Express Mail No. EV 473 970 846 US

**IN THE UNITED STATES PATENT AND TRADEMARK OFFICE**

| | | | |
|---|---|---|---|
| Application of: | Ternansky *et al.* | Confirmation No.: | 9257 |
| Serial No.: | 10/723,144 | Art Unit: | 1654 |
| Filed: | November 25, 2003 | Examiner: | Cordero Garcia, Marcela M. |
| For: | PEPTIDES WHICH INHIBIT ANGIOGENESIS, CELL MIGRATION, CELL INVASION AND CELL PROLIFERATION, COMPOSITIONS AND USES THEREOF | Attorney Docket No: | 9715-023-999 |

**DECLARATION OF DR. ANDREW P. MAZAR UNDER 37 C.F.R. § 1.132**

Mail Stop Amendment
Commissioner for Patents
P.O. Box 1450
Alexandria, VA 22313-1450

Sir:

I, Dr. Andrew P. Mazar, do hereby declare and state:

1. I am a co-inventor of the subject matter disclosed and claimed in the above-identified patent application (herein referred to as the '144 application).

2. I am currently the Chief Scientific Officer of Attenuon, LLC, which is the assignee of the '144 application.

3. My academic background, technical experience and list of publications are set forth in my *curriculum vitae*, attached hereto as **Exhibit 1**.

4. In the following paragraphs, I describe experiments conducted in the laboratories of Attenuon, LLC, which I personally supervised.

5. Compounds were tested in an in vivo assay for inhibition of tumor growth. On day 1 of the study, female C57BL/6 mice were inoculated subcutaneously with $3 \times 10^5$ Lewis lung carcinoma (3LL) cells. Compounds to be tested were dissolved in 50 mM citrate glycine buffer, pH 5.0, at a final concentration of 1.67 mM. Tumor bearing animals were treated

intravenously 3 times per week with either 100 µl of test compound, or vehicle control, starting on day 2 of the study. Treatment continued for a period of 17 days and tumor volumes were measured twice per week.

6. Table 1 displays the results of the in vivo assay described in paragraph 5 of various pentapeptides. The results are expressed as a ratio of the mean tumor volume of the treated group over the mean tumor volume of the control group.

Table 1.

| Compound | t/c ratio |
|---|---|
| Ac-PHSCN-$NH_2$ | 0.55 |
| Ac-PHSC(Me)N-$NH_2$ | 0.14 |
| Ac-PHSC(acetyl)N-$NH_2$ | 0.19 |
| Ac-PHSC(t-Butyl)N-$NH_2$ | 1.19 |
| Ac-PHSC(2-methoxyethyl)N-$NH_2$ | 1.67 |
| Ac-PHSC(pivoyl)N-$NH_2$ | 0.64 |
| Ac-PHSHoC(pivoyl)N-$NH_2$ | 0.60 |
| Ac-PHSC(cyclohexanoyl)N-$NH_2$ | 1.14 |
| Ac-PHSC(benzoyl)N-$NH_2$ | 0.91 |
| Ac-PHSC(alloc)N-$NH_2$ | 1.16 |
| Ac-PHSC(benzyl)N-$NH_2$ | 1.09 |
| Ac-PHSC(p-methylbenzyl)N-$NH_2$ | 1.35 |
| Ac-PHSC((phenylthio)acetyl)N-$NH_2$ | 0.94 |
| Ac-PHSHoC(benzoyl)N-$NH_2$ | 0.5 |
| Ac-PHSHoC(thiophene-2-carbonyl)N-$NH_2$ | 1.61 |
| Ac-PHSC(S-t-Butyl)N-$NH_2$ | 1.12 |
| Ac-PHSC(S-Methyl)N-$NH_2$ | 0.62 |
| Ac-PHSC(S-cysteine)N-$NH_2$ | 1.68 |
| Ac-PHSHoC(S-Methyl)N-$NH_2$ | 2.10 |
| Ac-PHSC(S-Phenyl)N-$NH_2$ | 0.51 |
| Ac-PHSMet(O)N-$NH_2$ | 1.00 |
| Ac-PHSMet($O_2$)N-$NH_2$ | 0.74 |
| Ac-PHSC($O_2$ benzyl)N-$NH_2$ | 0.81 |

7. The results in Table 1 show that the substitution of the side chain of the 4th amino acid of the pentapeptides had divergent effects upon activity, and show the lack of predictability around the substitution pattern of the side chain of the 4th amino acid of the pentapeptides. As indicated by the data above, Ac-PHSC(Me)N-$NH_2$ and Ac-PHSC(acetyl)N-$NH_2$ decreased the tumor volume over two and half to three times more than Ac-PHSCN-$NH_2$. These results were unexpected. Other alkyl substitutions on the S of the side chain of the 4th amino acid produced pentapeptides which were much less capable than Ac-PHSC(Me)N-$NH_2$ or Ac-PHSCN-$NH_2$, at inhibiting the growth of tumors. For example, the S-t-butyl compound (Ac-PHSC(t-Butyl)N-$NH_2$) and the S-( $CH_2$)O $CH_3$ compound (Ac-PHSC(2-methoxyethyl)N-$NH_2$) were much less active than either the Ac-PHSC(Me)N-$NH_2$ or Ac-PHSCN-$NH_2$ compounds. Moreover, other acyl substituted compounds were also much less capable of inhibiting tumor growth than Ac-PHSC(acetyl)N-$NH_2$. The S-pivoyl compound (Ac-PHSC(pivoyl)N-$NH_2$) had approximately the same activity as Ac-PHSCN-$NH_2$ and was much less active than Ac-PHSC(acetyl)N-$NH_2$, while the S-cyclohexanoyl (Ac-PHSC(cyclohexanoyl)N-$NH_2$), S-benzoyl (Ac-PHSC(benzoyl)N-$NH_2$) and S-alloc (Ac-PHSC(alloc)N-$NH_2$) compounds were all much less active than either Ac-PHSCN-$NH_2$ or Ac-PHSC(acetyl)N-$NH_2$.

8. Compounds Ac-PHSC(pivoyl)N-$NH_2$, Ac-PHSHoC(pivoyl)N-$NH_2$, Ac-PHSHoC(benzoyl)N-$NH_2$, Ac-PHSC(S-Methyl)N-$NH_2$, and Ac-PHSC(S-Phenyl)N-$NH_2$ had similar activity to Ac-PHSCN-$NH_2$, a result which could not have been predicted in view of the divergent effects on activity of different substituents.

9. The experiments described in paragraphs 11-13 below suggested that Ac-PHSCN-$NH_2$, may have a different mechanism for inhibiting angiogenesis than Ac-PHSC(Me)N-$NH_2$.

10. A previous study (as reported by Kim *et al*, J. Clin. Invest., 110, 933-941, 2002, a copy of which is attached hereto as Exhibit 2) suggested that antagonists of the integrin alpha5beta1 activate protein kinase A ("PKA"), leading to the activation of caspase-8 and the induction of apoptosis. When applied to endothelial cells, antagonists of alpha5beta1 induce apoptosis and inhibit angiogenesis (*id.* at 933). Previous studies from our laboratory had suggested that Ac-PHSCN-$NH_2$, is an alpha5beta1 antagonist and that it inhibits angiogenesis (see Khalili *et al*, Mol Cancer Ther 5, 2271-2280, 2006, a copy of which is attached hereto as Exhibit 3).

11. To determine if PKA activation is required for Ac-PHSCN-$NH_2$ or Ac-PHSC(Me)N-$NH_2$ activity, we measured the inhibition of angiogenesis mediated by Ac-PHSCN-$NH_2$ or Ac-PHSC(Me)N-$NH_2$, in the presence or absence of the PKA inhibitor, HA-1004 (N-(2-Guanidinoethyl)-5-isoquinolinesulfonamide).

12. The procedure followed in the experiment was substantially as described in section 5.4.8 on page 32, line 10 to page 33, line 2 of U.S. Application No. 10/723,144 as filed November 25, 2003. Ice-cold Matrigel® (e.g., 500 µL) (Collaborative Biomedical Products, Inc., Bedford, Mass.) was mixed with heparin (e.g., 50 µg/ml), FGF-2 (e.g., 400 ng/ml) and the compound to be tested. Basic fibroblast growth factor ("bFGF") was also added to the Matrigel as the angiogenic stimulus. The Matrigel® mixture was injected subcutaneously into 4-8 week-old althymic nude mice at sites near the abdominal midline at 3 different sites. The injected Matrigel® forms a palpable solid gel. Injection sites were chosen such that each animal received a positive control plug (such as basic fibroblast growth factor ("bFGF" also referred to as "FGF-2")+heparin), a negative control plug (e.g., buffer+heparin) and a plug that included the compound being tested for its effect on angiogenesis, e.g., (FGF-2+heparin+compound). All treatments were run in triplicate. Animals were sacrificed by cervical dislocation at about 7 days post injection. The mouse skin was detached along the abdominal midline, and the Matrigel® plugs were recovered and scanned immediately at high resolution. Plugs were then dispersed in water and incubated at 37°C overnight using Drabkin's method to detect haemoglobin as a measure of angiogenesis (Drabkin, *et al.*, J. Biol. Chem., 112, 51, (1935), a copy of which is attached hereto as Exhibit 4). Animals were injected prior to sacrifice with a 0.1 ml buffer (phosphate buffered saline ("PBS")) containing a high molecular weight dextran to which was conjugated a fluorophore. The amount of fluorescence in the dispersed plug, determined fluorimetrically, also served as a measure of angiogenesis in the plug.

13. As shown in Figure 1 (see Exhibit 5), the presence of the PKA inhibitor antagonized the effect of Ac-PHSCN-$NH_2$ (identified as ATN 161), suggesting that activation of PKA is an important part of the mechanism by which Ac-PHSCN-$NH_2$ inhibits angiogenesis. Surprisingly, inhibition of angiogenesis by the peptide, Ac-PHSC(Me)N-$NH_2$ (identified as ATN-220), was not affected by the presence of HA-1004, suggesting that the Ac-PHSC(*Me*)N-$NH_2$ peptide inhibits angiogenesis by a mechanism distinct from that of Ac-PHSCN-$NH_2$.

14. I hereby declare that all statements made herein of my own knowledge are true and that all statements made on information and belief are believed to be true; and further that I make these statements with the knowledge that willful false statements and the like so made are punishable by fine or imprisonment, or both, under Section 1001 of Title 18 of the United States Code, and that such willful false statements may jeopardize the validity of the application, and any patent issuing thereon.

Dated: 5/14/07

Andrew P. Mazar

**Andrew P. Mazar, Ph. D.**

1608 India Street, #403
San Diego, CA 92101
Office (858) 720-8797 x102
Home (619) 546-6619
Cell (858) 922-6618
mazar@attenuon.com

Experienced research director and senior manager with over 17 years of pharmaceutical and biotechnology industry experience. Extensive expertise in design, discovery and development of small molecules, peptides and biologicals for the treatment of cancer and other angiogenesis and inflammation-dependent diseases. Internationally recognized for research in angiogenesis and the urokinase plasminogen activator system. Inventor on multiple issued and filed patents. Established track record in scientific community which includes: presenting research seminars at national and international meetings; publication in peer-reviewed scientific journals; publication of invited reviews and book chapters; participation in NIH and VA study sections; and organizational roles in planning international scientific meetings. Expertise in translating oncology drugs from discovery through early clinical trials. Expertise in strategic assessment of external science, biotechnology licensing, partnership and alliance opportunities and leading the due diligence process.

## PROFESSIONAL EXPERIENCE

**Attenuon, LLC, San Diego, California** **2000-present**

Attenuon was founded in May 1998 with the goal of working with leading academic laboratories to rapidly translate advances in the understanding of tumor biology into less toxic drugs to control the growth and progression of cancer. Attenuon's staff includes leading researchers in tumor biology and synthetic chemistry as well as industry veterans knowledgeable in drug development. Attenuon's compounds – two of which are currently in clinical trials – are intended to target a broad range of tumors and the blood vessels that feed their growth without affecting healthy cells. The company believes that these compounds could thus be effective against many types of cancer.

**Chief Scientific Officer, Senior Vice President, Research and Development**

Responsible for scientific and managerial leadership of entire company as well as business development and fund raising. Attenuon has never had a CEO and thus I had to assume many of the responsibilities typically associated with the CEO position as well as carrying out the CSO functions. Attenuon has raised over $50M to date. Responsibilities included identifying and in-licensing compounds from academia or from government laboratories including management of due diligence process; building Attenuon's research and development capabilities from scratch including hiring entire scientific and clinical teams; initiation, propagation and prioritization of all internal research and development functions; initiation and management of multiple academic and government collaborations; recruitment and management of Scientific and Clinical Advisory Boards; management of all CRO interactions; management of Attenuon's IP portfolio; presentations at scientific and investor conferences including investment road show; development of business plan, private placement memorandum and all confidential and non-confidential scientific overviews; management of out-licensing presentations and discussions; and evaluation of additional business opportunities for parent company, D.E. Shaw and Co.

- First employee hired when Attenuon transitioned from a virtual company
  - Built biology group of four (4) Ph. D. level scientists, thirteen (13) Research Associates including internal *in vivo* team to carry out animal tumor model and pharmacology studies
  - Built chemistry group of seven (7) Ph. D. level scientists
  - Built clinical group including M.D. oncologist, Ph.D. level clinical scientists and two (2) project managers
  - Built regulatory team of two (2) people
  - Managed ~$10-12M annual budget over the past two (4) years with commitment for $25M budget for 2007 and 2008

- Led in-licensing efforts of compounds
- Recruited proactive thought leaders in oncology, angiogenesis and oncology drug development to join the Scientific and Clinical Advisory Boards (most advisors are also collaborators)
- Chaired all advisory board meetings since 2000

- Initiated, propagated and prioritized all research and development functions
  - Demonstrated expertise with *in vitro* and *in vivo* tumor models, assay development and validation, target identification and validation, chemical genomics and drug discovery and development
  - Rapidly prioritized from among six (6) projects to move ATN-161 and ATN-224 into development (both currently in phase II trials)
  - Led optimization, discovery and development of ATN-161 and ATN-224
  - Led regulatory teams on ATN-161 and ATN-224
  - Managed Attenuon's IP portfolio – developed IP strategy that led to identification of $2^{nd}$ – $4^{th}$ generation analogs of ATN-224 and $2^{nd}$ and $3^{rd}$ generation analogs of ATN-161
  - Identified and conducted proof-of-principle animal studies in non-oncology indications for both ATN-161 and ATN-224
  - Received $1.2M NIH grant to pursue analog of ATN-161 for tumor imaging
  - Built anti-urokinase plasminogen activator receptor (uPAR) antibody project from the ground up internally (lead antibodies discovered in-house) – led to funded collaboration with Kirin Pharmaceuticals
  - Identified and initiated development on lead anti-uPAR antibody, huATN-658 (2007)

- Demonstrated ability to rapidly move projects from bench through Phase I trials
  - ATN-161 moved from license to IND in thirteen (13) months and ATN-224 in eighteen (18) months
  - INDs allowed without clinical holds
  - Led internal team focused on understanding mechanisms of action and developing rationale and biomarkers to support clinical development as well as expanding existing IP on lead projects
  - Managed external CRO interactions on all projects
  - Developed bridging strategy that allowed Attenuon to use toxicology data from NCI RAID studies using the first generation version of ATN-224 to support the ATN-224 IND
  - Developed regulatory strategy for huATN-658

- Managed early clinical development
  - Developed protocols in collaboration with clinical collaborators
  - Initiated and propagated collaboration on ATN-224 with Cancer Research UK
  - Managed clinical and regulatory teams
  - Initiated two (2) co-operative research and development agreements (CRADAs) on ATN-161 and ATN-224 with Neuro-oncology branch (NOB at the NCI) where the NCI will develop ATN-161 and ATN-224 for the treatment of malignant glioma through Phase II trials
  - Recruited Chief Medical Officer
  - Moved two projects into multiple phase II trials in Oncology

- Reviewed and conducted due diligence on possible licensing opportunities from academia and government laboratories
  - Identified and obtained licenses for two (2) broad families of natural product anti-cancer agents from NCI and prepared licensing applications including research and development plan and budgets for the development of these compounds
  - Managed due diligence process
  - Resource limitations did not allow Attenuon to move forward with any of these opportunities

- Initiated and managed multiple academic and government collaborations
  - Maintain active collaborations with UCSD Cancer Center, McGill Health Center, University of Missouri, University of Pennsylvania, Fox Chase Cancer Center, Sunnybrook and Women's Hospital, Case Western Reserve School of Medicine, Scripps Research Institute, University of Chicago, University of Texas, Cancer Research UK and the NCI

- Resulted in forty one (41) full publications and twenty seven (27) meeting abstracts since 2000
- Service to the research community through participation in study sections, *Ad Hoc* grant review, manuscript review for leading scientific journals and organizational committee membership for international meetings

- Responsible for other senior management activities
  - Presented at scientific and investor conferences including investment road show – represented company at conferences including AACR, EORTC, ASCO and various investor conferences such as USCD Connect, BIO, SCBC and various partnership conferences
  - Developed business plan, private placement memorandum and all confidential and non-confidential scientific overviews
  - Managed out-licensing presentations and discussions
  - Authored scientific and development sections to all company literature – prepared scientific overview documents on all company programs
  - Developed non-hierarchical company culture and fostered team based approach to discovery and development
  - Raised >$50M since inception of company

**Ångstrom Pharmaceuticals, San Diego, California** **1997-2000**

Angstrom Pharmaceuticals, Inc. is a privately held, development stage pharmaceutical company. The Company is focused on development of proprietary products based on interfering with urokinase plasminogen activator (uPA) and its receptor (uPAR), which is a key biochemical system responsible for angiogenesis, cell migration and tissue invasion. Because of the near-universal involvement of uPA/uPAR in carcinoma, nearly all solid tumors in males and females are amenable to treatment with a uPA/uPAR antagonist. Because Å6 inhibits angiogenesis, the Company is also targeting wet age-related macular degeneration, the leading cause of blindness in people over age 50. Å6 has demonstrated excellent efficacy in several animal models of ophthalmic neo-vascularization, which are used to predict clinical efficacy in macular degeneration.

**Vice President, Biology**
**Senior Director, Biology**
**Director, Biology**
**Consultant**

Responsible for all biology functions of the company. Built entire biology research and development efforts that included three (3) internal research associates and numerous outside academic collaborators, one of which was partnered to Diatide, Inc. (now Schering AG) and the other which is now in Phase II trials. Drafted patent applications for these compounds; carried out due diligence on three in-licensing opportunities; responsible for a significant amount of funding through grants and funded collaborations. Participated in >100 road shows over a three year period; participated in partnership discussions with >20 companies.

- Responsible for all biology functions of the company
  - Built entire biology research and development efforts
  - Developed several novel models of metastasis with academic collaborators
  - Angstrom never obtained VC or other significant outside funding thus, we were only able to build a small internal team of three (3) research associates

- Able to advance several projects by virtue of extensive academic collaborator network that was willing to work on the compounds without significant funding
  - Invented three compounds, Å17, Å36 and Å6, targeting uPAR
  - Issued composition of matter protection on these compounds
  - Able to leverage robust biology data to bring in small amounts of capital from angel investors – this was used to initiate exploratory development studies on Å6
  - Partnered Å17 with Diatide, Inc. (now part of Schering AG) to bring in some capital to keep company going
  - Å6 now in Phase II trials
  - Identified in-licensing opportunities and carried out initial due diligence

- Responsible for a significant amount of funding through grants and funded collaborations
  - PI on two SBIR grants including a prestigious FLAIR grant from the NCI ($700K/two years)
  - Funded collaboration from another company on minimization of an anti-angiogenic protein ($750K/yr)
  - Extensive interactions with potential partners – went to term sheet with one potential partner (later decided they did not want to focus on oncology) and deep due diligence with a second, large Japanese pharmaceutical company

- Presented on road shows and partnership discussions

**Abbott Laboratories, Abbott Park, Illinois** **1989-1996**

Abbott Laboratories is an international company that develops and markets drugs, diagnostics and nutritional products. Abbott Laboratories is a recent entry to oncology drug development, having formed the oncology development group in 1997. During my tenure, the only efforts in oncology occurred at the pilot project level and were not formally part of pharmaceutical products research. The projects that were piloted during my tenure eventually evolved into recognized pharmaceutical projects and have led to at least two (2) clinical stage projects that are currently in development.

**Group Leader, Oncology Research**
**Senior Scientist**
**Research Scientist**

Responsible for a laboratory group of three (3) Ph.D. and four (4) Research Associates as Group Leader. Managed two (2) Research Associates as a Senior Scientist. Reported to Department Head.

- Developed analytical methods to support IND filing for two (2) thrombolytic agents
- Member of thrombolytic venture development team
- Piloted two (2) anti-angiogenesis research programs focusing on the urokinase plasminogen activator (uPA) system
- Validated uPA and uPAR as therapeutic targets
- Developed panel of reagents in uPA system including antibodies and purified proteins and fragments – made these available to the uPA research community
- Presented pilot data to senior management and Scientific Advisory Board
- Established *in vitro* angiogenesis assays and *in vivo* tumor models to support pilot projects
- Acted as internal advisor to other groups on tumor models and tumor biology
- Primary scientific reviewer on in-licensing opportunities in oncology
- Consulted to TAP Pharmaceuticals on development of TNP-470, one of the first anti-angiogenic agents to be evaluated clinically

**University of Texas Health Center at Tyler, Tyler, Texas** **2006-**
**Adjunct Associate Professor of Research**

**University of North Texas, Fort Worth, Texas** **1999-2003**
**Adjunct Professor**
**Board member, Institute for Cancer Research**
Doctoral Thesis Advisor, Geath Al-Atrash, MD, Ph.D.; Degree granted 2002

**Barat College, Lake Forest, Illinois** **1996-1997**
**Lecturer, Biology**

**Northwestern University School of Medicine, Chicago, Illinois** **1993-1998**
**Adjunct Assistant Professor**

## EDUCATION

Ph.D., Biochemistry
University of Illinois College of Medicine
Department of Biochemistry, Chicago, Illinois

B.S., Chemistry (honors), concentration in Biochemistry
University of Wisconsin – Parkside, Kenosha, Wisconsin

## AWARDS, HONORS AND COMMITTEES

Co-chair, State of the Art VIII: Receptors, International Congress on Fibrinolysis and Proteolysis (2006); Scientific Organizing Committee – International Congress on Fibrinolysis and Proteolysis (2006); Guest Editor, Current Cancer Drug Targets, Hot Topics Issue on Novel Targets for Anti-angiogenic and Cytostatic therapies (2005); Chairperson, AACR Annual Meeting, Symposium: *Expression of Metastasis-related Gene* (2002); Co-Chairperson, AACR Annual Meeting, Subsection BL3: *Tumor Progression, Invasion and Metastasis* (2002); Invited Participant, Banbury Center/Cold Spring Harbor: *New Concepts for Cancer Clinical Trials* (2001); Invited participant, ASCO Annual Meeting, Angiogenesis Expert Panel (2001); Advisory Board Member, Institute for Cancer Research, University of North Texas Health Science Center, Fort Worth, Texas (1999-2003); Young Investigator Award, 1st Osteosarcoma Research Conference, Allegheny-Singer Research Institute, Pittsburgh, Pennsylvania (1991); NSF Travel Grant (1989); Selected NATO Fellow to attend NATO sponsored Advanced Study Institute: *The enzyme catalysis process: energetics, mechanism and dynamics*, Barga, Italy (1989); University of Illinois Graduate College Fellowship, University of Illinois College of Medicine, Department of Biochemistry, Chicago, Illinois (1988).

## PEER REVIEW ACTIVITIES

**Editorial Review:**
Blood; BMC Cancer; Breast Cancer Research; British Journal of Cancer; Cancer Research; Clinical Cancer Research; Experimental Cell Research; FEBS Journal; Gene Therapy; Expert Opinion on Therapeutic Patents; International Journal of Cancer; Journal of Histochemistry and Cytochemistry; Medicinal Research Reviews; Molecular and Cellular Biochemistry; Molecular Cancer; Molecular Cancer Research; Molecular Cancer Therapeutics; Oncology Research; Recent Patents on Anti-Cancer Drug Discovery (PRA).

**Committees and Study Sections:**
NIH/NIDDK ZDK1 GRB4 O1&O2: STTR/SBIR (2006); Special Emphasis Panel/Scientific Review Group 2005/10 ZDK1 GRB-4 (O1) (2005); Phillip Morris External Research Program (2004, 2007); NIH/NHLBI SCCOR Study Panel ZHL1 CSR-R M1 R (2003); NIH/SBIR Study Section ZRG1 SSS-2 (2001-2002); VA Oncology Merit Review Study Section (1999-2001); American Heart Association, Ad Hoc Grant Reviewer (1999).

**Editorial Boards**
Recent Patent Reviews on Anti - Cancer Drug Discovery

## PROFESSIONAL SOCIETIES

American Society for Biochemistry and Molecular Biology; American Association for Cancer Research; American Association for the Advancement of Science; American Society of Clinical Oncology; International Society for Fibrinolysis and Proteolysis; Protein Society.

## BIBLIOGRAPHY

### ORIGINAL ARTICLES


Rabbani, S.A., Desjardins, J., Bell, A.W., Banville, D., Mazar, A., Henkin, J. and Goltzman, D. (1990) "An amino-terminal fragment of urokinase isolated from a prostate cancer cell line (PC-3) is mitogenic for osteoblast-like cells." Biochem. Biophys. Res. Comm. 173(3): 1058-1064.

Hoosein, N.M., Boyd, D.D., Hollas, W.J., Mazar, A., Henkin, J. and Chung, L.W.K. (1991) "Involvement of urokinase and its receptor in the invasiveness of human prostatic carcinoma cell lines." Cancer Comm. 3(8): 255-264.

Mazar, A.P., Buko, A., Petros, A.M., Barnathan, E.S. and Henkin, J. (1992) "Domain analysis of urokinase plasminogen activator (uPA): Preparation and characterization of intact A-chain molecules." Fibrinolysis 6 (suppl.1): 49-55.

Hollas, W., Soravia, E., Mazar, A., Henkin, J., Blasi, F. and Boyd, D. (1992) "Decreased urokinase receptor expression by overexpression of the plasminogen activator in a colon cancer cell line." Biochem. J. 285: 629-634.

Zini, J.M., Murray, S.C., Graham, C.H., Lala, P.K., Barnathan, E.S., Mazar, A., Henkin, J., Cines, D.B. and McCrae, K.R. (1992) "Characterization of urokinase receptor expression by human placental trophoblasts." Blood 79(11): 2917-2929.

Hansen, A.P., Petros, A.M., Mazar, A.P., Pederson, T.M., Rueter, A. and Fesik, S.W. (1992) "A practical method for uniform isotopic labeling of recombinant proteins in mammalian cells." Biochemistry 31(51): 12713-12718.

Rabbani, S.A., Mazar, A.P., Bernier, S.M., Haq, M., Bolivar, I., Henkin, J., and Goltzman, D. (1992) "Structural requirements for the growth factor activity of the amino-terminal domain of urokinase." J. Biol. Chem. 267(20): 14151-14156.

Novokhatny, V., Medved, L., Mazar, A., Marcotte, P., Henkin, P. and Ingham, K. (1992) "Domain structure and interactions of recombinant urokinase-type plasminogen activator." J. Biol. Chem. 267(6): 3878-3885.

Hollas, W., Hoosein, N., Chung, L.W.K., Mazar, A., Henkin, J., Kariko, K., Barnathan, E.S. and Boyd, D. (1992) "Expression of urokinase and its receptor in invasive and non-invasive prostate cancer cell lines." Thromb. and Haemos. 68(6): 662-666.

Nusrat, A.R., Mazar, A., Henkin, J. and Chapman, H.A. (1992) "A role for urokinase in mediating phorbol ester induced macrophage-like maturation and adhesion of U937 and other myeloid cells." Fibrinolysis (6 supp.1): 71-76.

Clayman, G., Wang, S.W., Nicolson, G.L., El-Naggar, A., Mazar, A., Henkin, J., Blasi, F., Goepfert, H. and Boyd, D.D. (1993) "Regulation of urokinase-type plasminogen activator expression in squamous cell carcinoma of the oral cavity." Int. J. Cancer 54: 73-80.

Hollas, W., Kariko, K., Barnathan, E., Mazar, A., Henkin, J. and Boyd, D. (1993) "Divergent effect of N, N-dimethylformamide on the expression of urokinase and its receptor." Fibrinolysis 7: 149-157.

Zhang, S., Laurent, M., Lopez-Alemany, R., Mazar, A., Henkin, J., Ronne, E., and Burtin, P. (1993) "Comparative localization of receptors for plasmin and for urokinase on MCF7 cells." Exp. Cell Res. 207: 290-299.

Novokhatny, V.V., Medved, L.V., Mazar, A. and Ingham, K.C. (1993) "Effect of tethered peptidylchloromethyl-ketone inhibitors on thermal stability and domain interactions of urokinase and other serine proteases." J. Biol. Chem. 268(23): 17211-17218.

Hansen, A.P., Petros, A.M., Meadows, R.P., Nettsesheim, D.G., Mazar, A.P., Olejniczak, E.T., Xu, R.X., Pederson, T.M., Henkin, J. and Fesik, S.W. (1994) "Solution structure of the amino terminal fragment of urokinase-type plasminogen activator." Biochemistry 33: 4847-4864.

Howell, A.L., Hunt, J.A., James, T.W., Mazar, A., Henkin, J. and Zacharski, L.R. (1994) "Urokinase inhibits HL-60 cell proliferation in vitro." Blood Coag. and Fibrinol. 5: 445-453.

Multhaupt, H.A.B., Mazar, A., Cines, D.B., Warhol, M., McCrae, K.R., (1994) "Expression of urokinase receptors by human trophoblast: a histochemical and ultrastructural analysis." Laboratory Investigation 71(3): 392-400.

Schnaper, H.W., Barnathan, E.S., Mazar, A.P., Maheshwari, S., Ellis, S., and Kleinman, H.K. (1995) "Plasminogen activators augment endothelial cell organization in vitro by two distinct pathways." J. Cell. Phys. 165: 107-118.

Rabbani, S.A., Harakidas, P., Davidson, D., Henkin, J. and Mazar, A.P. (1995) "Prevention of prostate cancer metastasis by a urokinase-type plasminogen activator (uPA) specific inhibitor in vivo." Int. J. Cancer 63: 840-845.

Higazi, A.A-R., Mazar, A., Wang, J., Reilly, R., Henkin, J., Kniss, D. and Cines, D. (1996) "Single-chain urokinase-type plasminogen activator bound to its receptor is relatively resistant to plasminogen activator inhibitor type 1." Blood 87(9): 3545-3549.

Higazi, A. A-R., Mazar, A., Wang, J., Quan, N., Griffin, R., Reilly, R., Henkin, J. and Cines, D.B. (1997) "Soluble human urokinase receptor is composed of two active subunits." J. Biol. Chem.272 (8): 5348-5353.

Weaver, A.M., Hussaini, I.M., Mazar, A., Henkin, J. and Gonias, S. (1997) "Embryonic fibroblasts that are genetically deficient in low density lipoprotein receptor-related protein demonstrate increased activity of the urokinase receptor system and accelerated migration on vitronectin." J. Biol. Chem. 272 (22): 14372-14379.

Wang, J., Mazar, A., Quan, N., Schneider, A. and Henkin, J. (1997) "Plasminogen activation by pro-urokinase in complex with its receptor: dependence on a tripeptide (spectrozyme plasmin)." Eur. J. Biochem. 247(1): 256-261.

Rabbani, S.A., Gladu, J., Mazar, A.P., Henkin, J. and Goltzman, D. (1997) "Induction in human osteoblastic cells (SaOS2) of the early response genes fos, jun and myc by the amino terminal fragment (ATF) of urokinase." J. Cell. Physiol. 172: 137-145.

Xing, R.H., Mazar, A., Henkin, J. and Rabbani, S.A. (1997) "Prevention of breast cancer growth, invasion and metastasis by anti-estrogen tamoxifen alone or in combination with urokinase inhibitor B-428." Cancer Res.57: 3585-3593.

Colman, R.W., Pixley, R.A., Najamunnisa, S., Yan, W., Wang, J., Quan, N., Mazar, A. and McCrae, K.R. (1997) "Binding of high molecular weight kininogen to human endothelial cells is mediated via a site within domains 2+3 of the urokinase receptor." J. Clin. Invest. 100(6): 1-7.

Gum, R., Juarez, J., Allgayer, H., Mazar, A., Wang, Y. and Boyd, D. (1998) "Stimulation of urokinase-type plasminogen activator receptor expression by PMA requires a JNK1-dependent signaling molecule." Oncogene 17: 213-225.

Allgayer, H., Wang, H., Gallick, G. E., Crabtree, A, Mazar, A., Jones, T., Kraker, A. J. and Boyd, D. D. (1999) "Transcriptional induction of the urokinase receptor (uPAR) gene by a constitutively active Src: requirement of an upstream motif (-152/-135) bound with Sp1." J. Biol. Chem. 274: 18428-37.

Guo, Y. J., Arakelian, A., Goldfarb, R. H., Higazi, A. A-R., Jones, T.R., Kwaan, H., Mazar, A.P. and Rabbani, S.A. (2000) "A peptide derived from the non-receptor binding region of urokinase plasminogen activator (uPA) inhibits tumor growth and metastasis and induces tumor cell death in vivo." FASEB J. 14: 1400-1410.

Haj-Yehia, A., Nassar, T., Sachais, B.S., Kuo, A., Bdeir, K., Al-Mehdi, A. B., Mazar, A., Cines D.B. and Higazi, A.A-R. (2000) "Urokinase-derived peptides regulate vascular smooth muscle contraction in vitro and in vivo." FASEB J. 14: 1411-1422.

Shliom, O., Huang, M., Sachais, B., Weisel, J. W., Nagaswami, C., Nassar, T., Bdeir, K., Hiss, E., Gawlak, S., Harris, S., Mazar, A. and Higazi, A.A. (2000) "Novel Interactions Between Urokinase and it Receptor." J. Biol.

Chem. 275(32): 24304-12.

Mishima, K., Mazar, A.P., Gown, A., Skelly, M., Ji, X.-D., Wang, X.D., Jones, T.R., Cavenee, W. D. and Huang, H.J.S. (2000) "Inhibition of glioblastoma growth and angiogenesis in vivo by a peptide derived from the non-receptor binding region of urokinase plasminogen activator (uPA) in combination with cisplatin." Proc. Natl. Acad. Sci. 97(15): 8484-8489.

Bdeir, K., Kuo, A., Mazar, A., Sachais, B.S., Xiao, W., Gawlak, S., Harris, S., Higazi, A.A. and Cines, D.B. (2000) "A region in domain II of the urokinase receptor required for urokinase binding." J. Biol. Chem. 275: 28532-28538.

Tarui, T., Mazar, A.P., Cines, D.B., Takada, T. (2001) "Urokinase Receptor (uPAR/CD87) is a genuine ligand for integrins and mediates cell-cell interaction." J. Biol. Chem. 276: 3983-3990.

Idell S., Mazar A.P., Bitterman P., Mohla S., Harabin A.L. (2001) " Fibrin Turnover in Lung Inflammation and Neoplasia." Am. J. Respir. Crit. Care Med. 2001 Feb 1: 163(2): 578-584.

Al-Atrash, G., Kitson, R., Xue, Y., Mazar, A., Kim, M. and Goldfarb, R. (2001) "uPA and uPAR contribute to NK cell invasion through the extracellular matrix." Anticancer Research 21: 1-8.

Zhang, J.C., Qi, X., Juarez, J., Plunkett, M., Donate, F., Sakthivel, R., Mazar, A.P., McCrae, K.R. (2002) "Inhibition of angiogenesis by two-chain high molecular weight kininogen (HKa) and kininogen-derived polypeptides." Can. J. Physiol. Pharmacol. 80: 85-90.

Guo, Y., Mazar, A.P., Lebrun, J.J. and Rabbani, S.A. (2002) "An Anti-Angiogenic Urokinase Derived Peptide (Å6) Combined with Tamoxifen (TAM) Decreases Tumor Growth and Metastasis in a Syngeneic Model of Breast Cancer." Cancer Res. 15: 4678-4684.

Zhang, J.C., Donate, F., Ziats, N.P., Juarez, J.C., Mazar, A.P., Pang, Y-P., McCrae, K.R. (2002) "The antiangiogenic activity of cleaved high molecular weight kininogen is mediated through binding to endothelial cell tropomyosin." Proc Nat Acad. Sci. 99: 12224-12229.

Juarez, J.C., Guan, X., Shipulina, N., Plunkett, M., Parry, G.C., Shaw, D.E., Zhang, J-C., McCrae, K.R., Mazar, A.P., Morgan, W.T., Donate, F. (2002) "The histidine-proline rich glycoprotein (HPRG) has potent anti-angiogenic and anti-tumor activities mediated through the histidine-proline rich domain." Cancer Res. 62: 5344-5358.

Idell, S., Mazar, A., Cines, D., Kuo, A., Parry, G., Gawlak, S., Juarez, J., Koenig, K., Azghani, A., Hadden, W., McLarty, J. and Edmund Miller (2002) "Single-chain Urokinase Alone or Complexed to its Receptor in Tetracycline-induced Pleuritis in Rabbits." Am. J. Respir. Crit. Care Med. 166: 920-926.

Datta, A., Kitson, R.P., Xue, Y., Al-Atrash, G., Mazar, A.P., Jones, T.R. and Goldfarb, R.H. (2002) "Combined chemo/anti-angiogenic therapy against Lewis Lung Carcinoma (3LL) pulmonary metastasis." In Vivo 16: 451-458.

Nassar T., Haj-Yehia A., Akkawi S., Kuo A., Bdeir K., Mazar A., Cines D.B., Higazi A.A. (2002) "Binding of urokinase to low density lipoprotein-related receptor (LRP) regulates vascular smooth muscle cell contraction." J. Biol. Chem. 277: 40499-40504.

Stoeltzing O., Liu W., Reinmuth N., Fan F., Parry G.C., Parikh A.A., McCarty M.F., Bucana C.D., Mazar A.P. and Ellis LM. (2003) "Inhibition of integrin alpha5 beta1 function with a small peptide (ATN-161) plus continuous 5-FU infusion reduces colorectal liver metastases and improves survival in mice." Int. J. Cancer 104: 496-503.

Tarui T., Andronicos N., Czerkay R.P., Mazar A.P., Bdeir K., Parry G.C., Kuo A., Loskutoff D.J., Cines D.B. and Takada Y.J. (2003) "Critical role of integrin alpha5 beta1 in urokinase (uPA)/urokinase receptor (uPAR, CD87) signaling." J. Biol. Chem. 278: 29863-29872.

Bdeir, K., Kuo, A., Sachais, B.S., Ruxl, A.H., Bdeir, Y., Mazar, A.P., Higazi, A.A-R. and Cines, D.B. (2003) "The kringle stabilizes urokinase binding to the urokinase receptor." Blood 102: 3600-3608.

Chang D.I., Hosomi N., Lucero J., Heo J.H., Abumiya T., Mazar A.P. and del Zoppo, G.J. (2003) "Activation systems for latent matrix metalloproteinase-2 are upregulated immediately after focal cerebral ischemia." J. Cereb. Blood Flow Metab. 23: 1408-1419.

Hall, C.L., Tsan, R., Mugnai, R., Mazar, A., Radinsky, R. and Pettaway, C.A. (2004) "Enhanced Invasion of Hormone Refractory Prostate Cancer Cells through Hepatocyte Growth Factor (HGF) Induction of Urokinase-Type Plasminogen Activator (u-PA)." Prostate 59: 167-176.

Guan, X., Juarez, J.C., Qi, X., Shipulina, N.V., Shaw, D.E., Morgan, W.T., McCrae, K.R., Mazar, A.P. and Doñate, F. (2004) "Histidine-Proline Rich Glycoprotein (HPRG) binds and transduces anti-angiogenic signals through cell surface tropomyosin on endothelial cells." Thromb. Hemostat. 92: 403-412.

Doñate, F., Juarez, J.C., Guan, X., Shipulina, N.V., Plunkett, M.L., Tel-Tsur, Z., Shaw, D.E., Morgan, W.T. and Mazar, A.P. (2004) "Peptides derived from the Histidine-Proline (H/P) domain of the Histidine-Proline Rich Glycoprotein (HPRG) bind to tropomyosin and have anti-angiogenic and anti-tumor activities." Cancer Res. 64: 5812-5817.

Bauer, T.W., Fan, F., Liu, W., Johnson, M., Parikh, N.U., Parry, G.C., Callahan, J., Mazar, A.P., Gallick, G. and Ellis, L.M. (2005) "Insulin-like growth factor-1-mediated migration and invasion of human colon carcinoma cells requires activation of c-Met and urokinase plasminogen activator receptor." Annals of Surgery 241: 748-758.

Huang, M., Mazar, A.P., Parry, G.C., Kuo, A. and Cines, D.B. (2005) "Crystallization of soluble urokinase receptor (suPAR) in complex with urokinase amino terminal fragment (1-143)." Acta. Crystallograph D61: 697-700.

Shetty, S., Gyetko, M.R., Mazar, A.P. (2005) "Induction of p53 by urokinase in lung epithelial cells." J. Biol. Chem. 280: 28133-28141.

Bauer, T.W., Liu, W., Fan, F., Camp, E.R., Yang, A., Somcio, R.J., Avila, H.C., Bucana, C.D., Callahan, J., Parry, G.C., Boyd, D.D., Mazar, A.P. and Ellis, L.M. (2005) "Urokinase Plasminogen Activator Receptor Antibody Inhibits Orthotopic Growth of Human Pancreatic Carcinoma, Local Tumor Invasion, and Development of Liver Metastases in Mice." Cancer Res. 65: 7775-7781.

Mazar A.P. (2005) Editorial. Novel non-cytotoxic approaches for cancer therapy: Potential targets and pathways amenable to single agent multimodal therapeutic approaches. Curr. Cancer Drug Targets 5: p.469-470.

Li, Y., Shi, X., Parry, G., Chen, L., Callahan, J.A., Mazar, A.P. and Huang, M. (2005) "Optimization of crystals of an inhibitory antibody of urokinase plasminogen activator receptor (uPAR) with hydrogen peroxide and low protein concentration." Protein and Peptide Lett. 12; 655-658.

Huai, Q., Mazar, A.P., Kuo, A., Parry, G.C., Shaw, D.E., Callahan, J., Li, Y., Yuan, C., Bian, C., Chen, L., Furie, B., Furie, B.C., Cines, D.B., Huang, M. (2006) "Structure of human urokinase plasminogen activator in complex with its receptor." Science 311:656-9.

Tarui, T., Akakura, N., Majumdar, M., Andronicos, N., Takagi, J., Mazar, A.P., Bdeir, K., Kuo, A., Yarovoi, S.V., Cines, D.B. and Takada, Y. (2006) "Direct interaction of the kringle domain of urokinase-type plasminogen activator (uPA) and integrin alphavbeta3 induces signal transduction and enhances plasminogen activation. Thromb Haemost. 95: 524-34."

Cianfrocca, M.E., Kimmel, K.A., Gallo, J.,Cardoso, T., Brown, M.M., Hudes, G., Lewis, N., Weiner, L., Lam, G.N., Brown, S.C., Shaw, D.E., Mazar, A.P. and Cohen, R.B. (2006). "Phase I Trial Of The Antiangiogenic Peptide ATN 161 (Ac-PHSCN-$NH_2$)$_2$, a Beta Integrin Antagonist, In Patients With Solid Tumors." Br J Cancer 94:1621-6.

Juarez, J.C., Betancourt Jr., O., Pirie-Shepherd, S.R., Guan, X., Price, M.L., Shaw, D.E., Mazar, A.P. and Doñate, F. (2006). "Copper binding by tetrathiomolybdate attenuates angiogenesis and tumor cell proliferation through the inhibition of superoxide dismutase 1 (SOD1)." Clin Cancer Res 12: 4974-4982.

Khalili, P., Arakelian, A., Chen, G., Plunkett, M.L., Beck, I., Parry, G.C., Doñate, F., Shaw, D.E., Mazar, A.P. and Rabbani, S.A. (2006). "A non-RGD based integrin binding peptide (ATN-161) blocks breast cancer growth and metastasis in vivo." Mol Cancer Ther 5: 2271-2280.

Chidlow, J.H., Langston, W., Greer, J.J., Ostanin, D., Abdelbaqi, M., Houghton, J., Senthilkumar, A., Shukla, D., Mazar, A.P., Grisham, M.B. and Kevil, C.G.(2006) "Differential Angiogenic Regulation of Experimental Colitis." Am J Pathol 2006 169: 2014-2020.

Barinka, C., Parry, G., Callahan, J., Shaw, D.E., Kuo, A., Bdeir, K., Cines, D.B., Mazar, A. and Lubkowski, J. (2006). "Structural Basis of Interaction between Urokinase-type Plasminogen Activator and its Receptor." J Mol Biol. 363:482-95.

Li, Y., Parry, G., Chen, L., Callahan, J.A., Shaw, D.E., Meehan, E.J., Mazar, A.P.and Huang M. (2006). "An Anti-urokinase Plasminogen Activator Receptor (uPAR) Antibody: Crystal Structure and Binding Epitope." J Mol Biol 365(4):1117-1129.

Danese, S., Sans, M., Spencer, D., Beck, I., Donate, F., Plunkett, M., de la Motte, C., Redline, R., Shaw, D. Levine, A., Mazar, A., Fiocchi, C. (2006) "Angiogenesis blockade as a new therapeutic approach to experimental colitis." Gut. 2006 Dec 14; [Epub ahead of print].

Idell, S., Allen, T., Chen, S., Koenig, K., Mazar, A., Azghani, A.(2007) "Intrapleural Activation, Processing, Efficacy and Duration of Protection of Single Chain Urokinase in EvolvingTetracycline-induced Pleural Injury in Rabbits." Am J Physiol Lung Cell Mol Physiol. 292: L25-32.

Shetty, S., Velusamy, T., Idell, S., Shetty, P.K., Mazar, A.P., Bhandary, Y.P. and Shetty, R.S. (2007) "Regulation of Urokinase Receptor Expression by p53: A Novel Role in Stabilization of uPAR mRNA." Mol Cell Biol (in press).

**BOOK CHAPTERS AND REVIEW ARTICLES**

Mazar, A.P., Henkin, J., Goltzman, D. and Rabbani, S.A. (1991) "A N-terminal fragment of urinary plasminogen activator which is mitogenic in SaOS-2 cells is generated proteolytically by PC-3 cells." in Frontiers of Osteosarcoma Research, J.F. Novak and J.H. McMaster, eds. Toronto: Hogrefe and Huber, pp. 319-322.

Mazar, A., Henkin, J. and Goldfarb, R. H. (1999) "The urokinase plasminogen activator (uPA/uPAR/PAI-1) system in cancer: implications for angiogenesis, invasion and tumor metastasis." Angiogenesis 3(1): 15-32.

Mazar, A.P., Gawlak, S., Goldfarb, R.H., Kitson, R.P., Rabbani, S.A., Guo, J., Gown, A. and Jones, T.R. (2000) "The urokinase plasminogen activator receptor (uPAR) is a choke-point for carcinoma metastasis and angiogenesis." Recent Research Developments in Cancer 2: 1-12.

Mazar, A.P. (2001) "The Urokinase Receptor as a Target for the Diagnosis and Therapy of Cancer." Anticancer Drugs 12(5): 387-400.

Rabbani, S.A. and Mazar, A.P. (2001) "The Role of the Plasminogen Activation System in Angiogenesis and Metastasis." Surg. Oncol. Clin. N. America 10(2): 393-416.

Rabbani, S.A., Shukeir, N., Mazar, A.P (2004). "Prostate Cancer: Models for Developing Novel Therapeutic Approaches." in Bone Metastasis and Molecular Mechanisms: G. Singh and F.W. Orr (Eds.), Kluwer Academic Publishers (Boston): 163-186.

Donate, F., McCrae, K., Shaw, D.E. and Mazar, A.P. (2004) "Extracellular tropomyosin: a novel common pathway target for anti-angiogenic therapy." Curr. Cancer Drug Targets 4: 543-553.

Parry, G.C., Doñate, F., Plunkett, M.L., Shaw, D.E., Pirie-Shepherd, S. and Mazar, A.P. (2005) "Integrins: Novel targets for the treatment of bone metastasis." in Bone Metastasis: Experimental and Clinical Therapeutics. S. Rabbani and G. Singh (Eds.) Humana Press: 201-227.

## MEETING ABSTRACTS

Mazar, A., Buko, A., Sarin, V., Menon, G., Petros, A. and Henkin, J. (1990) "The growth factor domains of both tissue plasminogen activator and urokinase contain a novel fucosylation at a homologous threonine residue." Molecular Biology of Plasminogen Activators, Florence, Italy.

Rabbani, S.A., Mazar, A., Bolivar, I., Henkin, J. and Goltzman, D. (1991) "The amino terminal fragment (ATF) of uPA is generated by PC-3 cells in culture and is mitogenic in osteoblastic cells." Molecular and Cellular Biology of Plasminogen Activators, Elsinore, Denmark.

Rabbani, S.A., Mazar, A., Bolivar, I., Henkin, J. and Goltzman, D. (1991) "Characteristics of the production of urokinase and its fragments by several cell lines and its preferential action in osteoblastic cells." Meeting of the American Society for Bone and Mineral Research, San Diego, California.

Ho, Y-K., Goldin, S., Mazar, A. and Falco, W (1991) "Functional role of oligomeric transducin." Invest. Ophthalmol. Visual Sci. 32: 1052.

Howell, A.L., Hunt, J.A., Mazar, A., Henkin, J. and Zacharski, L.R. (1992) "Anti-proliferative effect of urokinase (uPA) and uPA fragments on myeloid leukemia cells (HL-60)." The American Society for Hematology 34th Annual Meeting, Boston, Massachusetts.

Novokhatny, V., Medved, L., Mazar, A. and Ingham, K. (1992) "Effect of synthetic inhibitors on the domain structure and stability of the serine protease module of urokinase." Biophys. J. 61 Part 2: A324.

Petros, A.M., Hansen, A.P., Mazar, A.P., Xu, R.X. and Fesik, S.W. (1993) "NMR studies on the structure of the amino terminal fragment of urokinase." Molecular and Cellular Biology of Plasminogen Activation, Cold Spring Harbor, New York, #184.

Rabbani, S.A., Gladu, J., Mazar, A., Henkin, J. and Goltzman, D. (1993) "Amino terminal fragment of urokinase induces c-fos expression in human osteoblasts." Molecular and Cellular Biology of Plasminogen Activation, Cold Spring Harbor, New York, #3.

Achbarou, A., Kaiser, S., Tremblay, G., Mazar, A., Davidson, D., Weitzberg, M., Henkin, J., Goltzman, D. and Rabbani, S.A. (1993) "A homologous rat model for tumor metastasis results in increased skeletal metastasis by prostate cancer cells overexpressing urokinase." Molecular and Cellular Biology of Plasminogen Activation, Cold Spring Harbor, New York, #21.

Rabbani, S.A., Mazar, A., Henkin, J. and Goltzman, D. (1993) "Expression of uPA, uPAR and matrilysin by various human tumor cell lines in vitro: Correlation with the production of ATF 1-143." Molecular and Cellular Biology of Plasminogen Activation, Cold Spring Harbor, New York, #58.

Smith, R.A., Matayoshi, E., Mazar, A., Henkin, J. and Holzman, T.F. (1993) "Hydrodynamic, fluorescence polarization and kinetic studies on the activation of recombinant plasminogen activators." Molecular and Cellular Biology of Plasminogen Activation, Cold Spring Harbor, New York, #159.

Hansen, A.P, Petros, A.M., Mazar, A.P., Pederson, T.M., Rueter, A. and Fesik, S.W. (1993) "A practical method for the uniform labeling of recombinant proteins in mammalian cells." J. Cell. Biochem. Vol. 0, No. 17 Part C: p. 253.

Khodjasteh, Z.F., Mercer, L.J., Obernesser, M., Verrusio, E.N. and Mazar, A. (1994) "The plasminogen activators/ inhibitors in peritoneal fluid of patients with endometriosis." XIIth International Congress on Fibrinolysis, Belgium.

Khodjasteh, Z.F., Mercer, L.J., Obernesser, M. and Mazar, A. (1994) "Tissue type plasminogen activator and its inhibitor in the peritoneal fluid of patients with and without endometriosis at different phases of the menstrual cycle." XIIth International Congress on Fibrinolysis, Belgium.

Schnaper, H. William, Mazar, A., Barnathan, E. and Kleinman, H.K. (1994) "Urokinase-type plasminogen activator enhances endothelial cell differentiation through a non-proteolytic mechanism involving uPA receptor binding."" Pediatric Research 35, No. 4 Part 2: 373A.

Liu, D.F., Davidson, D., Achbarou, A., Mazar, A., Henkin, J. and Rabbani, S.A. (1994) "Rat prostate MatLyLu cells overexpressing rat uPA metastasized in a syngeneic rat model." Proc. American Association for Cancer Research, #35.

Manupello, J., Zhou, W., Mazar, A., Wang, J., Quan, N., Reilly, R., Henkin, J., Higazi, A.A-R. and Cines, D.B. (1996) "Epitope mapping of monoclonal antibodies (MA) to the human urokinase receptor (CD87)" Tissue Antigens 48(4-2): 368.

Higazi, A.A-R., Mazar, A., Wang, J., Reilly, R., Henkin, J., Kniss, D. and Cines, D. (1996) "Single chain urokinase type plasminogen activator bound to its receptor is relatively resistant to plasminogen activator inhibitor type 1." Fibrinolysis 10(3): #92.

Crosby, S.D., Mazar, A.P., Henkin, J. and Okasinski, G.F. (1996) "SPR detection of Low Molecular Weight analytes." 6th Annual North American BIA Symposium.

Colman, R.W., Pixley, R.A., Najamunnisa, S., Yan, W., Wang, J., Mazar, A. and McCrae, K. (1996) "High molecular weight kininogen binds to the vitronectin binding domain(s) on the urokinase receptor." Circulation 94(8): I42-I43.

Wang, J., Mazar, A., Quan, N., Schneider, A. and Henkin, J. (1997) "Plasminogen activation by pro-urokinase in complex with its receptor: dependence on a tripeptide (Spectrozyme plasmin)." Proc. American Association for Cancer Research, #38:2756.

Xing, R., Henkin, J., Mazar, A.P. and Rabbani, S.A. (1997) "Prevention of breast cancer growth, invasion and metastasis by a urokinase inhibitor B-428 alone or in combination with anti-estrogen Tamoxifen." Proc. American Association for Cancer Research, #38:2760.

Ennis, B.W., Mazar, A.P., Davidson, D., Quan, N., Henkin, J. and Rabbani, S.A. (1997) "Overexpression of uPA by the MatLyLu rat prostatic cancer cell line results in enhanced tumor angiogenesis." Proc. American Association for Cancer Research, #38:3518.

Xing, R.H., Mazar, A., Henkin, J. and Rabbani, S. (1997) "Role of urokinase (uPA) and its receptor (uPAR) in breast cancer growth, invasion and metastasis: potential therapeutic strategies." Fibrinolysis and Proteolysis 11(3): 28.

Colman, R.W., Pixley, R.A., Najamunnisa, S., Yan, W., Wang, J., Mazar, A. and McCrae, K.R. (1997) "Binding of high molecular weight kininogen to human endothelial cells is mediated via a site within domains 2+3 of the urokinase receptor." Fibrinolysis and Proteolysis 11(3): 36.

Mazar, A. and Jones, T. (1999) "High-affinity, small cyclic peptide ligands localize reporter and therapeutic conjugates to the surfaces of tumor cells and stimulated endothelial cells." Proc. American Association for Cancer Research, #40:146.

Guo, Y.J., Arakelian, A., Kwaan, H., Jones, T.R., Mazar, A.P. and Rabbani, S.A. (1999) "An 8-mer peptide derived from the non-receptor binding region of urokinase plasminogen activator inhibits breast cancer growth and metastasis through the induction of apoptosis in vivo." Proc. American Association for Cancer Research, #40:3431.

Guo, Y.J., Mazar, A.P. and Rabbani, S.A. (1999) "Combination therapy with TAM and an inhibitor of invasion and angiogenesis (Å6) leads to significant inhibition of hormone-dependent breast cancer cell growth in vivo" Clin. Cancer Res. 5 (11): 3741s.

Al-Atrash, G., Kitson, R.P., Kim, M.H., Mazar, A.P. and Goldfarb, R.H. (2000) "Urokinase Plasminogen Activator and its receptor in NK cells: contribution to extracellular matrix degradation and impact on NK cell accumulation into cancer metastases." FASEB J 14 (supp. 6): A1024.

Zhang, J-C., Juarez, J., Shaw, D.E., Mazar, A.P. and McCrae, K.R. (2000) "Peptides derived from high molecular weight kininogen (HK) domains 3 and 5 inhibit endothelial cells proliferation and induce endothelial cell apoptosis." Proc. American Society for Hematology.

Rabbani, S.A., Gladu, J. and Mazar, A.P. (2001) "Induction of c-fos oncogene in human osteosarcoma cells (SaOS2) by urokinase (uPA) via the Ras-Raf-MAPK signaling pathway." Proc. American Association for Cancer Research, #42:72.

Al-Atrash, G., Kitson, R.P., Xue, Y., Mazar, A.P., Kim, M.H., Goldfarb, R.H. (2001) "uPA and uPAR contribute to NK cell invasion through the extracellular matrix: co-operation of uPA/uPAR and matrix metalloproteinases in NK cell invasion." Proc. American Association for Cancer Research, #42:5090.

Stoeltzing, O., Liu, W., Reinmuth, N., Fan, F., Livant, D.L., Mazar, A.P. and Ellis, L.M. (2001) "Reduction of colon cancer growth by a novel antiangiogenic agent that targets the integrin $\alpha_5\beta_1$." Clin. Cancer Res. 7(11, suppl.): 3656s.

Higazi, A.A-R., Nassar, T., Akkawi, S., Kuo, A., Bdeir, K., Mazar, A. and Cines, D.B. (2002) "Urokinase plasminogen activator is a link between fibrinolysis and vascular smooth muscle cell contraction." Blood 100: 2728.

Stoeltzing, O., Liu, W., F. Fan, Reinmuth, N., Parikh, A.A., Mazar, A.P. and Ellis, L.M. (2002) "Combination of a novel anti-angiogenic agent that targets the integrin $\alpha_5\beta_1$ with continuous 5-FU infusion reduces metastases formation in a murine model of colorectal hepatic metastases." Ann. Surg. Onc. 9 (Suppl.): S35.

Plunkett, M.L., Tel-Tsur, Z., Bera, M., Beck, I., Avery, J., Livant, D.L., Mazar, A.P. (2002) "A novel anti-angiogenic/anti-metastatic peptide, ATN-161 (Ac-PHSCN-NH2), which targets multiple fully activated integrins including alpha-5 beta-1 and alpha-v beta-3, leads to increased anti-tumor activity and increased survival in multiple tumor models when combined with chemotherapy." European Journal of Cancer 38, (Suppl. 7): 79.

Parry, G.C., Plunkett, M.L., Tarui, T., Takada, Y., Tel-Tsur, Z., Truong, F., Mazar, A.P. (2002) "Development of monoclonal antibodies targeting the uPA system for diagnosis and therapy." European Journal of Cancer 38 (Suppl. 7): 151.

M.L. Plunkett and Mazar, A.P. (2002) "Dose and schedule optimization of a novel anti-angiogenic/anti-metastatic peptide, ATN-161 (Ac-PHSCN-NH2), which targets multiple fully activated integrins including alpha-5 beta-1 and alpha-v beta-3." European Journal of Cancer 38 (Suppl. 7): 82.

Doñate, F., Juarez, J.C., Guan X., Hopkins, S.A., Yoon, W.H., O'Hare, S.M., Gladstone, P.L., Price, M.L., Allan, A.K., Ternansky, R.J., Mazar, A.P. (2002) "Minimization of the anti-angiogenic Histidine-Proline Rich Glycoprotein (HPRG) protein." European Journal of Cancer 38 (Suppl. 7): 79.

Plunkett, M.L., Beck, I., Avery, A.J., Tel-Tsur, Z., Yu, M., Livant, D., Arimura, J., Truong, F. and Mazar, A.P. (2003) "Combining low dose chemotherapy with low dose anti-angiogenic agents (ATN-161 and ATN-224) leads to increased anti-tumor activity in prostate cancer xenograft models." Proc. American Association of Cancer Research, #44:3730.

Doñate, F., Guan, X., Callahan, J.A., Mazar, A.P. and Parry, G.C. (2003) "ATN-161 (Ac-PHSCN-$NH_2$) has potent anti-angiogenic activity through multiple mechanisms of action and localizes to newly formed blood vessels in vivo." Proc. American Association of Cancer Research, #44:63.

Hensley, H.H. and Mazar, A.P. (2003) "Evaluation of the anti-angiogenic agent ATN-161 by dynamic magnetic resonance imaging in a mouse model." Proc. American Association of Cancer Research, #44:59.

Rabbani, S.A., Khalili, P. and Mazar, A.P. (2003) "A non-RGD based integrin binding peptide (ATN-161) that targets activated alpha-5 beta-1 and alpha-v beta-3 blocks the development of osteolytic skeletal metastases in a xenograft model of breast cancer." Clin. Cancer Res. 9 (Suppl.): 6181S.

Parry, G.C., Callahan, J.A., Truong, F., Tel-Tsur, Z., Plunkett, M.L. and Mazar, A.P. (2003) "Evaluation of monoclonal antibodies targeting the uPA system for internalization and delivery of cytotoxic agents." Clin. Cancer Res. 9 (Suppl.): 6195 Clin. Cancer Res. 9 (Suppl.): 6181S S.

Khalili, P., Plunkett, M., Beck, I., Arimura, J., Mazar, A. and Rabbani, S. (2004) "Regression of primary breast tumor and blockage of osteolytic skeletal metastasis by a non-RGD based integrin binding peptide (ATN-161) targeting$\alpha_5\beta_1$ and$\alpha_v\beta_3$ in a xenograft model of breast cancer." Proc. American Association for Cancer Research #45: 4001.

Betancourt, O., Donate, F., Guan, X., Shaw, D.E., Mazar, A., and Pirie-Shepherd, S. (2004) "Inhibition of cytosolic superoxide dismutase (SOD1) in endothelial cells: a possible mechanism for the antiangiogenic properties of the copper depleting drug ATN-224." Eur. J. Cancer 2: 49.

Juarez, J.C., Betancourt, O., Pirie-Shepherd, S., Au, J.L.-S., Mazar, A.P. and Donate, F. (2005) "Inhibition of CuZn superoxide dismutase (SOD1) in tumor cells by the copper binder tetrathiomolybdate (ATN-224) leads to apoptosis and cell death." Proc. AACR 46: 1388 (Abstract #5897).

Callahan, J.A., Beck, I., Bauer, T.W., Ellis, L.M., Mazar, A.P. and Parry, G.C. (2005) "*In vitro* and *in vivo* characterization of a monoclonal antibody, ATN-658, targeting the uPA system." Proc. AACR 46: 1454 (Abstract #6179).

Parry, G.C., Beck, I., Callahan, J.A. and Mazar, A.P. (2005) "Inhibition of uPA binding to uPAR by monoclonal antibodies prevents tumor cell migration *in vitro* and tumor growth *in vivo*." Thromb. And Haemost. 93: A27.

Danese, S., Sans, M., Spencer, D., Beck, I., Donate, F., Plunkett, M., Campbell, M., West, G.A., Redline, R., Gasbarrini, A., Mazar, A., de la Motte, C., Levine, A.D. and Fiocchi, C. (2005). "Starving the inflamed gut: Angiogenesis blockade as a novel therapeutic approach to experimental colitis." Gastroenterology 128 (4, supp. 2): 289.

Juarez, J.C., Manuia, M.M., Betancourt, O., Mazar, A.P. and Donate, F. (2006). "The inhibition of CuZn superoxide dismutase (SOD1) by ATN-224, a second generation tetrathiomolybdate, interferes with multiple signaling pathways in tumor and endothelial cells in vitro." Proc. AACR 47: 4687.

Campbell, R.A.,Gordon, M.S., Betancourt, O., Juarez, J., Donate, F., Mazar, A. and Berenson, J.R. (2006). "ATN-224, an orally available small molecule inhibitor of SOD1, inhibits multiple signaling pathways associated with myeloma progression and has antitumor activity in a murine model of refractory myeloma growth." Proc. AACR 47: 4859.

S. A. Lowndes, A. Adams, A. Timms, M. Middleton, C. Hayward, S. D. Reich, A. P. Mazar, A. L. Harris (2006) "Phase I study of ATN-224 in patients (pts) with advanced solid tumours." J. Clin Oncology, 2006 Part I. Vol 24, No. 18S (June 20 Supp).

Donate, F., Juarez, J., Maunia, M., Burnett, M., Trapp, V., Fruhauf, J., and Mazar, A. (2006) "SOD1 inhibition by tetrathiomolybdate demonstrates differential sensitivity against melanoma cell lines in vitro and in vivo: a possible method for identifying patients most likely to benefit from the second generation tetrathiomolybdatye, ATN-224." Eur. J. Cancer 4: 126.

Donate, F., Lowndes, S., Juarez, J., Maunia, M., Smith, E., Liu, N., Hayward, C., Batuman, O., Harris, A. and Mazar, A. (2006) "Translation of in vitro markers of the SOD1 inhibitor ATN-224 to clinical trials." Eur. J. Cancer 4: 43.

---

## PATENTS AND INVENTIONS

### ISSUED PATENTS

Mazar, A.P. and Jones, T.R. "Anti-invasive and anti-angiogenic compositions and methods." US5994309.

Mazar, A.P. and Jones, T.R. "Anti-invasive and anti-angiogenic compositions and methods." US6696416.

Mazar, A.P. and Jones, T.R. "Anti-invasive and anti-angiogenic compositions and methods." Australian 752205

Mazar, A.P. and Jones, T.R. "Cyclic peptides targeting the urokinase receptor." US6277818.

Mazar, A.P. and Jones, T.R. "Cyclic peptides targeting the urokinase receptor." EP1144604.

Doñate, F. and Mazar, A.P. "Human Kininogen D3 domain polypeptide as an anti-angiogenic and anti-tumor agent." US 7,098,187.

### PATENT APPLICATIONS

Mazar, A.P. and Jones, T.R. "Anti-invasive and anti-angiogenic compositions and methods." US20030027768.

Mazar, A.P. and Jones, T.R. "Anti-invasive and anti-angiogenic compositions and methods." EP00950096A1.

Mazar, A.P. and Jones, T.R. "Anti-invasive and anti-angiogenic compositions and methods for treating brain tumors and other diseases." WO02069885A2.

Mazar, A.P. and Jones, T.R. "Diagnostic probes and therapeutics targeting uPA and uPAR." EP1218496A2.

Mazar, A.P., Varga, J. and Jones, T.R. "Chimaeric uPAR-targeting cyclic peptide therapeutic and diagnostic compositions and methods." WO 00026353A1.

Mazar, A.P. and Jones, T.R. "Diagnostic probes and therapeutics targeting uPA and uPAR", WO 00125410A2.

Mazar, A.P. and Jones, T.R. "Anti-invasive and anti-angiogenic compositions and methods for treating brain tumors and other diseases." WO 02069885.

Juarez, J.C. and Mazar, A.P. "Human kininogen D5 polypeptides." WO 0214369 (PCT/US01/23185).

Juarez, J.C. and Mazar, A.P. "Human kininogen D5 polypeptides." EP1305342A2.

Doñate, F., Harris, S., Plunkett, M.L. and Mazar, A.P. "Histidine proline rich glycoprotein (HPRG) as an anti-angiogenic and anti-tumor agent." WO 02064621.

Juarez, J.C., Mazar, A.P., McCrae, K.M., Guan, X. and Doñate, F. "Cell surface tropomyosin as a target of angiogenesis inhibition." WO03077872A2.

Allan, A.L., Doñate, F., Hopkins, S.A., Gladstone, P., Mazar, A.P., O'Hare, S.M., Parry, G., Plunkett, M., Ternansky, R.J. and Yoon, W.H. "Peptides which inhibit angiogenesis, cell migration, cell invasion and cell proliferation-compositions and uses thereof." 60/429,174.

Allan, A.L., Donate, F., Hopkins, S.A., Gladstone, P., Mazar, A.P., O'Hare, S.M., Parry, G., Plunkett, M., Ternansky, R.J. and Yoon, W.H. "Peptides which inhibit angiogenesis, cell migration, cell invasion and cell

proliferation-compositions and uses thereof." 60/475,539.

Allan, A.L., Doñate, F., Hopkins, S.A., Gladstone, P., Mazar, A.P., O'Hare, S.M., Parry, G., Plunkett, M., Ternansky, R.J. and Yoon, W.H. "Peptides which inhibit angiogenesis, cell migration, cell invasion and cell proliferation-compositions and uses thereof." 10/723,144.

Allan, A.L., Doñate, F., Hopkins, S.A., Gladstone, P., Mazar, A.P., O'Hare, S.M., Parry, G., Plunkett, M., Ternansky, R.J. and Yoon, W.H. "Peptides which inhibit angiogenesis, cell migration, cell invasion and cell proliferation-compositions and uses thereof." PCT/US03/38175.

Ternansky, R.J., Gladstone, P.L., Allan, A.L., Price, M.L.P. and Mazar, A.P. "Thiotungstate analogs and uses thereof." US 60/473, 937.

Ternansky, R.J., Mazar, A.P., Pirie-Shepherd, S.R., Coucouvanis, D., Gladstone, P.L., Allan, A.L., O'Hare, S.M., Price, M.L.P. and Doñate, F. "Thiomolybdate analogs and uses thereof." 60/434,742.

Ternansky, R.J., Mazar, A.P., Pirie-Shepherd, S.R., Coucouvanis, D., Gladstone, P.L., Allan, A.L., O'Hare, S.M., Price, M.L.P. and Doñate, F. "Thiomolybdate analogs and uses thereof." 10/436,958.

Ternansky, R.J., Mazar, A.P., Pirie-Shepherd, S.R., Coucouvanis, D., Gladstone, P.L., Allan, A.L., O'Hare, S.M., Price, M.L.P. and Doñate, F. "Thiomolybdate analogs and uses thereof." 10/447,585.

Ternansky, R.J., Mazar, A.P., Pirie-Shepherd, S.R., Coucouvanis, D., Gladstone, P.L., Allan, A.L., O'Hare, S.M., Price, M.L.P. and Doñate, F. "Thiomolybdate analogs and uses thereof." WO 04009034A2.

Allan, A.L., Yoon, W.H., Gladstone, P.L., Ternansky, R.J., Parry, G., Doñate, F. and Mazar, A.P. "Peptides which target tumor and endothelial cells: compositions and uses thereof." PCT/US03/37895.

Parry, G.C., Gladstone, P., Ternansky, R.J., Gawlak, S. and Mazar, A.P. "Antibodies and/or conjugates thereof which bind to the amino terminal fragment of urokinase, compositions and uses thereof." 60/523,255.

Pirie-Shepherd, S., Mazar, A.P. and Betancourt, O. "Inhibition of Superoxide Dismutase by Tetrathiomolybdate: Identification of New Anti-angiogenic and Antitumor agents." Filed 2004.

Parry, G.C., Gawlak, S., Callahan, J. and Mazar, A.P. "Ligands Binding the Complex of Urokinase-type Plasminogen Activator (uPA) and its Receptor (uPAR) That Inhibit Downstream uPAR Interactions: Identification and Use in Diagnosis or Therapy." Filed 2004.

Mazar, A.P., Heiati, H., Schrier, J., Li, M., and Harris, S. "Improved formulations of anti-angiogenic compounds." US APP. 60/648, 391.

Donate, F. and Mazar, A.P. "Identification of Novel Protein Targets on the Surface of Stressed Cells" US APP 60/728,757.

Ternansky, R.J., Gladstone, P., Mazar, A.P. and Allan, A.L. "Acid addition salts of Ac-PHSCN-$NH_2$." US APP 60/649, 308.

Danese, S., Fiocchi, C., and Mazar, A.P. "Treatment of Inflammatory Bowel Disease (IBD) With Anti-Angiogenic Compounds." US APP 60/679, 977.

Huang, M., Huai, Q., Parry, G.C., Mazar, A.P., and Cines, D. "Crystal Structure of Human uPA ATF Bound to its Receptor." US APP 60/722, 402.

Mazar, A.P. "Antibodies to Urokinase-Type Plasminogen Activator Receptor (uPAR) Bind Cancer Stem Cells: Use in Diagnosis and Therapy." Filed June, 2006

Price, M., Ternansky, R. and Mazar, A.P. "Methods and Compositions for Increasing Bioavailability of

Thiomolybdate and Thiotungstate Compounds." Filed June 2006

# Inhibition of endothelial cell survival and angiogenesis by protein kinase A

See the related Commentary beginning on page 913.

Semi Kim, Manjiri Bakre, Hong Yin, and Judith A. Varner

University of California, San Diego Comprehensive Cancer Center, La Jolla, California, USA

**Receptors for the provisional ECM are important regulators of angiogenesis. One of these receptors, integrin α5β1, plays a critical role in tumor- and growth factor–induced angiogenesis, because antagonists of this integrin potently inhibit angiogenesis and tumor growth. Here we show that the integrin α5β1 promotes endothelial cell survival during angiogenesis in vivo by suppressing the activity of protein kinase A (PKA). Antagonists of integrin α5β1 activate PKA, which then leads to the activation of caspase-8 and induction of apoptosis. Direct activation of PKA by cAMP or by expression of the PKA catalytic subunit also induces endothelial cell apoptosis, resulting in angiogenesis inhibition in vivo. Our studies indicate that ligation of integrin α5β1 during angiogenesis suppresses an apoptotic program that is dependent on PKA. These studies also indicate that induction of endothelial cell apoptosis in vivo by genetic or pharmacological activation of PKA may be a useful strategy to inhibit angiogenesis.**

*J. Clin. Invest.* **110**:933–941 (2002). doi:10.1172/JCI200214268.

## Introduction

New blood vessels develop from preexisting vessels (1) or from circulating endothelial progenitor cells (2) in response to growth factors and/or hypoxic conditions (angiogenesis). Angiogenesis promotes embryonic development, wound healing, and the female reproductive cycle (1), as well as solid tumor cancer, neovascular eye disease, psoriasis, and rheumatoid arthritis (1). While growth factors are required to elicit new blood vessel growth, adhesion to provisional ECM proteins such as fibronectin, vitronectin, and fibrinogen is required for endothelial cell survival, proliferation, and motility during new blood vessel growth (3–8).

The integrin family of ECM receptors mediates not only cellular adhesion to and migration on the ECM proteins found in intercellular spaces and basement membranes, but also cell survival (9–19). Prevention of cell attachment to the ECM induces a form of apoptosis termed anoikis in primary cells and some tumor cells (9–19). However, some integrin antagonists can also suppress cell survival in cells that are still attached to the ECM by other adhesion proteins. For example, antagonists of the integrin αvβ3 inhibit angiogenesis in vivo, even though endothelial cells remain attached to the ECM through integrins α5β1 and αvβ5 (4, 6). Similarly, unligated integrin α5β1 inhibits tumor cell survival and proliferation in vitro and in vivo, even when tumor cells adhere to the ECM through other integrins (20–22). Thus, integrins play key roles in the regulation of cellular survival.

Integrins also regulate vascular development and angiogenesis (4, 6–16). Antagonists of integrin αvβ3 inhibit tumor angiogenesis and growth by causing endothelial cells in tumors, but not in normal tissues, to die (4, 6). Fibronectin and its receptor integrin α5β1 also regulate angiogenesis (17). Integrin α5β1 expression is upregulated on human tumor vasculature in many tumors and in healing wounds (17–18). Growth factor and tumor-induced angiogenesis, as well as tumor growth, are inhibited by antagonists of α5β1 (Ab's, cyclic peptides, and small organic molecules) and by Ab antagonists of fibronectin, the major ligand for α5β1 (17, 19). Loss of the gene encoding the α5 subunit is also embryonic lethal and is associated with vascular and cardiac defects (23–25). Integrin α5β1 thus plays a vital role in angiogenesis.

The mechanisms whereby integrin α5β1 antagonists block angiogenesis are unknown. We show here that antagonists of α5β1 inhibit endothelial cell survival in vitro and in vivo without affecting cell attachment to the ECM. Perturbing α5β1 ligation activates cAMP-dependent kinase, protein kinase A (PKA), which then activates an initiator (caspase-8), but not a stress-mediated (caspase-9) apoptotic pathway. Integrin α5β1 antagonists thereby suppress cell survival in vitro and during angiogenesis in vivo in a PKA-dependent manner. These studies reveal a novel and important mechanism whereby integrin antagonists induce cell apoptosis and regulate key in vivo processes such as angiogenesis.

*Received for publication September 21, 2001, and accepted in revised form July 30, 2002.*

**Address correspondence to:** Judith A. Varner, University of California, San Diego Cancer Center, 9500 Gilman Drive, La Jolla, California 92093-0912, USA. Phone: (858) 822-0086; Fax: (858) 822-1325; E-mail: jvarner@ucsd.edu.

**Conflict of interest:** No conflict of interest has been declared.

**Nonstandard abbreviations used:** protein kinase A (PKA); green fluorescent protein (GFP); poly (ADP ribose) polymerase (PARP); human umbilical vein endothelial cell (HUVEC); endothelial basal medium (EBM); defined endothelial growth medium-2 (EGM-2); endothelial growth medium (EGM); PKA catalytic ($PKA_{cat}$); mutationally inactive PKA (dnPKA); 4′,6-diamidine-2-phenylindole dihydrochloride (DAPI); chick chorioallantoic membrane (CAM); integrin-mediated death (IMD).

## Methods

*General.* Anti-α5β1 and anti-α2β1 were from Chemicon International (Temecula, California, USA). Anti-αvβ3, anti-MHC, and N1-green fluorescent protein (N1-GFP) vector were from David Cheresh (The Scripps Research Institute, La Jolla, California, USA). Anti-caspase Ab's were from New England Biolabs Inc. (Beverly, Massachusetts, USA). Anti-poly (ADP ribose) polymerase (PARP) and FITC-annexin V were from PharMingen (San Diego, California, USA). Fibronectin and collagen I were from Collaborative Biomedical Products (Bedford, Massachusetts, USA). Vitronectin was purified from outdated human plasma by denaturing heparin-Sepharose chromatography as described (26). Poly-L-lysine was from Sigma-Aldrich (St. Louis, Missouri, USA). HA1004 was obtained from Biomol Research Laboratories (Plymouth Meeting, Pennsylvania, USA). Caspase inhibitors and activity assays were from Calbiochem-Novabiochem Corp. (La Jolla, California, USA). Ten-day-old chicken embryos were from McIntyre Poultry (Ramona, California, USA), and bFGF was from Genzyme Pharmaceuticals (Cambridge, Massachusetts, USA). Human umbilical vein endothelial cells (HUVECs), endothelial basal medium (EBM), defined endothelial growth medium-2 (EGM-2) (EBM + bFGF, VEGF, and no serum), and endothelial growth medium (EGM) (EBM + bFGF, VEGF, and 2% serum) were from Clonetics Corp. (San Diego, California, USA). PKA catalytic ($PKA_{cat}$) and mutationally inactive (*dnPKA*) cDNAs were from Susan Taylor and Renate Pilz (University of California, San Diego, California, USA), respectively. The cDNAs were subcloned into topoTA-pcDNA 3.1 V5/His according to manufacturer's directions (Invitrogen Corp., Carlsbad, California, USA). HUVECs were cultured in EGM. All statistical analyses were performed using the Student *t* test.

*Annexin V-FITC staining.* Culture plates were coated with 10 μg/ml of fibronectin, vitronectin, collagen, or poly-L-lysine at 4°C for 16 hours and blocked with denatured BSA. Plates were also coated with 25 μg/ml goat anti-mouse IgG (Southern Biotechnology Associates Inc., Birmingham, Alabama, USA) at 37°C for 2 hours, rinsed, blocked with denatured BSA, and then incubated with 10 μg/ml anti-α5β1 or control IgG (anti-MHC) at 4°C for 16 hours. HUVECs were incubated on plates in the presence or absence of 10 μg/ml anti-α5β1, anti-αvβ3, anti-α2β1, or isotype-matched anti-MHC in defined endothelial growth medium containing bFGF and VEGF for 0–24 hours. In some experiments, HUVECs were incubated with Ab's and 100 μM caspase-3, -8, or -9 inhibitors or vehicle control (0.5% DMSO). Cells were then incubated with FITC-annexin V for 15 minutes at room temperature in the dark. Washed cells were fixed in 1% paraformaldehyde, then incubated in 4′,6-diamidine-2-phenylindole dihydrochloride (DAPI). The percentage of annexin-positive cells in five microscopic fields was determined at ×200 magnification by fluorescence microscopy.

*Apoptosis assays.* HUVECs were incubated on ECM or Ab-coated plates for 0–24 hours. DNA fragmentation was detected by agarose gel electrophoresis as described (27). Alternatively, HUVECS on plates were lyzed with RIPA buffer (100 mM Tris, pH 7.2, 150 mM NaCl, 1% deoxycholate; 1% Triton X-100, 0.1% SDS) (19) on ice. Lysates were electrophoresed on 8% SDS-PAGE gels and immunoblotted with anti-PARP, -caspase-3, -caspase-9, -cleaved caspase-3, or -cleaved caspase-9 Ab's. Immunoreactive bands were identified by chemiluminescence and quantified by densitometry. Caspase-3 and -8 activities were determined in cell lysates according to manufacturer's instructions (Calbiochem-Novabiochem Corp.).

*Role of PKA in cell survival.* HUVECs were plated for 24 hours on ECM protein–coated plates in the presence of anti-αvβ3 or anti-α5β1, 1 μM HA1004 (a PKA inhibitor), and anti-αvβ3 or anti-α5β1 with 1 μM HA1004. Cells were stained with FITC-annexin V or immunoblotted with anti-cleaved caspase-3 Ab's as described above. HUVECs ($5 \times 10^6$) were electroporated in 300 μl of EGM with 30 μg of DNA (20 μg *dnPKA* or $PKA_{cat}$ plasmids, 2 μg *N1-GFP*, and 8 μg pBluescript) at 300 V, 450 μF, as described previously (28). Expression of transgenes was determined by Western blotting of cell lysates with anti-V5 and anti-GFP Ab's. Transfection efficiency was quantified by determining the percentage of cells that were cotransfected with GFP expression vectors. Eighty percent transfection efficiency was generally achieved using this electroporation method.

*Chick chorioallantoic membrane angiogenesis assay.* Chick chorioallantoic membrane (CAM) assays were performed as described (17). Saline or bFGF-stimulated CAMs were treated for 24 hours with 20 μg anti-α5β1, anti-αvβ3, or control Ab's and then injected intravenously with 50 μl annexin V-FITC. CAMs were harvested after 2 hours, then analyzed by confocal microscopy. Alternatively, CAMs treated as above were excised, minced on ice, and treated with 0.1% dispase/0.1% collagenase for 1 hour at 37°C. Single-cell suspensions were incubated with FITC-annexin V and analyzed as described above. The bFGF-stimulated CAMs were also treated with anti-α5β1 or anti-αvβ3 in the presence or absence of 500 μM caspase-3, -8 or -9 inhibitors. The bFGF-stimulated CAMs were also transfected with 4 μg *N1-GFP*, *dnPKA*, or $PKA_{cat}$ expression plasmids. Freshly excised CAMs were homogenized in ice-cold RIPA buffer containing protease inhibitors and immunoblotted to detect intact and cleaved caspase-3 or -8. For all treatment groups, $n = 10$. CAMs were fixed with 3.7% paraformaldehyde prior to excision. The average number of blood vessel branch points per treatment group plus or minus SEM is presented. Some excised CAMs were cryopreserved, cut into 5-μm sections, immunostained with anti-cleaved caspase-3, anti-cleaved caspase-8, and anti-vFW Ab's (to detect blood vessels). CAMs were also stained by the TUNEL method to detect fragmented DNA.

## Results

*Integrin α5β1 promotes endothelial cell survival in vitro and in vivo.* Antagonists of α5β1 and fibronectin inhibit

growth factor and tumor-induced angiogenesis (17, 19). Because integrins have been shown to promote cell survival, we examined the roles of α5β1 and fibronectin in endothelial cell survival. Endothelial cells (HUVECs) cultured on poly-L-lysine (which mediates nonspecific cell attachment to the substratum) and fibronectin substrates were analyzed for the binding of annexin V, a $Ca^{2+}$-dependent phospholipid-binding protein that binds to apoptotic cells with exposed phosphatidyl serine (29). HUVECs attached to fibronectin bind little annexin V, whereas over 85% of cells on poly-L-lysine-coated plates bound annexin V (Figure 1a, $P = 0.01$). Additionally, lysates from HUVECs cultured in suspension or on poly-L-lysine and fibronectin were immunoblotted for PARP, an enzyme involved in DNA repair that is cleaved by caspase-3 during the early stages of apoptosis to produce 85-kDa and 2-kDa fragments, resulting in loss of normal PARP function (30, 31). Cells in suspension or attached to poly-L-lysine displayed significant PARP cleavage, while cells attached to fibronectin showed little PARP cleavage (Figure 1b, $P = 0.006$). Similarly, attachment to fibronectin, but not poly-L-lysine, protects HUVECs from DNA fragmentation associated with apoptosis (Figure 1c, $P = 0.0001$). These studies indicate that fibronectin attachment promotes the survival of proliferating endothelial cells.

To determine if integrin α5β1 is the fibronectin receptor supporting HUVEC survival in vitro, HUVECs were cultured on surfaces coated with anti-α5β1 or control Ab's. Immobilized anti-integrin Ab's cluster integrins, thereby acting as agonists (6, 32). Cells attached to surfaces coated with Ab's directed against α5β1 bound little annexin (Figure 1d, $P = 0.001$) and thus remained viable. In contrast, more than 75% of cells attached to control Ab's were annexin positive. Cells attached to α5β1 Ab-coated surfaces also showed significantly less PARP cleavage (Figure 1e, $P = 0.007$) and DNA fragmentation (Figure 1f, $P = 0.003$) than cells attached to control Ab's. These results indicate that α5β1 promotes endothelial cell survival.

Antagonists of integrin α5β1 block angiogenesis in vivo but have no effect on unstimulated blood vessels (17). To determine if these antagonists induce endothelial cell apoptosis during angiogenesis in vivo, CAMs were stimulated with bFGF, treated with saline, function-blocking anti-α5β1 Ab's, and isotype-matched control Ab's, and then analyzed for markers of apoptosis. Intravenous injection of fluorescently labeled annexin V demonstrated that α5β1 antagonists induce endothelial cell apoptosis in vivo. Anti-α5β1 Ab's, but not saline or control Ab's, induced annexin V staining of blood vessels in living CAMs, indicating that α5β1 regulates survival in vivo of proliferating endothelial cells (Figure 2a). In fact, vessels in anti-α5β1-treated CAMs bound eight times more annexin V than control-treated CAMs (Figure 2b, $P = 0.015$). These anti-α5β1

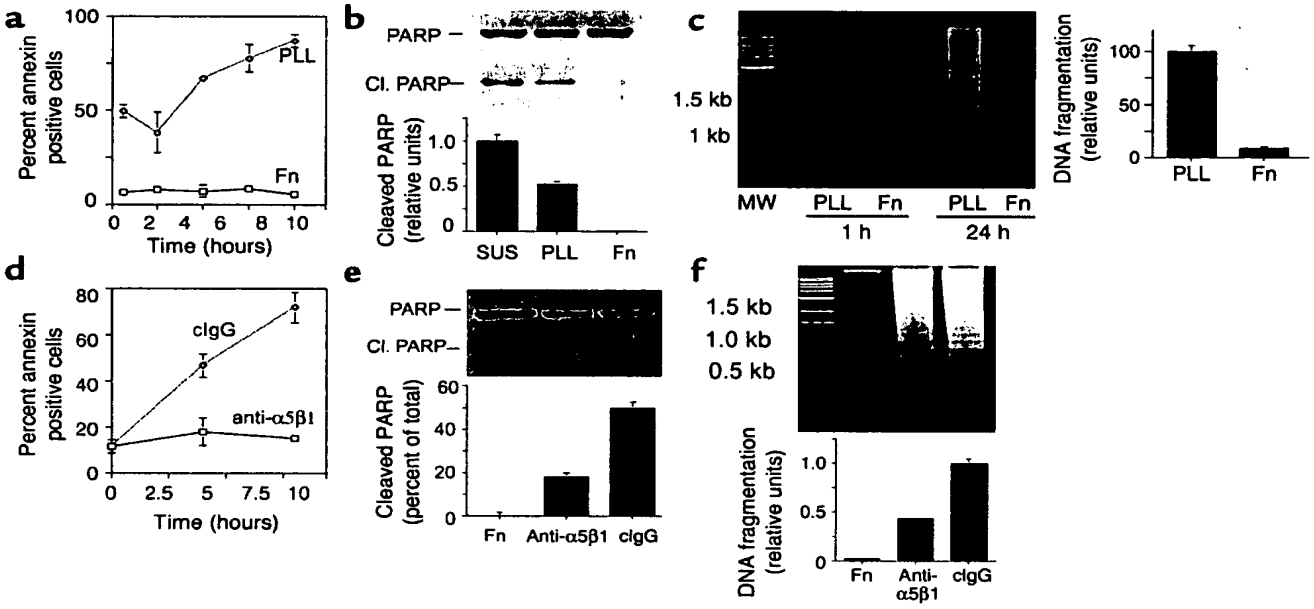


**Figure 1**

Fibronectin and integrin α5β1 support endothelial cell survival. (**a**–**c**) HUVECs were maintained in suspension (SUS) or on fibronectin-coated (Fn) or poly-L-lysine-coated (PLL) plates. (**a**) The percentage of annexin V-positive cells on poly-L-lysine- or fibronectin-coated dishes was determined at regular intervals from 0 to 8 hours. (**b**) Cell lysates prepared after 4 hours of attachment were immunoblotted to detect intact (116 kDa) and cleaved PARP (85 kDa). The ratio of intact to cleaved PARP was determined by densitometry. Cl., cleaved. (**c**) Soluble DNA extracted from cells attached to poly-L-lysine or fibronectin was electrophoresed on 1.6% agarose gels. Relative DNA cleavage was determined by densitometry. (**d**–**f**) HUVECs were plated on fibronectin, anti-α5β1, or control Ab-coated plates. (**d**) The percentage of annexin V-positive cells was determined from 0 to 8 hours. (**e**) Cell lysates were immunoblotted to detect intact and cleaved PARP. (**f**) DNA fragmentation was evaluated as in **c**. cIgG, control immunoglobulin.

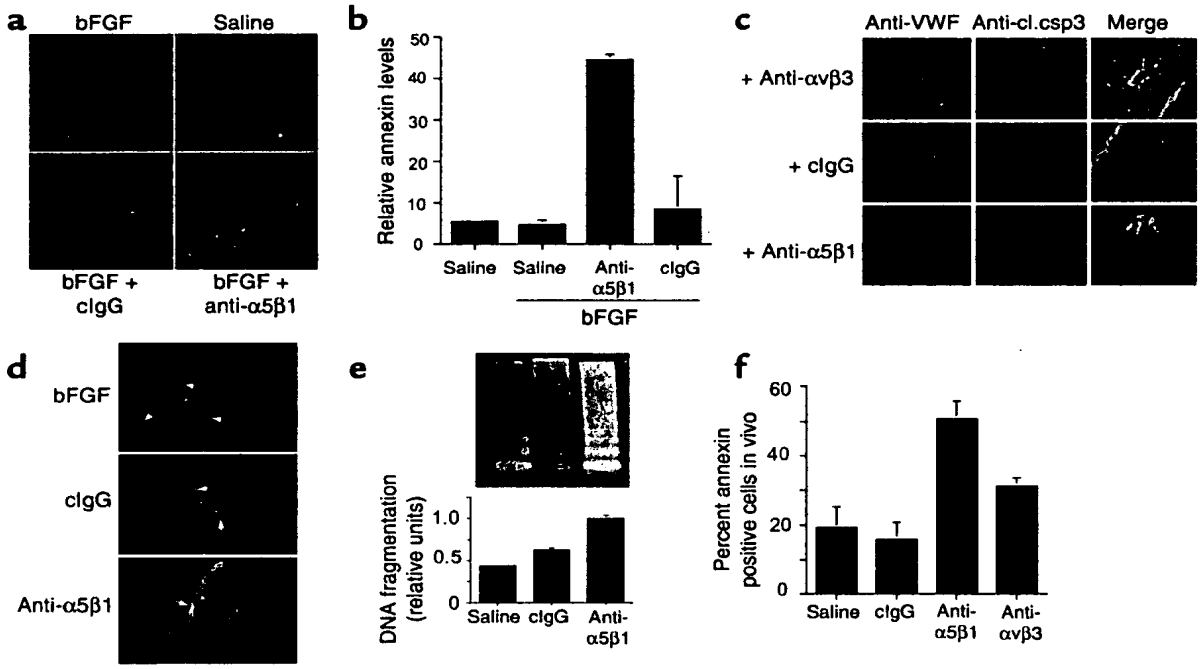


**Figure 2**

Integrin α5β1 supports endothelial cell survival during angiogenesis in vivo. (**a**) CAMs were stimulated with bFGF or saline and then treated for 24 hours with saline, anti-α5β1, and control Ab's. CAMs were then injected with 50 μl FITC-annexin V, harvested 2 hours later, and analyzed directly by confocal microscopy. (**b**) Green pixels (annexin V positive) present per optical section were quantified. (**c**) CAMs treated as in **a** were cryosectioned and immunostained with anti-cleaved caspase-3 (anti-cl.csp3) (green) and anti-vWF (red). Cleaved caspase-3-positive blood vessels are yellow (arrows). (**d**) CAMs treated as in **a** were cryosectioned and immunostained with anti-vWF (red) and for DNA fragmentation (TUNEL staining, green). Arrows indicate blood vessels. Yellow structures are apoptotic blood vessels. (**e**) Soluble DNA isolated from CAMs treated as in **a** was electrophoresed on 1.6% agarose gels. Molecular-weight markers are 1-kb DNA ladders. Relative DNA cleavage was determined by densitometry. (**f**) Individual cells isolated from CAMs treated as in **a** were stained with FITC-annexin V.

Ab's were shown previously to react with α5β1 on chicken endothelial cells and to block its function in vitro and in vivo (17). Because α5β1 is only expressed at significant levels on proliferating endothelial cells (17), α5β1 function-blocking Ab's target proliferating endothelial cells. Because peptide and small molecule antagonists of α5β1 also inhibit angiogenesis (17) and induce apoptosis (not shown), Ab-mediated complement activation is not likely to play a significant role in this apoptosis induction. Thus, these results suggest that integrin α5β1 antagonists induce endothelial cell apoptosis in vivo.

To determine further whether α5β1 antagonists cause apoptosis in vivo, sections of CAMs were analyzed for the expression of cleaved caspase-3 in blood vessels (Figure 2c, $P = 0.01$). Cleavage of caspase-3 into 17- and 12-kDa fragments is an indication of caspase-3 activation; the amount of cleaved caspase-3 is a quantitative index of apoptosis induction. Ab's directed against mammalian caspases cross-react with avian caspases, because avian caspases exhibit 65% overall sequence identity and 100% activation domain sequence identity with mammalian caspases (33). Treatment with either α5β1 or αvβ3 antagonists induces caspase-3 cleavage (green) in blood vessels (red) in growth factor–stimulated CAMs. Antagonists of α5β1 but not control Ab's also induce DNA fragmentation in bFGF-stimulated endothelial cells, as evaluated by TUNEL staining (Figure 2d) and by analysis of DNA fragmentation of agarose gels (Figure 2e, $P = 0.003$). Furthermore, isolated cells from CAMs treated with α5β1 and αvβ3 function-blocking Ab's bound significantly more FITC-annexin V than in cells from control CAMs (Figure 2f, $P = 0.0002$ and 0.003, respectively). These studies definitively show that α5β1 antagonists induce endothelial cell apoptosis during angiogenesis.

*Unligated integrin α5β1 induces apoptosis in adherent endothelial cells.* To determine how α5β1 antagonists interfere with cell survival during angiogenesis, proliferating HUVECs in complete culture medium were plated on poly-L-lysine–, fibronectin-, vitronectin-, or collagen-coated culture plates in the presence of Ab antagonists of integrins α5β1, αvβ3, or α2β1 for 24 hours. Cells were then stained with FITC-annexin V. While fibronectin and vitronectin promote the survival of proliferating endothelial cells (Figure 3, a and c), collagen does not (ref. 34; data not shown). Integrin antagonists that block cell attachment to the substratum (Figure 3, b and d) induce apoptosis, or anoikis, in endothelial cells (Figure 3, a and c). For example, antagonists of α5β1 induce apoptosis on fibronectin (Figure 3a, $P = 0.001$), while antagonists of αvβ3 induce apop-

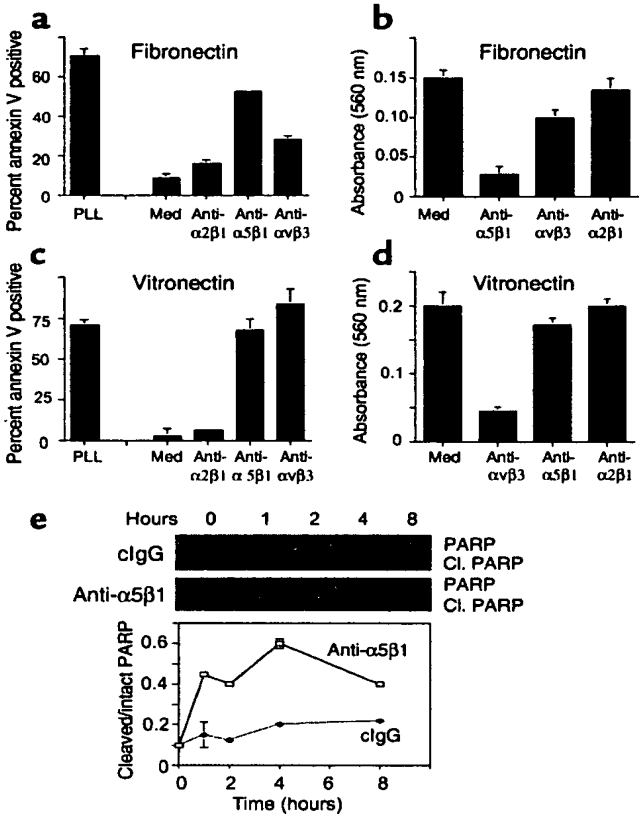


**Figure 3**
Unligated integrin α5β1 regulates endothelial cell survival. HUVECs were plated on poly-L-lysine-coated, fibronectin-coated (**a** and **b**), or vitronectin-coated (**c** and **d**) culture plates in culture medium (med) or culture medium containing anti-α5β1, anti-αvβ3, anti-α2β1 Ab's. After 1 hour, cell attachment was determined (**b** and **d**). After 24 hours, the percentage of FITC-annexin V-positive (**a** and **c**) cells was determined. (**e**) HUVECs plated on vitronectin-coated plates in the presence of function-blocking anti-α5β1 or control Ab's were collected at regular intervals from 0 to 8 hours and PARP cleavage assessed by Western blotting. Relative PARP cleavage levels were determined by densitometry.

tosis on vitronectin (Figure 3c, $P = 0.02$) by blocking cell attachment to the substratum.

In vivo, however, anoikis induced by loss of attachment to the ECM is unlikely to occur because endothelial cells are attached to multiple matrix proteins through multiple integrins at any one time. Therefore, we also examined the ability of integrin antagonists to induce apoptosis in cells that remain attached through other integrins. In fact, α5β1 antagonists induce apoptosis of cells on vitronectin (Figure 3c, $P = 0.05$) without affecting their attachment to vitronectin (Figure 3d). Anti-α5β1, but not control Ab's, also induce PARP cleavage in HUVECs plated on vitronectin substrates (Figure 3e, $P = 0.003$). Thus, unligated α5β1 inhibits endothelial cell survival on provisional matrix proteins such as fibronectin and vitronectin. These studies indicate that integrin α5β1 provides critical survival signals to proliferating endothelial cells such as those participating in angiogenesis. These studies indicate that integrin α5β1 can directly and indirectly regulate survival of proliferating endothelial cells.

*Unligated integrin α5β1 activates a caspase-8–mediated apoptosis pathway in vitro and in vivo.* To determine the nature of the cell death pathway induced by α5β1 antagonists, endothelial cells were plated on ECM protein-coated culture plates in the presence of integrin antagonists and caspase inhibitors or vehicle control (0.33% DMSO). Cell death induced by anti-α5β1 Ab's was blocked by caspase-3 inhibitors, whether the cells were attached to fibronectin ($P = 0.0005$, Figure 4a) or vitronectin ($P = 0.02$, Figure 4b). Cell attachment to poly-L-lysine rapidly activated caspases-3 and -8 while attachment to vitronectin did not (Figure 4, c and d). Anti-α5β1 Ab's but not control Ab's also activated cas-

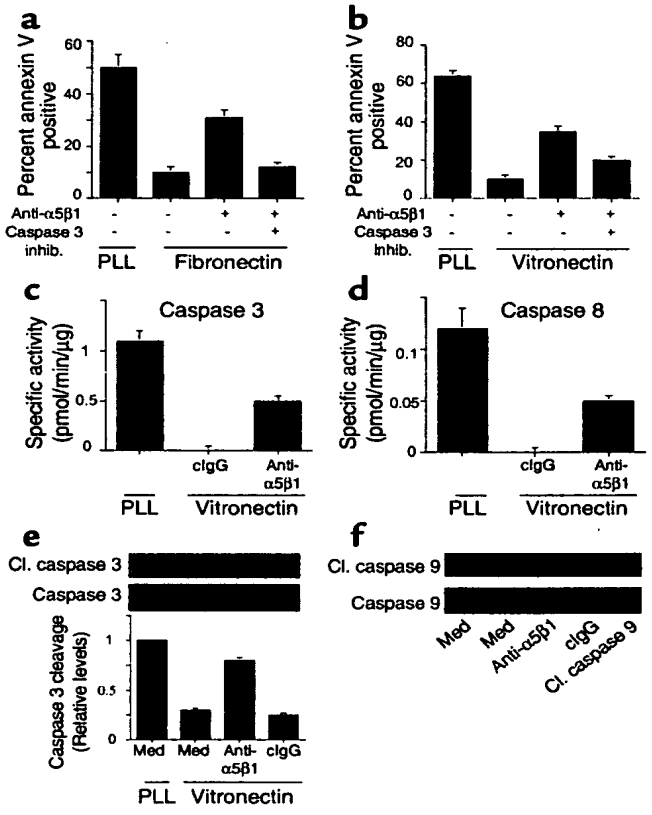


**Figure 4**
Unligated integrin α5β1 induces caspase-3 and -8, but not -9, activation. HUVECs were plated on (**a**) fibronectin-, (**b**) vitronectin-, or (**a** and **b**) poly-L-lysine-coated culture plates in the presence of anti-α5β1 Ab's and 50 μM z-DEVD-fmk (caspase-3) or z-IETD-fmk (caspase-8) inhibitors or vehicle control (0.33% DMSO) for 24 hours. The percentage of annexin V-positive cells was then determined. inhib, inhibitor. (**c** and **d**) Caspase-3 and -8 activities were determined in HUVECs plated on vitronectin-coated or poly-L-lysine-coated plates in the presence of culture medium, anti-α5β1, or control Ab's. (**e**) Cell lysates were immunoblotted with anti-caspase-3 and anti-cleaved caspase-3 Ab's. Relative caspase-3 cleavage was determined by densitometry. (**f**) Cell lysates were immunoblotted with anti-caspase-9 and anti-cleaved caspase-9 Ab's.

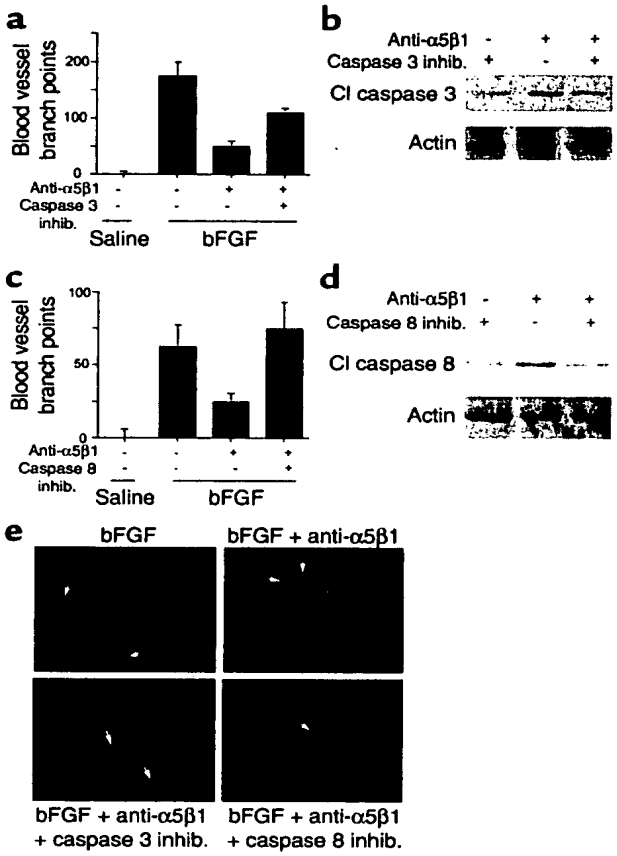


**Figure 5**

Integrin antagonists induce caspase-3- and -8-dependent apoptosis in vivo. (**a–d**) CAMs stimulated with saline or bFGF were treated with 2.5% DMSO (vehicle control), anti-α5β1, or anti-α5β1 with 500 μM caspase-3 (**a** and **b**) or caspase-8 (**c** and **d**) inhibitors. (**a** and **c**) Blood vessel branch points were quantified after 48 hours. (**b** and **d**) Caspase-3 and -8 cleavage was evaluated by Western blotting with (**b**) anti-cleaved caspase-3 or (**d**) anti-cleaved caspase-8 Ab's and anti-actin Ab's. (**e**) Cryosections of CAMs treated as in **a–d** were immunostained for vWF expression (red) and to detect DNA fragmentation (TUNEL staining, green). Arrows indicate blood vessels. Apoptotic vessels appear yellow.

pase-3 and -8 ($P = 0.0001$ and $P = 0.002$, respectively) in cells attached to vitronectin (Figure 4, c and d) and fibronectin (not shown). Caspase-3 cleavage was also readily detected in cells treated with anti-α5β1 but not control Ab's ($P = 0.01$, Figure 4e). In contrast, caspase-9 cleavage was not detected in cells treated with α5β1 antagonists (Figure 4f). These studies show that integrin α5β1 antagonists induce a proapoptotic pathway in proliferating endothelial cells that results from activation of initiator caspases (8) rather than stress caspase (9) pathways. These results also indicate that blocking α5β1 ligation induces caspase-8- and -3-mediated death even when cells are still attached to provisional matrix ligands through other integrins.

Our studies show that integrin-mediated survival depends on suppression of caspase-3 and -8 activity in vitro. As α5β1 antagonists block angiogenesis in vivo, these antagonists may induce caspase-3 and -8 activation in vivo. CAMs stimulated with bFGF were treated with saline, vehicle control (DMSO), caspase-3 or -8 inhibitors, and anti-integrin Ab's in the presence or absence of caspase inhibitors. Angiogenesis was inhibited by anti-α5β1 Ab's (Figure 5, a–d); this inhibition was partially reversed by cell-permeable caspase-3 inhibitors ($P = 0.04$, Figure 5a) and fully reversed by caspase-8 inhibitors ($P = 0.05$, Figure 5c). Caspase-3 inhibitors partially blocked caspase-3 activity in vivo (Figure 5b), while caspase-8 inhibitors completely blocked its activity in vivo (Figure 5d). Furthermore, caspase-3 and -8 inhibitors prevented in vivo endothelial cell DNA fragmentation induced by α5β1 inhibition (Figure 5e). Caspase-9 inhibitors had little effect on angiogenesis (not shown). Caspase inhibitors alone had no effect on angiogenesis or on unstimulated CAMs. These results indicate that α5β1 antagonists activate caspases-8 and -3 in vivo, thereby inhibiting angiogenesis.

*Unligated integrins induce PKA-dependent apoptosis.* Integrin ligation activates signaling pathways that promote cell migration, proliferation, and survival. Typically, integrin-mediated signaling is characterized by increases in tyrosine phosphorylation of signaling intermediates such as focal adhesion kinase, src, and ERK family members. However, integrin ligation also suppresses the activation of at least one kinase, PKA (19). Importantly, we found that integrin ligation suppresses PKA activation, while antagonists of integrins activate this enzyme (Figure 6a). Notably, antagonists of integrin α5β1 activate endothelial cell PKA whether endothelial cells are plated on fibronectin or on vitronectin (Figure 6a). Therefore, we investigated the contribution of PKA to integrin-mediated cell death. We found that a pharmacological inhibitor of PKA, HA1004, substantially suppressed the apoptosis induced by integrin antagonists anti-αvβ3 ($P = 0.05$) or anti-α5β1 ($P = 0.05$) in cells attached to vitronectin, as detected by annexin V binding to intact cells (Figure 6b). PKA inhibitors also blocked caspase-3 cleavage induced by anti-α5β1 ($P = 0.002$, Figure 6c). Expression of dnPKA, but not a control transgene (GFP), also prevented integrin antagonist-induced cell death ($P = 0.004$; Figure 7, a and b). More than 80% of cells expressed the transgene, which was also detected by Western blotting (Figure 7d). These studies indicate that both direct (anoikis) and indirect integrin antagonist-mediated cell death is PKA dependent.

*PKA activation induces endothelial cell apoptosis in vitro and in vivo.* Our studies show that inhibition of PKA suppresses integrin antagonist-induced cell death. To determine whether activation of PKA directly induces endothelial cell death, endothelial cells were treated with dibutyryl cAMP or were transiently transfected with the active, catalytic subunit of PKA. Both cAMP and expression of the catalytic subunit of PKA significantly induce apoptosis ($P = 0.009$ and $P = 0.003$, respectively) in endothelial cells in vitro (Figure 7c). Thus, PKA directly induces apoptosis in endothelial cells.

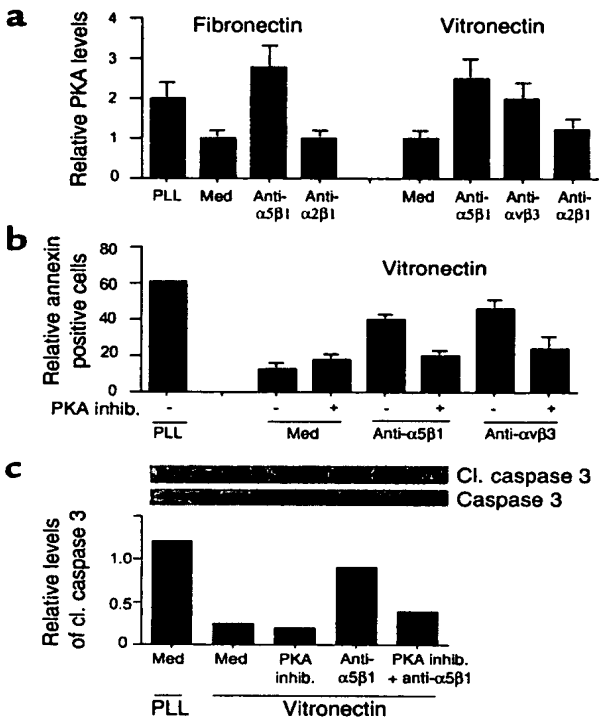


**Figure 6**
Unligated α5β1-mediated death is PKA dependent. (a) PKA activity was measured in HUVECs attached to poly-L-lysine, fibronectin, or vitronectin in the presence or absence of integrin antagonists. (**b**) HUVECs were plated on vitronectin-coated or poly-L-lysine-coated culture plates in the presence or absence of anti-α5β1 or anti-αvβ3 Ab's, a selective PKA inhibitor (1 μM HA1004), or anti-integrin Ab's in combination with 1 μM HA1004. After 24 hours, the percentage of FITC-annexin-positive cells was determined. (**c**) Cell lysates from **b** were immunoblotted with anti-caspase-3 and anti-cleaved caspase-3 Ab's. Relative caspase-3 cleavage was determined by densitometry.

To determine whether PKA plays a role in the negative regulation of angiogenesis in vivo, bFGF-stimulated CAMs were transfected with expression plasmids encoding GFP and dnPKA and treated with α5β1 Ab's. While α5β1 antagonists block angiogenesis (Figure 8a, $P = 0.004$), dnPKA reverses this inhibition (Figure 8a, $P = 0.02$). Expression of dnPKA also prevents α5β1 antagonist-induced DNA fragmentation in vivo as detected by TUNEL staining (Figure 8b) and inhibits activation of caspase-3 and -8 in vivo (Figure 8c). Since integrin antagonists induce PKA-dependent apoptosis in vivo, direct activation of PKA may also inhibit angiogenesis. Expression of the PKA catalytic subunit during angiogenesis in vivo completely suppresses angiogenesis ($P = 0.0005$), as does exposure to cAMP ($P = 0.001$, Figure 8d). VEGF-stimulated angiogenesis is also inhibited by activation of PKA (data not shown). This inhibition results from apoptosis induction, because it is accompanied by DNA fragmentation detected by TUNEL staining (Figure 8e) and caspase-3 cleavage in vivo (Figure 8f). The expression of transgenes could be demonstrated in endothelial cells in vivo by immunohistochemical staining for the presence of His-tagged proteins (Figure 8g). Thus, activation of PKA by integrin antagonists, by cAMP, or by expression of the catalytic subunit of PKA induces endothelial cell apoptosis and inhibits angiogenesis.

These studies demonstrate that the unligated integrin α5β1 induces endothelial cell apoptosis in vivo in a PKA-dependent manner, thereby inhibiting angiogenesis. These studies demonstrate that activation of PKA by unligated integrins is an essential step in the induction of apoptosis. Importantly, our studies demonstrate that direct activation of PKA in vivo induces endothelial cell apoptosis and inhibition of angiogenesis.

## Discussion

During normal embryonic development and during adult tissue repair processes, unwanted cells are elimi-

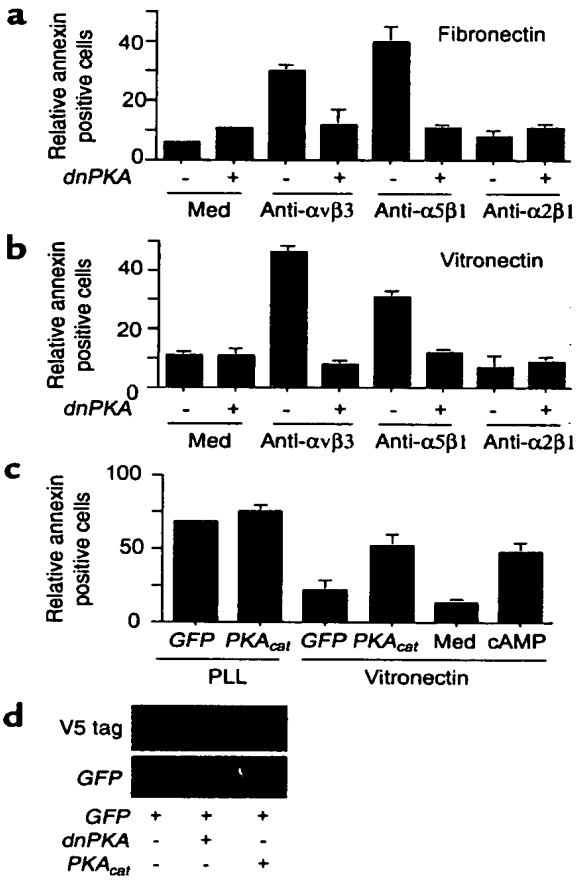


**Figure 7**
PKA negatively regulates cell survival. (**a** and **b**) HUVECs transfected with *GFP* (-) or a *dnPKA* (+) were plated on (**a**) fibronectin-coated, (**b**) vitronectin-coated, or poly-L-lysine-coated plates in the absence or presence of anti-α5β1, anti-αvβ3, or anti-α2β1. After 24 hours, the percentage of annexin V-positive cells was determined. (**c**) HUVECs treated with culture medium or dibutyryl cAMP (250 μM) and HUVECs transfected with *GFP* or the catalytic subunit of PKA ($PKA_{cat}$) were plated on vitronectin-, or poly-L-lysine-coated plates. After 24 hours, the percentage of annexin V-positive cells was determined. (**d**) Expression of transgenes was detected by Western blotting cell lysates with anti-*GFP* or anti-V5.

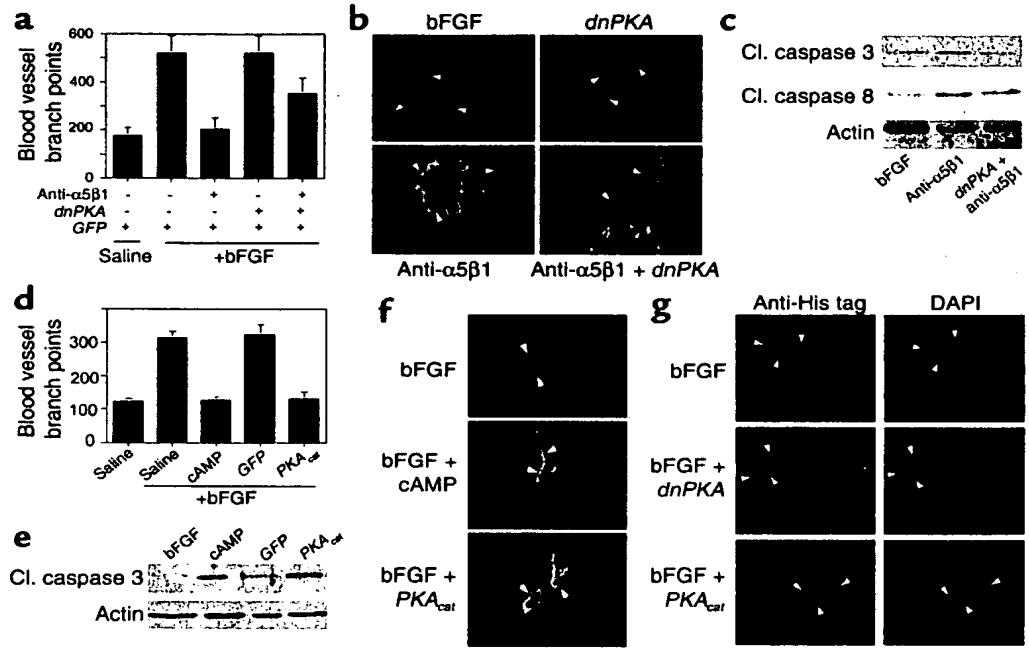


**Figure 8**

PKA inhibits angiogenesis by inducing apoptosis. (**a**) CAMs stimulated with bFGF were transfected 24 hours later by placing 4 μg *pcDNA/V5/His dnPKA* or *N1-GFP* expression plasmid on CAMs. CAMs were treated on the same day with saline or anti-α5β1 Ab's and were harvested 48 hours later. Blood vessel branch points were quantified. (**b**) Cryosections of CAMs from **a** were immunostained with anti-vWF (red) and were stained to detect fragmented DNA by the TUNEL method (green). Arrows indicate blood vessels. Apoptotic blood vessels appear yellow. (**c**) Western blots of lysates prepared from CAMs treated as in **a** were immunoblotted with anti-cleaved caspase-3 and anti-cleaved caspase -8, as well as anti-actin as a loading control. (**d**) CAMs stimulated with bFGF were treated with saline or 250 μM cAMP or were transfected by placing 4 μg *pcDNA/V5/His* $PKA_{cat}$ or *N1-GFP* expression plasmid on stimulated CAMs. Blood vessel branch points were quantified 48 hours later. (**e**) Cryosections of CAMs from **d** were immunostained with anti-vWF (red) and were stained to detect fragmented DNA by the TUNEL method (green). Arrows indicate blood vessels. Apoptotic blood vessels appear yellow. (**f**) Detergent lysates prepared from freshly excised CAMs from **d** were immunoblotted for expression of cleaved caspase-3 and actin as a loading control. (**g**) Cryosections of CAMs from **a** and **d** were immunostained with anti-pentaHis (red) to detect expression of His-tagged transgenes in the transfected CAM tissue. Sections were counterstained with DAPI. Arrows indicate blood vessels.

nated by apoptosis (35). Cell death is also induced by environmental stress, activation of death receptors, and loss of contact with the ECM (35). Apoptosis is initiated by activation of caspases, cysteine proteins that cleave target proteins after aspartic acid residues (36). Initiator and stress caspases are activated by extracellular stimuli and, in turn, activate effector caspases. Effector caspases cleave important cellular proteins such as focal adhesion kinase and p21-activated kinase, which regulate cell shape as well as enzymes that are important for DNA repair and nuclear integrity (36).

Integrin-mediated cell attachment promotes cell survival (37), while interruption of cell attachment induces anoikis or detachment-induced apoptosis (38, 39). Our studies indicate that key unligated integrins can also induce cell death when cells are still attached to the ECM. We show here that unligated integrin α5β1 inhibits endothelial cell survival and angiogenesis in ECM-adherent cells by activating PKA and, subsequently, caspase-8. In proliferating endothelial cells, α5β1 is ligated by endothelial cell–secreted fibronectin (19, 40). Antagonists of either α5β1 or fibronectin inhibit α5β1 function, thereby activating PKA and inducing cell death, even when cells remain attached to the ECM through integrin αvβ3 or other integrins. Recent studies suggest that unligated integrin αvβ3 actively induces apoptosis by a pathway termed integrin-mediated death (IMD). IMD may be initiated by the interaction of unligated integrin β subunit cytoplasmic tails with caspase-8 (41). Our studies indicate that unligated α5β1 also induces IMD and that IMD is dependent on the activity of PKA.

Here we show that direct activation of PKA with cAMP or by overexpression of the PKA catalytic subunit induces apoptosis in proliferating endothelial cells and inhibits angiogenesis. PKA activation has been implicated previously in the regulation of apoptosis in some, but not all, transformed cells (42). In some cells, PKA phosphorylates and inhibits the tyrosine kinase Raf, thereby blocking the MAP kinase pathway and inducing apoptosis (43). Alternatively, PKA may negatively regulate cell survival by hyperphosphorylating Bcl-2 and suppressing Bcl-2 binding to Bax, thus lowering the Bcl-2/Bax ratio (44). Since integrin ligation activates Bcl-2 (45), integrin antagonism may inhibit Bcl-2 in a PKA-dependent manner. PKA activation also inhibits Akt, a prosurvival serine/threonine kinase that phosphorylates and inacti-

vates BAD, a member of the proapoptotic Bcl-2 family (46). Phosphorylation of BAD inhibits its association with and inactivation of the prosurvival proteins, Bcl-2 and Bcl-x (46). Alternatively, since PKA and caspase-8 are rapidly activated upon inhibition of integrin ligation (19), PKA may play an early role in endothelial cell death by activating caspase-8. Thus, PKA may negatively regulate one or more cell survival signaling pathways.

Unligated integrins may play important roles in suppressing cell survival during tissue remodeling, such as occurs during development, angiogenesis, and wound healing. In these circumstances, cell viability may be promoted when cells remain in the proper environment. Primary cells that inappropriately wander into other microenvironments lacking the correct ECM ligands would be induced to undergo apoptosis. Tumor cells that are more resistant to apoptotic stimuli than normal cells may escape this IMD pathway and wander to distant environments, causing metastases. The studies presented here indicate that in primary cells, unligated integrins induce apoptosis by a PKA-dependent and caspase-8–dependent pathway.

## Acknowledgments

This work was supported by grants CA-71619 and CA-83133 from the NIH to J.A. Varner. J.A. Varner is a member of the Comprehensive Cancer Center of the University of California, San Diego.

1. Varner, J.A. 1997. The role of vascular cell integrin αvβ3 and αvβ5 in angiogenesis. *EXS.* **79**:361–390.
2. Asahara, T., et al. 1999. VEGF contributes to postnatal neovascularization by mobilizing bone marrow derived endothelial progenitor cells. *EMBO J.* **18**:3964–3972.
3. Meredith, J.E., Jr., Fazeli, B., and Schwartz, M.A. 1993. The ECM as a cell survival factor. *Mol. Biol. Cell.* **4**:953–961.
4. Brooks, P.C., et al. 1994. Integrin αvβ3 antagonists promote tumor regression by inducing apoptosis of angiogenic blood vessels. *Cell.* **79**:1157–1164.
5. Boudreau, N., Sympson, C.J., Werb, Z., and Bissell, M. 1995. Suppression of ICE and apoptosis in mammary epithelial cells by ECM. *Science.* **267**:891–893.
6. Stromblad, S., Becker, J.C., Yebra, M., Brooks, P.C., and Cheresh, D.A. 1996. Suppression of p53 activity and p21WAF1/CIP1 expression by vascular cell integrin αvβ3 during angiogenesis. *J. Clin. Invest.* **98**:426–433.
7. Clark, R.A.F., Tonneson, M.G., Gailit, J., and Cheresh, D.A. 1996. Transient functional expression of αvβ3 on vascular cells during wound repair. *Am. J. Path.* **148**:1407–1421.
8. Friedlander, M., et al. 1995. Definition of two angiogenic pathways by distinct alpha v integrins. *Science.* **270**:1500–1502.
9. Arap, W., Pasqualini, R., and Ruoslahti, E. 1997. Cancer treatment by targeted drug delivery to tumor vasculature in a mouse model. *Science.* **279**:377–380.
10. Brooks, P.C., Clark, R.A., and Cheresh, D.A. 1994. Requirement of vascular integrin alpha v beta 3 for angiogenesis. *Science.* **264**:569–571.
11. Carron, C.P., et al. 1998. A peptidomimetic antagonist of the integrin αvβ3 inhibits Leydig cell tumor growth and development of hypercalcemia of malignancy. *Cancer Res.* **58**:1930–1955.
12. Christofidou-Solomidou, M., Bridges, M., Murphy, G., Albelda, S., and DeLisser, H.M. 1997. Expression and function of endothelial cell αv integrin receptors in wound-induced human angiogenesis in human skin/SCID mice chimeras. *Am. J. Path.* **151**:975–983.
13. Drake, C.J., Cheresh, D.A., and Little, C.D. 1995. An antagonist of integrin αvβ3 prevents maturation of blood vessels during embryonic neovascularization. *J. Cell Sci.* **108**:2655–2661.
14. Friedlander, M., et al. 1996. Involvement of integrin αvβ3 and αvβ5 in ocular neovascular diseases. *Proc. Natl. Acad. Sci. USA.* **93**:9764–9769.
15. Varner, J.A., Nakata, M.T., Jordan, R.E., and Coller, B.S. 1999. Inhibition of angiogenesis and tumor growth by murine 7E3, the parent antibody of c7E3 Fab (abciximab; ReoPro™). *Angiogenesis.* **3**:53–61.
16. Bader, B.L., Rayburn, H., Crowley, D., and Hynes, R.O. 1998. Extensive vasculogenesis, angiogenesis, and organogenesis precede lethality in mice lacking all αv integrins. *Cell.* **95**:507–520.
17. Kim, S., Bell, K., Mousa, S., and Varner, J.A. 2000. Regulation of angiogenesis in vivo by ligation of integrin α5β1 with the central cell binding domain of fibronectin. *Am. J. Path.* **156**:1345–1362.
18. Kloss, C., et al. 1999. Integrin family of cell adhesion molecules in the injured brain: regulation and cellular localization in the normal and regenerating mouse facial motor nucleus. *J. Comp. Neurol.* **411**:162–178.
19. Kim, S., Harris, M., and Varner, J.A. 2000. Regulation of integrin αvβ3-mediated endothelial cell migration and angiogenesis by integrin α5β1 and protein kinase A. *J. Biol. Chem.* **275**:33920–33928.
20. Varner, J.A., Emerson, D.A., and Juliano, R.L. 1995. Integrin α5β1 expression negatively regulates cell growth: reversal by attachment to fibronectin. *Mol. Biol. Cell.* **6**:725–740.
21. Giancotti, F.G., and Ruoslahti, E. 1990. Elevated levels of alpha 5 beta 1 fibronectin receptor suppress the transformed phenotype of Chinese hamster ovary cells. *Cell.* **60**:849–859.
22. Plath, T., et al. 2000. A novel function for the tumor suppressor p16 INK4a: induction of anoikis via upregulation of the α5β1 fibronectin receptor. *J. Cell. Biol.* **150**:1467–1477.
23. George, E. L., Georges, E.N., Patel-King, R.S., Rayburn, H., and Hynes, R.O. 1993. Defects in mesodermal migration and vascular development in fibronectin-deficient mice. *Development.* **119**:1079–1091.
24. Yang, J.T., Rayburn, H., and Hynes, R.O. 1993. Embryonic mesodermal defects in α5 integrin-deficient mice. *Development.* **119**:1093–1105.
25. Goh, K.L., Yang, J.T., and Hynes, R.O. 1997. Mesodermal defects and cranial neural crest apoptosis in α5 integrin-null embryos. *Development.* **124**:4309–4319.
26. Yatohgo, T., Izumi, M., Kashiwagi, H., and Hayashi, M. 1988. Novel purification of vitronectin from human plasma by heparin affinity chromatography. *Cell Struct. Funct.* **13**:281–292.
27. Herrmann, M., et al. 1994. A rapid and simple method for the isolation of apoptotic DNA fragments. *Nucleic Acids Res.* **22**:5506–5507.
28. Dormond, O., Foletti, A., Paroz, C., and Rüegg, C. 2001. NSAIDs inhibit alpha V beta 3 integrin-mediated and Cdc42/Rac-dependent endothelial-cell spreading, migration and angiogenesis. *Nat. Med.* **7**:1041–1047.
29. Raynal, P., and Pollard, H. B. 1994. Annexins: the problem of assessing the biological role for a gene family of multifunctional calcium and phospholipid-binding proteins. *Biochem. Biophys. Acta.* **1197**:63–93.
30. Nicholson, D.W., et al. 1995. Identification and inhibition of the ICE/CED-3 protease necessary for mammalian apoptosis. *Nature.* **376**:37–43.
31. Partel, T., Gores, G.J., and Kaufmann, S.H. 1996. The role of protease during apoptosis. *FASEB J.* **10**:587–597.
32. Leaveley, D.I., Schwartz, M.A., Rosenfeld, M., and Cheresh, D.A. 1993. Integrin β1 and β3-mediated endothelial cell migration is triggered through distinct mechanisms. *J. Cell Biol.* **121**:163–170.
33. Johnson, A.L., and Bridgham, J.T. 2000. Caspase-3 and -6 expression and enzyme activity in hen granulosa cells. *Biol. Reprod.* **62**:589–598.
34. Montgomery, A.M.P, Reisfeld, R.A., and Cheresh, D.A. 1994. Integrin αvβ3 rescues melanoma from apoptosis in a three-dimensional dermal collagen. *Proc. Natl. Acad. Sci. USA.* **91**:8856–8860.
35. Ashkenazi, A., and Dixit, V.M. 1998. Death receptors: signaling and modulation. *Science.* **281**:1305–1308.
36. Thornberry, N., and Lazebik, Y. 1998. Caspases: enemies within. *Science.* **281**:1312–1316.
37. Schwartz, M.A. 1997. Integrins, oncogenes and anchorage independence. *J. Cell Biol.* **139**:575–578.
38. Frisch, S.M., and Francis, H. 1994. Disruption of epithelial cell-matrix interactions induces apoptosis. *J. Cell. Biol.* **124**:619–626.
39. Rytomaa, M., Martins, L.M., and Downward, J. 1999. Involvement of FADD and caspase 8 signaling in detachment induced apoptosis. *Curr. Biol.* **9**:1043–1046.
40. Magnusson, M.K., and Mosher, D.F. 1998. Fibronectin: structure, assembly, and cardiovascular implications. *Arterioscler. Thromb. Vasc. Biol.* **18**:1363–1370.
41. Stupack, D.G., Puente, X.S., Butsaboualoy, S., Storgard, C.M., and Cheresh, D.A. 2001. Apoptosis of adherent cells by recruitment of caspase-8 to unligated integrins. *J. Cell Biol.* **155**:459–470.
42. Weissinger, E., et al. 1997. Inhibition of Raf-1 kinase by cyclic AMP agonists causes apoptosis of v-abl-transformed cells. *Mol. Cell. Biol.* **17**:3229–3241.
43. D'Angelo, G., Lee, H., and Weiner, R.I. 1997. CAMP-dependent protein kinase inhibits the mitogenic action of vascular endothelial growth factor and fibroblast growth factor in capillary endothelial cells by blocking Raf activation. *J. Cell. Biochem.* **67**:353–366.
44. Srivastava, R.K., et al. 1998. Involvement of microtubules in the regulation of Bcl-2 phosphorylation and apoptosis through cyclic AMP-dependent protein kinase. *Mol. Cell. Biol.* **18**:3509–3517.
45. Zhang, Z., Vuori, K., Reed, J.C., and Ruoslahti, E. 1995. The α5β1 integrin supports survival of cells on fibronectin and upregulates bcl-2 expression. *Mol. Biol. Cell.* **6**:841–850.
46. Kim, S., Jee, K., Kim, D., Koh, H., and Chung, J. 2001. Cyclic AMP inhibits Akt activity by blocking the membrane localization of PDK1. *J. Biol. Chem.* **276**:12864–12870.

Exhibit 3

Figure 1
The effect of ATN-161 and ATN-220 on growth factor induced angiogenesis was tested in the matrigel plug assay in the presence or absence of the PKA inhibitor HA1004. As shown in the upper panel ATN-161 significantly inhibited growth factor induced angiogenesis and this inhibition was in large part attenuated by the presence of HA1004. In contrast, although ATN-220 significantly inhibited angiogenesis (lower panel) this inhibition was not affected by the presence of HA1004. Taken together these data suggest that, unexpectedly, ATN-220 inhibits angiogenesis by a mechanism distinct from that by which ATN-161 inhibits angiogenesis.

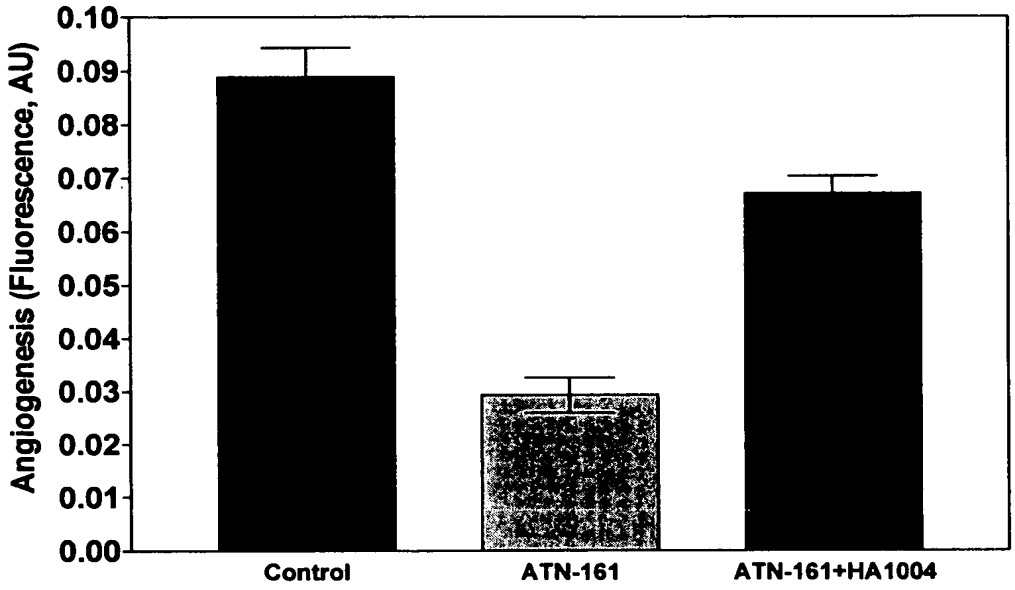


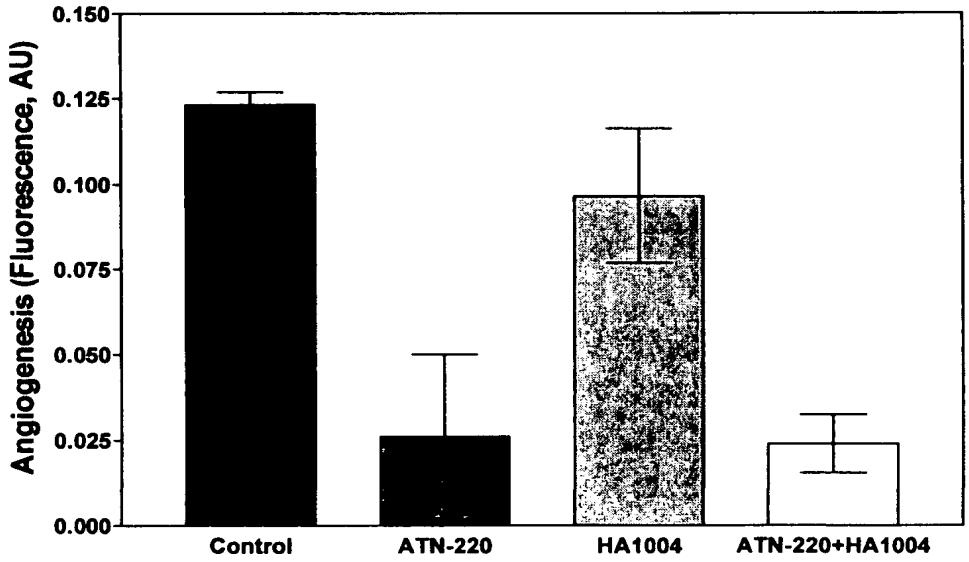

# A non–RGD-based integrin binding peptide (ATN-161) blocks breast cancer growth and metastasis *in vivo*

**Parisa Khalili,[1] Ani Arakelian,[1] Gaoping Chen,[1] Marian L. Plunkett,[2] Ivy Beck,[2] Graham C. Parry,[2] Fernando Doñate,[2] David E. Shaw,[3] Andrew P. Mazar,[2] and Shafaat A. Rabbani[1]**

[1]Department of Medicine and Oncology, McGill University Health Center, Montreal, Quebec, Canada; [2]Attenuon, LLC, San Diego, California; and [3]DE Shaw Research, LLC, New York, New York

## Abstract

***Purpose:*** **Integrins are expressed by numerous tumor types including breast cancer, in which they play a crucial role in tumor growth and metastasis. In this study, we evaluated the ability of ATN-161 (Ac-PHSCN-$NH_2$), a 5-mer capped peptide derived from the synergy region of fibronectin that binds to $\alpha_5\beta_1$ and $\alpha_v\beta_3$ *in vitro*, to block breast cancer growth and metastasis.** ***Experimental design:*** **MDA-MB-231 human breast cancer cells were inoculated s.c. in the right flank, or cells transfected with green fluorescent protein (MDA-MB-231-GFP) were inoculated into the left ventricle of female BALB/c *nu/nu* mice, resulting in the development of skeletal metastasis. Animals were treated with vehicle alone or by i.v. infusion with ATN-161 (0.05–1 mg/kg thrice a week) for 10 weeks. Tumor volume was determined at weekly intervals and tumor metastasis was evaluated by X-ray, microcomputed tomography, and histology. Tumors were harvested for histologic evaluation.** ***Result:*** **Treatment with ATN-161 caused a significant dose-dependent decrease in tumor volume and either completely blocked or caused a marked decrease in the incidence and number of skeletal as well as soft tissue metastases. This was confirmed histologically as well as radiographically using X-ray and microcomputed tomography. Treatment with ATN-161 resulted in a significant decrease in the expression of phosphorylated mitogen-activated protein kinase, microvessel density, and cell proliferation in tumors grown *in vivo*.** ***Conclusion:*** **These studies show that ATN-161 can block breast cancer growth and metastasis, and provides a rationale for the clinical development of ATN-161 for the treatment of breast cancer. [Mol Cancer Ther 2006; 5(9):2271–80]**

Received 2/22/06; revised 5/16/06; accepted 7/12/06.

**Grant support:** Canadian Institutes of Health Research grant MOP 10630 (S.A. Rabbani).

The costs of publication of this article were defrayed in part by the payment of page charges. This article must therefore be hereby marked advertisement in accordance with 18 U.S.C. Section 1734 solely to indicate this fact.

**Requests for reprints:** Shafaat A. Rabbani, Department of Medicine and Oncology, McGill University Health Center, Room H4.61, 687 Pine Avenue West, Montreal, Quebec, Canada H3A 1A1.
Phone: 514-843-1632; Fax: 514-843-1712.
E-mail: shafaat.rabbani@mcgill.ca



doi:10.1158/1535-7163.MCT-06-0100

## Introduction

Integrins are $\alpha/\beta$ heterodimeric membrane-associated proteins that promote cell adhesion to the surrounding extracellular matrix and activate a number of intracellular signaling pathways that can alter cell behavior (1). It has been hypothesized that selective integrin expression allows tumor cells to metastasize to different organs (2). For example, lung colonization by breast cancer cells is associated with tumor cell expression of $\alpha_4\beta_6$, whereas the ability of multiple myeloma to grow in the bone microenvironment is dependent on the expression of $\alpha_4\beta_7$ (3, 4). Solid tumors (breast, prostate, and lung) which metastasize to the bone often express high levels of $\alpha_v\beta_3$ (5). In particular, bone-residing breast cancer cells have been shown to express significantly higher levels of $\alpha_v\beta_3$ compared with primary breast carcinoma (6). The multistep process of breast cancer metastasis to the bone involves the invasion of tumor cells into the bone marrow cavity. This process is facilitated by the capacity of $\alpha_v\beta_3$ integrins, expressed by tumor cells, to recognize several plasma and extracellular matrix proteins such as vitronectin, fibronectin, and fibrinogen (7). The expression of $\alpha_v\beta_3$ by human breast cancer cells is therefore directly associated with an increased ability to promote the osteolytic skeletal metastases that are often associated with breast cancer (8). Similarly, the expression of $\alpha_v\beta_3$ by osteoclasts may also play a critical role in breast cancer metastasis by mediating the bone resorption that is typically associated with breast cancer metastasis (9). Finally, angiogenesis may also contribute to the growth and metastasis of breast cancer, and the integrin $\alpha_5\beta_1$ has recently been implicated as a major mediator of tumor angiogenesis (10).

Despite recent advances in early detection and novel hormone therapies for breast cancer, metastasis has continued to be a challenging clinical problem (11). ATN-161 is a capped five–amino acid peptide that has shown antitumor activity as well as the ability to inhibit soft tissue metastasis in models of colon and prostate cancer (12, 13). ATN-161 was derived from the synergy region of fibronectin and has been proposed to antagonize synergy function, suggesting that ATN-161 may interact with integrin $\alpha_5\beta_1$ (12). Preliminary data has also shown that ATN-161 interacts primarily with the $\beta_?$ subunit as well as with other $\beta$-integrin subunits such as $\beta_3$ and that these interactions depend on the covalent interaction of ATN-161 with the free sulfhydryl residues in these $\beta$-integrin

subunits (13). Unlike other integrin-binding peptides, ATN-161 is unique in that it is not based around the arginine, glycine, aspartic acid (RGD) integrin adhesion epitope and, unlike RGD-based antagonists, does not inhibit cell adhesion *in vitro*. The evaluation of ATN-161 in patients with advanced cancer in a phase I trial has recently been completed and a biomarker-driven phase II trial of ATN-161 in patients with renal cell carcinoma has recently been initiated. However, little is known about the effects of ATN-161 on breast cancer growth and metastasis to bone. In this study, we used MDA-MB-231 breast cancer cells in well-characterized models of tumor growth and metastasis to evaluate the potential of ATN-161 in this therapeutic setting.

## Materials and Methods

### Cells and Cell Culture

Human MDA-MB-231 breast cancer adenocarcinoma cells were obtained from American Type Tissue Culture Collection (Rockville, MD) and cells transfected with green fluorescent protein (MDA-MB-231-GFP) were prepared and maintained in culture as previously described (14, 15). ATN-161 and scrambled peptide ATN-165 were manufactured by Peptisyntha (Brussels, Belgium) using solution phase methodologies under cyclic guanosine 3',5'-monophosphate.

### Binding Assays

The binding of ATN-161 to MDA-MB-231 tumor cells and to immobilized purified integrins, $\alpha_5\beta_1$ and $\alpha_v\beta_3$, was evaluated using a biotinylated version of ATN-161 (ATN-453; Ac-PHSCNGGK-Biotin). ATN-453 has previously been shown to retain the entire binding activity of ATN-161 (16). Briefly, cells were harvested using trypsin, washed twice in binding buffer [10 mmol/L HEPES (pH 7.4), 150 mmol/L NaCl, 0.1% bovine calf serum, and 2 mmol/L $MnCl_2$] and resuspended at a final concentration of $1 \times 10^6$ cells/mL. Cells ($1 \times 10^6$ per treatment) were incubated for 2 hours at 4°C with various concentrations of ATN-453 in the presence or absence of ATN-161 (Ac-PHSCN-$NH_2$), washed extensively with binding buffer and incubated with streptavidin–horseradish peroxidase for another 30 minutes at 4°C. After additional washes, cells were incubated with *o*-phenylenediamine substrate and absorbance was recorded at OD 490 nm. Binding to purified integrins was evaluated in a similar manner except that the purified integrins (5 μg/mL in PBS) were first immobilized onto high-protein binding microtiter plates for 1 hour at 37°C followed by blocking with 0.1% bovine serum albumin (1 hour, 37°C). Binding data was analyzed using Prism software (GraphPad Software, San Diego, CA) and binding curves were fit using nonlinear regression approaches.

### Cell Proliferation Assay and Western Blotting

MDA-MB-231 cells were plated in triplicate in six-well plates in the presence of 2% fetal bovine serum with vehicle alone or with different concentrations (1–100 μmol/L) of ATN-161 (15, 17). Triplicate wells were trypsinized and counted using a Coulter counter on alternate days (model ZF, Coulter Electronics, Harpenden, Hertfordshire, United Kingdom). Cell culture medium was replenished daily or every other day.

For Western blotting, MDA-MB-231 ($1 \times 10^6$) cells were plated in 100 mm Petri dishes for 24 hours, then serum-starved overnight before treatment with vehicle or ATN-161 (1–100 μmol/L) for different time periods (15–60 minutes). Western blot analyses were carried out using antibodies against focal adhesion kinase (FAK; Santa Cruz Biotechnology, Inc. Santa Cruz, CA), phosphorylated FAK (P-FAK; BioSource International, Inc. Camarillo, CA), mitogen-activated protein kinase (MAPK), phosphorylated MAPK (P-MAPK; Cell Signaling Technology, Inc., Beverly, MA), and β-tubulin (BD Biosciences, Mississauga, Ontario, Canada) as previously described (17). Western blots were detected using enhanced chemiluminescence detection reagents (Perkin-Elmer Life Sciences, Inc., Boston, MA).

### Cell Migration Assay

MDA-MB-231 cells ($3 \times 10^5$ per well) were plated in a six-well plate. Approximately 48 hours later, when the cells were 100% confluent, the monolayer was scratched using a 1 mL pipette tip. Media and nonadherent cells were aspirated, the adherent cells were washed once, and new medium containing various concentrations of ATN-161 (0.1–100 μmol/L) were added. Cells were observed under the microscope at different times and the inhibition of migration was assessed when wounds in the control treated group were closed.

### Animal Protocols

For xenograft studies, 5-week-old (15–20 g) female BALB/c *nu/nu* mice (Charles River, St. Constant, Quebec, Canada) were used throughout (18, 19). Prior to inoculation, MDA-MB-231 cells grown in serum containing culture medium were washed with Hank's balanced buffer and centrifuged at 1,500 rpm for 5 minutes. Cell pellets ($5 \times 10^5$ cells/mouse) were resuspended in 100 μL of Matrigel (Becton Dickinson Labware, Mississauga, Ontario, Canada) and saline mixture (20% Matrigel), and injected s.c. into the right flank of mice. All animals were numbered and kept separately in a temperature-controlled room on a 12-hour light/dark schedule with food and water *ad libitum*. Alternatively, MDA-MB-231-GFP ($1 \times 10^5$) cells were injected in 0.1 mL of cell suspension into the left ventricle of the heart (intracardiac) using a 26-gauge needle (17, 19). In the case of animals inoculated with MDA-MB-231 cells via the s.c. route, tumors were allowed to grow to 20 to 40 $mm^3$. At this stage, animals were randomized and treated with vehicle alone or with different doses of ATN-161 (i.v., 0.05–1 mg/kg/d, thrice a week for 6 weeks). Tumor volumes were determined from caliper measurements obtained weekly. For animals inoculated with MDA-MB-231-GFP cells via the intracardiac route, animals were treated with vehicle alone or with ATN-161 (i.v., 1 mg/kg/d, thrice a week) from the day of tumor cell inoculation for 10 weeks (17, 19–21). In other studies, tumor bearing animals were also treated with scrambled peptide ATN-165 as a control. All animal protocols were in accordance with and approved by the institutional review board.

### Radiologic and Histologic Analysis

High-resolution total body radiologic analysis were carried out as previously described (17, 19–21). The area and number of skeletal lesions ($mm^2$) was determined in both femora and tibia from all animals by using BioQuant image analysis software, version 6.50.10 (BioQuant Image Analysis Corporation, Nashville, TN). All radiographs were carefully evaluated by at least three investigators (including one radiologist) who were blinded to experimental protocols (17, 19–21). Microcomputed tomographic scans on femora were done on a standard desktop micro-CT instrument (model 1072, SkyScan, Aartselaar, Belgium). Images were captured using a 12-bit, cooled CCD camera.

Following completion of the experimental metastasis model (using intracardiac inoculation of cells), mice were sacrificed and their lungs, liver, and spleen were removed. Fresh tissue was sliced at 1 to 5 mm thickness and observed directly under a fluorescence microscope. The number of tumor cells per field of examination from 10 random sites were counted, photographed, and plotted as described previously (14, 15). In addition, radiologically affected and unaffected long bones were excised, fixed, decalcified, and paraffin-embedded (17, 19–21). Sections of 5-μm thickness were prepared for immunohistochemistry and histologic analysis. Histologic measurement of total tumor volume was done in representative sections in the mid-portion of the bone with maximum tumor burden of the tibia from all animals. The tumor volume / tissue volume was measured with BioQuant image analysis software (BioQuant Image Analysis Corporation) and the percentage of tumor volume / total tissue volume was calculated as previously described (17, 19–21).

Immunohistochemical staining was done on tumors harvested from the s.c. model as previously described (17, 19, 22). The staining was done following the protocol described in the Vectastain ABC-AP kit (Vector Laboratories, Inc., Burlingame, CA). The antibodies used were against FAK, P-FAK, MAPK, and P-MAPK as listed above. Anti-Ki-67 (clone MIB-1) was from DAKO Cytomation, Inc. (Mississauga, Ontario, Canada). Immunostaining was quantified by using BioQuant image analysis software as previously described (17, 19, 22). Determination of mitotic index was carried out on H&E-stained sections of control and experimental tumors. Mitotic figures in tumor cells were counted in 10 randomly selected fields under high magnification (×400). Total mitotic index was calculated as the percentage of total tumor cells (23). The Ki-67 index was expressed as the ratio of positive cells to all tumor cells (17, 19).

### Statistical Analysis

All results are expressed as mean ± SE. The statistical significance of the difference in numbers of osteolytic metastases and tumor volume between control and ATN-161–treated groups were analyzed by Mann-Whitney test for nonparametric samples. Statistical comparisons of tumor progression data from image analysis of sections were made using Student's $t$ tests or ANOVA. $P < 0.05$ was considered statistically significant.

## Results

### Effect of ATN-161 on MDA-MB-231 Cell Growth

An analogue of ATN-161 (ATN-453; Ac-PHSCNGGK-biotin-$NH_2$) binds to MDA-MB-231 cells *in vitro*, and this binding can be fit to a two-site binding model with a high-affinity site having a $K_d$ = 2.0 ± 0.9 μmol/L, and a low-affinity site with a $K_d$ = 100.5 ± 32.8 μmol/L (Fig. 1A). This binding can be competed using ATN-161 with an $IC_{50}$ of ~1 μmol/L (data not shown), indicating that extending the COOH terminus of ATN-161 in order to create a binding tracer (ATN-453) has no significant effect on the binding activity. The use of ATN-453 (which is detected using a colorimetric detection system) yields binding data such that a $K_d$ can be determined, but the number of binding sites cannot. The binding of ATN-453 was dependent on the presence of $Mn^{2+}$ (Fig. 1B), which is known to fully activate integrins (24). Very little specific binding was observed in the absence of $Mn^{2+}$ (Fig. 1B) or when $Mg^{2+}$ or $Ca^{2+}$ (data not shown) were used to activate integrins prior to initiating the binding assay. The binding to purified integrins was best-fit using a single-site binding model. The $K_d$ observed for the binding of ATN-453 to either purified immobilized $\alpha_5\beta_1$ (Fig. 1C) or $\alpha_v\beta_3$ (Fig. 1D) was 1.0 ± 0.2 and 0.69 ± 0.1 μmol/L, respectively, consistent with the high-affinity site observed on MDA-MB-231 cells. It should be noted that ATN-161 ultimately forms a disulfide bond with its integrin target and that the $K_d$ represents the reversible portion of the "pulled" binding reaction.

Integrins have been implicated in cell proliferation and migration (25). Thus, we evaluated the effect of ATN-161 on MDA-MB-231 cell proliferation and migration *in vitro*. For the proliferation assay, cells were seeded in six-well plates and incubated in the absence or presence of 2% fetal bovine serum or 2% fetal bovine serum + different doses (1–100 μmol/L) of ATN-161, which was added daily or every other day for 5 days. Cells from triplicate wells in each group were trypsinized and counted at different time points. ATN-161 treatment up to 100 μmol/L showed no significant effect on tumor cell proliferation compared with the vehicle-treated control group of cells (Fig. 2A). Migration assays were done as described in Materials and Methods, and concentrations of ATN-161 up to 100 μmol/L were also evaluated with no observed effect (data not shown). We also evaluated the effect of ATN-161 on integrin-mediated signaling *in vitro*. Treatment of MDA-MB-231 cells with various doses (1–100 μmol/L) of ATN-161 for different time points (15–60 minutes) was followed by the extraction of cellular proteins and Western blot analysis using antibodies directed against FAK and P-FAK. No effect on FAK or P-FAK levels was observed (Fig. 2B). However, ATN-161 significantly inhibited MAPK phosphorylation with maximal effects observed at 20 μmol/L of ATN-161 after 30 minutes of treatment (Fig. 2B).

### Effect of ATN-161 on MDA-MB-231 Tumor Growth

Despite the lack of direct antitumor cell activity *in vitro*, ATN-161 has shown potent antitumor activity in both s.c. and orthotopic mouse models of tumor progression

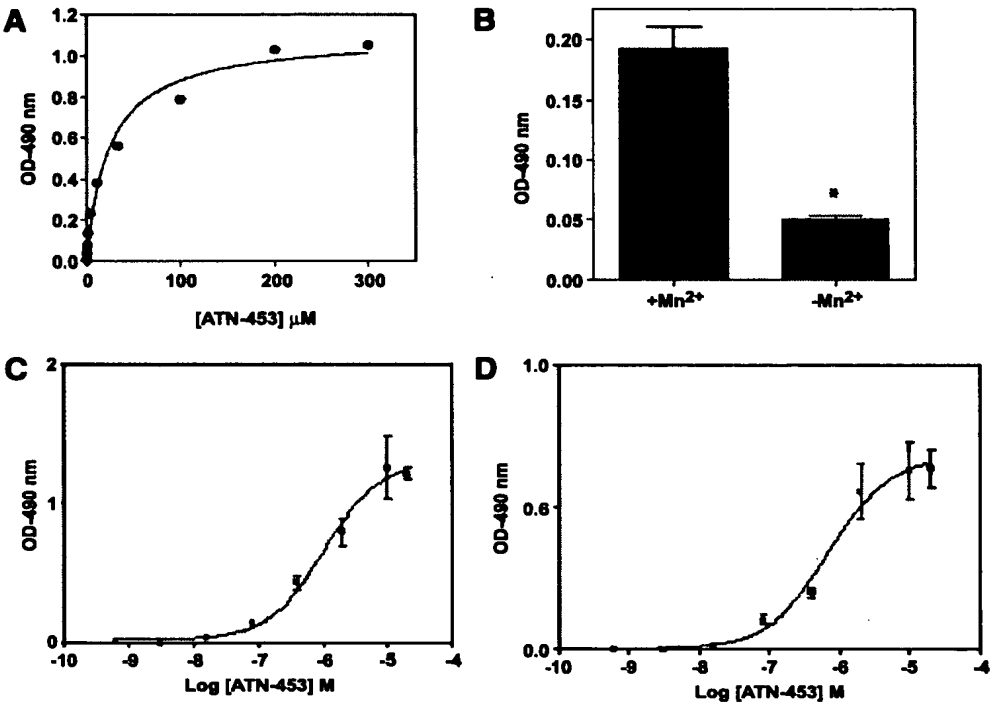


**Figure 1.** Binding of ATN-453 to purified integrins and cells. MDA-MB-231 cells were incubated with increasing concentrations of ATN-453 and bound peptide detected using avidin–horseradish peroxidase as described in "Materials and Methods." Nonspecific binding was determined in the presence of a 100-fold molar excess of ATN-161. Results of a typical experiment (specific binding only) are shown. **A,** ATN-453 binds to a high-affinity ($K_d$ = 2.0 ± 0.9 μmol/L) and a low-affinity site ($K_d$ = 100.5 ± 32.8 μmol/L) on MDA-MB-231 cells. **B,** binding of ATN-453 to cells is dependent on $Mn^{2+}$. Cells were incubated with ATN-453 (1 μmol/L) in the presence or absence of 2 mmol/L of $Mn^{2+}$. *Columns,* mean of two separate experiments; *bars,* ±SE. *, $P < 0.05$, significant difference in the absence of $Mn^{2+}$. **C,** the $K_d$ observed for the binding of ATN-453 binds to purified immobilized $\alpha_5\beta_1$ with a $K_d$ = 1.0 ± 0.2 μmol/L. **D,** ATN-453 binds to purified immobilized $\alpha_v\beta_3$ with a $K_d$ = 0.69 ± 0.1 μmol/L.

(12, 13). In order to evaluate the effect of ATN-161 on MDA-MB-231 tumor growth, $5 \times 10^5$ cells (in 20% Matrigel) were inoculated s.c. into the right flank of female BALB/c *nu/nu* mice. Tumors were allowed to reach a palpable stage (20–40 $mm^3$) approximately 4 weeks post-tumor cell inoculation. Animals were then randomized and treated with vehicle alone or with different doses of ATN-161 (i.v., 0.05–1 mg/kg/d thrice a week) for 6 weeks. Previous

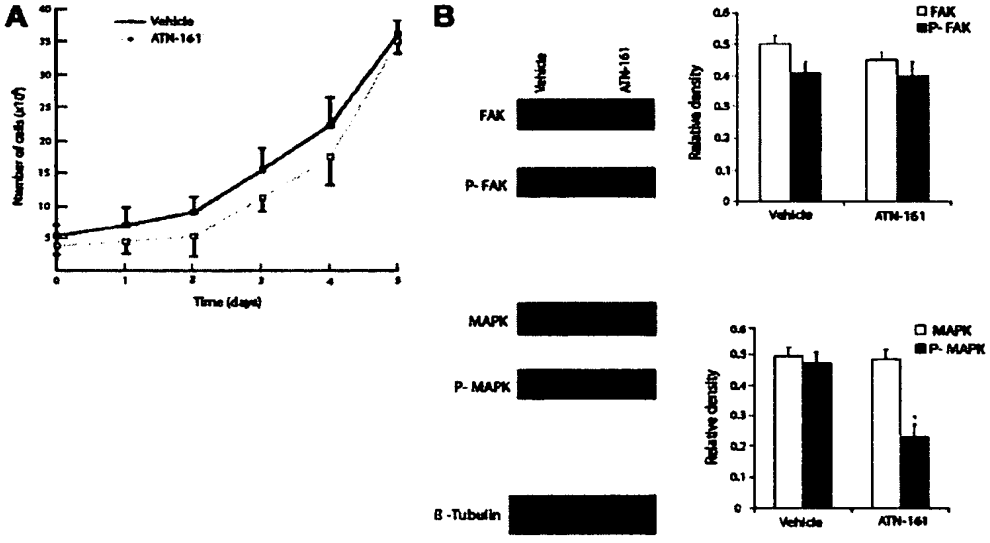


**Figure 2.** Effect of ATN-161 on human breast cancer cells MDA-MB-231 growth and on integrin-mediated signaling pathways *in vitro*. **A,** MDA-MB-231 cells were seeded at a density of $4 \times 10^4$ cells/well in six-well plates and treated with vehicle alone or different doses (1–100 μmol/L) of ATN-161 and were trypsinized and counted using a Coulter counter as described in "Materials and Methods." Effect of 100 μmol/L of ATN-161 on MDA-MB-231 cell growth for 5 d. **B,** MDA-MB-231 cells ($1 \times 10^6$ cells) were plated in Petri dishes and treated with vehicle alone or with 20 μmol/L of ATN-161 for 30 min. Total cellular proteins were extracted and analyzed for the levels of expression of FAK, P-FAK, MAPK, and P-MAPK by Western blotting as described in "Materials and Methods." Expression of β-tubulin was used as a loading control. Representative immunoblots and relative densities to β-tubulin. *Columns,* mean of two separate experiments; *bars,* ±SE. *, $P < 0.05$, significant difference from controls.

studies showed that a scrambled peptide version of ATN-161, Ac-HSPNC-$NH_2$, was inactive *in vivo* and behaved identically to vehicle alone (12, 26). Thus, vehicle alone was used as a control for all the animal studies presented here. Tumor volume was determined at weekly intervals. Treatment with ATN-161 showed a dose-dependent effect in reducing tumor volume as compared with control groups of animals receiving vehicle alone (Fig. 3). Although both 0.1 and 1 mg/kg of ATN-161 had a marked effect on reducing tumor volume, no statistically significant increment in these antitumor effects were seen between doses of 0.1 and 1 mg of ATN-161. It should be noted that the plasma $C_{max}$ of ATN-161 measured in preclinical pharmacokinetic studies in mice at a 1 mg/kg dose was ~2 to 5 μmol/L,[4] which is high enough to bind to $\alpha_5\beta_1$ and $\alpha_v\beta_3$ in the host, as well as to the high-affinity binding site on MDA-MB-231 cells. Higher doses of ATN-161 did not improve the antitumor activity that was observed at the 1 mg/kg dose, which was subsequently selected for all future *in vivo* studies. Treatment of tumor-bearing animals with scrambled peptide ATN-165 had no significant effect on tumor volume (data not shown). In addition, no significant differences in animal weight were observed between control and treated groups indicating that ATN-161 treatment was well-tolerated (data not shown).

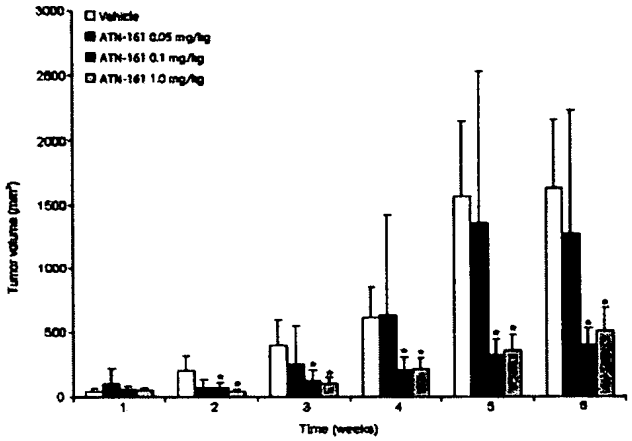


**Figure 3.** Effect of ATN-161 on MDA-MB-231 tumor growth *in vivo*. Female BALB/c *nu/nu* mice were injected s.c. into the right flank with $5 \times 10^6$ MDA-MB-231 cells. Once the tumor volume reached 20 to 40 $mm^3$ (week 4), animals were randomized and treated with vehicle alone or different doses (i.v., 0.05–1 mg/kg/d thrice a week) for 6 wks as described in "Materials and Methods." Tumor volume was measured weekly and comparisons were made with tumor-bearing animals receiving vehicle control. *Columns*, mean of 10 animals in each group from two different experiments; *bars*, ±SE. *, $P < 0.05$, significant differences from control tumor-bearing animals receiving vehicle alone.

### Effect of ATN-161 on MDA-MB-231 Skeletal Metastasis

Because skeletal metastasis is a common complication associated with human breast cancer, we examined the effect of ATN-161 in a xenograft model of experimental skeletal metastasis using MDA-MB-231 cells transfected with GFP. We have extensively characterized these experimental cells both *in vitro* and *in vivo* (14, 15, 19). The use of these MDA-MB-231-GFP cells allowed us to evaluate the effect of ATN-161 on tumor metastasis to both skeletal and nonskeletal sites. In these studies, MDA-MB-231-GFP cells were inoculated into the left ventricle of 5-week-old female BALB/c *nu/nu* mice. This route of tumor cell inoculation routinely results in the development of tumor metastasis to the long bone (tibia, femur), which can be visualized by radiologic examination (17, 19–21). From the day of tumor cell inoculation, animals were treated with vehicle alone or ATN-161 (i.v., 1 mg/kg, thrice a week) for 10 weeks. Radiologic analysis of animals treated with vehicle alone showed the presence of lesions in the tibia and femur from week 5 post-tumor cell inoculation, and the size and number of these skeletal lesions continued to increase over time. Animals in both control and experimental groups were evaluated by radiographic analysis at weekly intervals. In these studies, 10% of animals developed tumors in their heart due to the inoculation of tumor cells in the cardiac muscle and died by week 3 post-tumor cell inoculation. These animals were not included in the statistical analysis to evaluate the antitumor effects of ATN-161 (data not shown). In the control group of animals receiving vehicle alone, >90% animals ($n = 22/24$) showed the presence of distinct skeletal lesions at week 5, and continued to show progressive increases over time. At week 10 post-tumor cell inoculation, all control animals showed radiologic or histologic evidence of skeletal lesions. In contrast, at week 10 post-tumor cell inoculation, only 70% ($n = 17/24$) of the animals receiving ATN-161 (1 mg/kg/d) showed radiologic evidence of skeletal lesions. In addition, the skeletal lesion area was markedly lower in ATN-161–treated animals as compared with the control group of animals receiving vehicle alone. However, at this time point, no radiologic evidence of skeletal lesions was observed in 30% of the animals in the ATN-161–treated group. Statistical analysis of lesion in the long bones of control and ATN-161–treated groups of animals showed a significant decrease in the frequency and incidence of skeletal lesions following treatment with ATN-161 (Fig. 4A). Animals were sacrificed at week 11 and their long bones removed and subjected to further analysis by microcomputed tomography. These studies showed that animals receiving vehicle alone had significantly larger lesion areas than animals receiving ATN-161 (Fig. 4B). Following microcomputed tomography analysis, long bones were decalcified, fixed, and subjected to histologic analysis, which showed the presence of tumor cells in the bone marrow cavity and the destruction of both trabecular and cortical bone. A significant decrease in tumor volume / tissue volume ratio was also observed in the ATN-161–treated animals as compared with controls (Fig. 4C).

[4] Unpublished results.

### Effect of ATN-161 on Soft Tissue Metastases

The use of MDA-MB-231-GFP cells allowed us to detect the presence of tumor cells in different organs by quantifying the number of GFP-positive tumor cells. Following 10 weeks of treatment with vehicle alone or of ATN-161 (i.v., 1 mg/kg/d thrice a week), animals were sacrificed and different organs (lungs, liver, and spleen) were removed. Evaluation of these organs for the presence of microscopic tumor foci revealed the presence of disseminated GFP-positive tumor cells. The number of these metastatic tumor cells was significantly lower in animals treated with ATN-161 as compared with the cohort of animals receiving vehicle alone (Fig. 5).

### Effect of ATN-161 on Tumor Vascularization and Tumor Cell Proliferation *In vivo*

Because integrins are known to play a major role in tumor angiogenesis, a key event in tumor metastasis, we evaluated the effect of ATN-161 on tumor vascularization. Immunohistochemical analysis of primary tumors treated with vehicle alone or ATN-161 (1 mg/kg/d) showed significantly decreased (43%) microvessel density following treatments with ATN-161 (Fig. 6A). In addition, we evaluated the effect of ATN-161 on MDA-MB-231 proliferation *in vivo*. Primary tumors were subjected to H&E staining and evaluated for the number of mitotic cells. These studies showed a significantly lower number of mitotic cells in experimental tumors from animals treated with ATN-161 (Fig. 6A). In order to establish greater specificity for the antiproliferative response observed in ATN-161–treated animals, tumor sections were analyzed by immunohistochemistry using an antibody directed against Ki-67. The Ki-67 immunostaining was significantly lower in tumor sections from animals treated with ATN-161 as compared with controls, confirming the mitotic index results (Fig. 6A). Immunostaining for FAK, P-FAK, MAPK, and P-MAPK showed no differences in the levels of FAK or P-FAK in tumors *in vivo*, but showed decreased expression of P-MAPK, consistent with the *in vitro* results (Fig. 6B).

## Discussion

During the past decade, despite numerous advances in the identification of agents with activity in the advanced breast cancer setting, metastatic breast cancer continues to represent a huge unmet medical need. The effective treatment of tumors that metastasize to the bone will likely require targeting several compartments, including the tumor cells themselves, the neovessels that are formed to support the tumor cells, and the osteoclasts that are involved in bone remodeling and the formation of osteolytic metastatic lesions. Recent studies have implicated integrins, and specifically, $\alpha_v\beta_3$ as having a causal role in the metastasis to bone, and more precisely, in the osteolytic variant that is usually observed in patients with breast cancer. In addition, breast cancer metastases induces angiogenesis locally when arrested in the bone, which may also fuel the growth of the metastatic lesions (27). Although the integrin $\alpha_5\beta_1$ has not been specifically implicated in angiogenesis arising from the metastasis of breast cancer

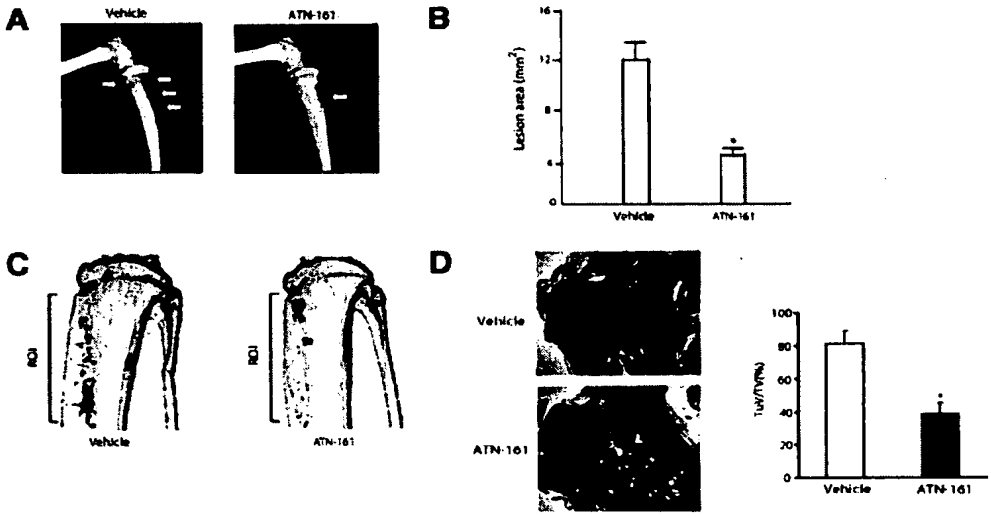


**Figure 4.** Radiographic and histologic analysis of MDA-MB-231-GFP tumor-bearing animals receiving vehicle alone or ATN-161. **A**, representative radiograph of female BALB/c *nu/nu* mice at week 10 after the inoculation of MDA-MB-231-GFP via the intracardiac route, and treatment with vehicle alone or of ATN-161 (i.v., 1 mg/kg/d thrice a week) for 10 wks. Area of skeletal lesions in control and ATN-161 – treated animals (*arrowheads*) was scored at week 10 post-tumor cell inoculation as described in "Materials and Methods." **B**, long bones were removed and subjected to analysis by microcomputed tomography. Images were rendered three-dimensionally and the area of skeletal metastasis was highlighted as the region of interest (*ROI*). Results are representative of five animals in each group. **C**, all long bones were removed and subjected to bone histology. Histologic analysis of tibia of all mice treated with vehicle alone or ATN-161 was carried out as described in "Materials and Methods." *Columns*, mean of at least 12 animals in each group from two different experiments; *bars*, ±SE. *, $P < 0.05$, significant differences in tumor volume / tissue volume (*TuV/TV*) from control animals.

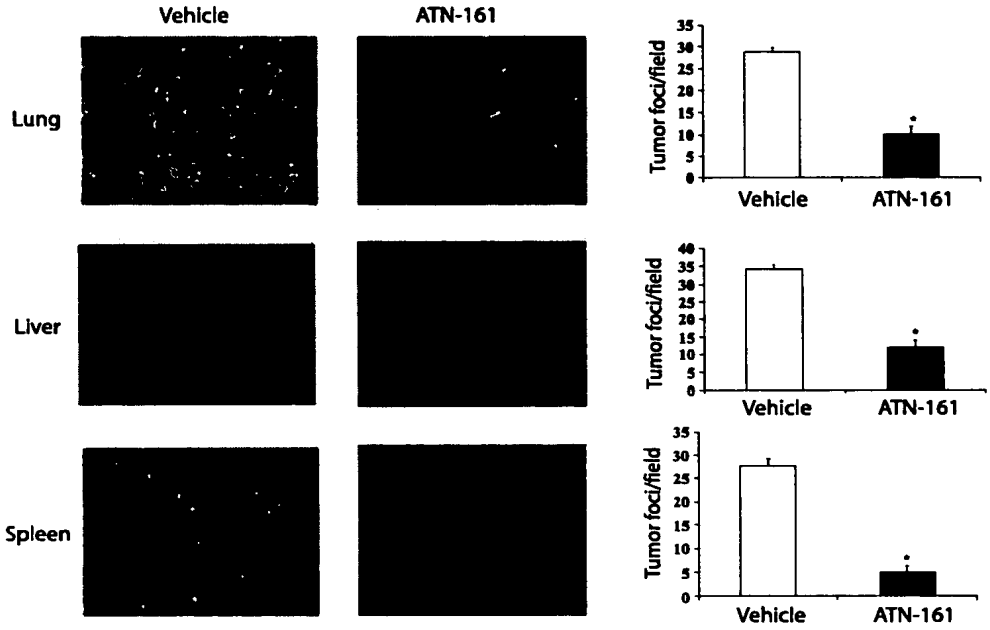


**Figure 5.** Effect of ATN-161 on MDA-MB 231-GFP breast cancer micrometastases. To evaluate the effect of ATN-161 on micrometastasis to various organs, female BALB/c *nu/nu* mice were inoculated with human breast cancer cells ($1 \times 10^5$) transfected with green fluorescent protein (MDA-231-GFP) into the left ventricle (intracardiac). Animals were treated with vehicle alone or ATN-161 (i.v., 1 mg/kg/d thrice a week) for 10 wk as described in "Materials and Methods." Animals were sacrificed at week 11 post-tumor cell inoculation and different organs were collected. One-millimeter-thick slices of lungs, liver, and spleen were cut, placed on glass slides, and examined directly under a fluorescent microscope for the presence of GFP-expressing tumor foci. Tumor foci in 10 random fields per slide (five slides per organ) were counted to determine the average number of tumor foci in these organs. Results are representative of 12 animals in each group from two different experiments. *Columns*, mean of at least 12 animals in each group from two different experiments; *bars*, ±SE. *, $P < 0.05$, significant changes in tumor foci per field.

cells, it has been shown to be critical for tumor angiogenesis in general as well as for the metastasis of other tumor types (27–29). Thus, we hypothesized that pharmacologic targeting of both $\alpha_v\beta_3$ and $\alpha_5\beta_1$ would lead to significant effects on the establishment and outgrowth of breast cancer metastasis in bone and in soft tissue.

In order to test this hypothesis, we used an integrin-binding peptide, ATN-161, derived from the synergy region of fibronectin, which binds to both $\alpha_5\beta_1$ and $\alpha_v\beta_3$ *in vitro*. The synergy region of fibronectin has been shown to interact with $\alpha_5\beta_1$ and mediates the high-affinity RGD-dependent adhesion of cells to fibronectin (30). Although several integrin binders have been described in the literature, ATN-161 is unique because it is not an RGD-based sequence and does not affect or alter cell adhesion, indicating that it may affect integrin signaling in a manner different and more subtle than the RGD-based integrin antagonists (31, 32).

Despite the fact that ATN-161 was able to bind to MDA-MB-231 cells with an affinity consistent with the binding to purified $\alpha_5\beta_1$ and $\alpha_v\beta_3$, ATN-161 did not seem to affect serum-driven MDA-MB-231 cell proliferation *in vitro*. At least one report has implicated $\alpha_v\beta_3$ as being important to the proliferation of MDA-MB-231 cells (33), which raises the issue of the target for ATN-161 on MDA-MB-231 cells. However, there is some controversy in the literature as to the level of expression of $\alpha_5\beta_1$ and $\alpha_v\beta_3$ in parental MDA-MB-231 cells. Isolated reports claim high levels of $\alpha_5\beta_1$ and $\alpha_v\beta_3$ expression in these cells (34), whereas other studies have shown low-level expression of these integrins with increased expression observed in subclones isolated from metastatic lesions (8). In general, the expression levels of these integrins in breast cancer and other cell lines have been analyzed using semiquantitative methods such as Western blotting, immunohistochemistry, and flow cytometry. There is also a striking lack of quantitative binding data in the literature that measures the receptor copy number of $\alpha_5\beta_1$ and $\alpha_v\beta_3$ on cells or in tumor tissues. Our binding assay does not allow the determination of the number of binding sites for ATN-161 on MDA-MB-231, making it impossible to compare the expression of $\alpha_5\beta_1$ and $\alpha_v\beta_3$ observed in these cells by other investigators. Thus, the lack of an antiproliferative effect of ATN-161 on MDA-MB-231 cells *in vitro* could be explained by the low copy number of $\alpha_5\beta_1$ and $\alpha_v\beta_3$ or the binding of ATN-161 to an alternate target and studies to resolve these issues are currently under way. To that end, one feature of ATN-161 that initially concerned us was the presence of a free cysteine residue that could lead to promiscuous binding to a number of cysteine or disulfide-containing proteins. However, a preliminary analysis of the binding of ATN-453 to blood cells and plasma proteins has shown

substantial specificity, with appreciable binding occurring only to platelets (which display $\alpha_v\beta_3$) and albumin. Additional studies attempting to isolate the target in MDA-MB-231 and endothelial cells are also under way.

Serum-starved conditions were used to isolate the effect of ATN-161 on integrin ligated cells in the absence of other pro-proliferative or pro-migratory stimuli. In these experiments, MDA-MB-231 cells are initially plated in the presence of serum, which is abundant in fibronectin and vitronectin, and these serum proteins ligate cell surface integrins in the MDA-MB-231 cells, leading to the adhesion of these cells. The cells are then transferred to serum-free conditions. Because ATN-161 does not inhibit integrin-mediated adhesion, it was not surprising that it did not affect FAK activation under the conditions of our assay. In contrast with FAK, MAPK phosphorylation was inhibited *in vitro*. Constitutive MAPK activation is known to occur in tumor cells and high basal levels of activated MAPK have been described, specifically, in MDA-MB-231 (35) although adhesion of these cells could also up-regulate MAPK activation (36). However, the inhibition of MAPK by ATN-161 in MDA-MB-231 tumor cells *in vitro* was insufficient by itself to affect the proliferation or migration of these cells, and some studies have shown that the simultaneous inhibition of both FAK and MAPK signaling is required to attenuate integrin-mediated migration or proliferation (36). In addition to low copy numbers or an alternate receptor for ATN-161, this could also explain the lack of an effect on proliferation of MDA-MB-231 cells *in vitro*. In contrast, ATN-161 had significant effects on the proliferation of MDA-MB-231 tumors *in vivo* (Fig. 6). A significant inhibition of angiogenesis was also observed in the ATN-161–treated animals, suggesting the possibility that the inhibition of proliferation observed in tumor

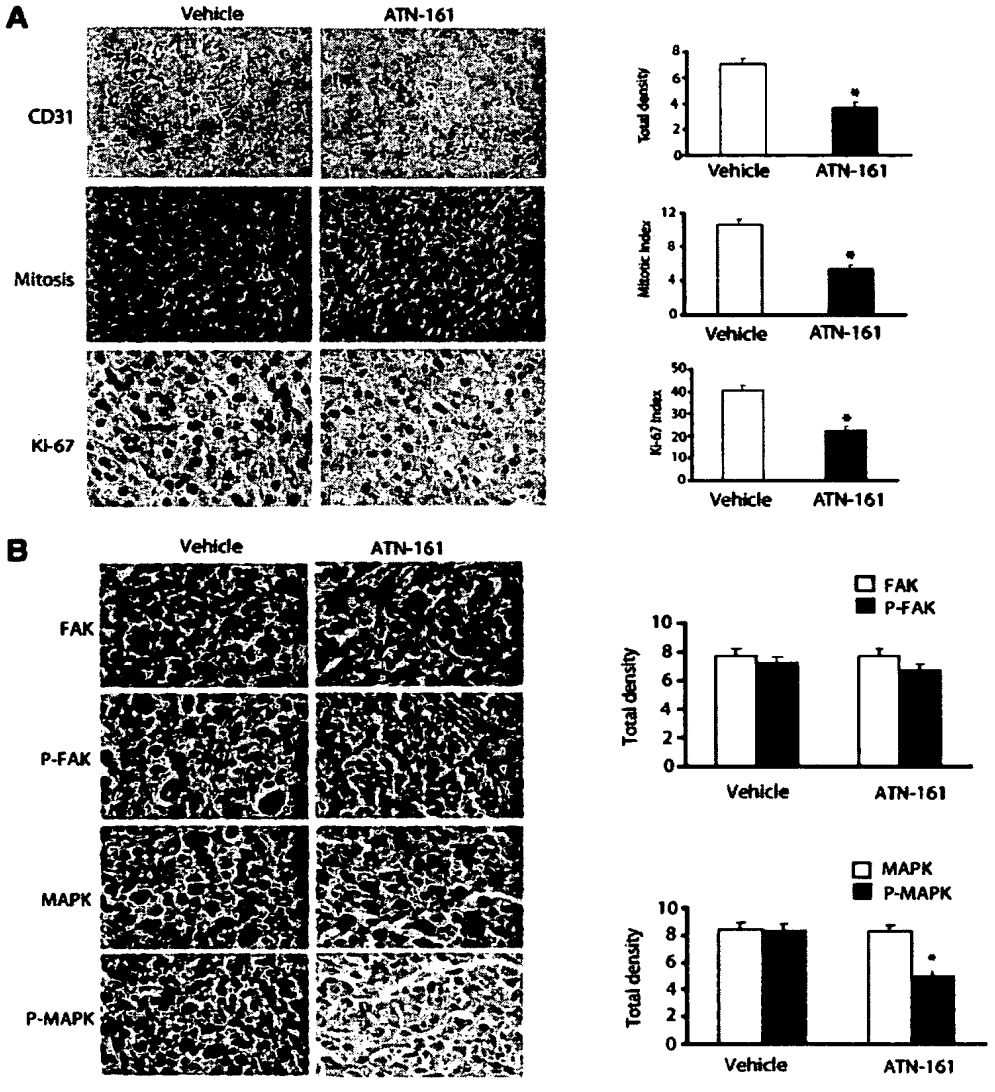


**Figure 6.** Effect of ATN-161 on vascularization, mitotic index, and integrin-mediated signaling pathway in primary MDA-MB-231 tumors. **A,** expression of CD31 as an index of tumor vessel density, mitotic index, and Ki-67 immunohistochemical analysis as an index of tumor cell proliferation *in vivo* was determined in MDA-MB-231 tumors as described on "Materials and Methods." **B,** expression of FAK, P-FAK, MAPK, or P-MAPK was determined and quantified on histologic sections of MDA-MB-231 tumors from animals treated with vehicle control or ATN-161 as described in "Materials and Methods." Quantitative analysis was carried out in 10 high-power fields in control and experimental sections (*arrowheads,* mitotic cells; magnification, ×400). *Columns,* mean of six animals in each group from two separate experiments; *bars,* ±SE. *, $P < 0.05$, significant difference from controls (*right*).

xenografts is indirect and results from decreased neovascularization of the tumor. The indirect effects of inhibiting angiogenesis have also been observed on extracellular signal-regulated kinase phosphorylation in other tumor types, raising this possibility for the MDA-MB-231 tumors used in this study (37). This inhibition of extracellular signal-regulated kinase phosphorylation could account for the decreased proliferation of MDA-MB-231 tumors because activated extracellular signal-regulated kinase is known to mediate the proliferation of this tumor cell line. Finally, the lack of inhibition of proliferation of MDA-MB-231 cells treated with ATN-161 *in vitro* is consistent with the hypothesis that the effects of ATN-161 on proliferation *in vivo* are indirect and require the inhibition of angiogenesis.

In addition to direct effects on MDA-MB-231 cells, the antitumor effects of ATN-161 could also be indirect through effects on osteoclast function or angiogenesis. ATN-161 has previously been shown to inhibit angiogenesis, although in that study, the inhibition of angiogenesis alone was insufficient to affect tumor growth and soft tissue metastasis (26). ATN-161 could affect endothelial cells directly or angiogenesis indirectly. For example, the inhibition of MAPK activation in MDA-MB-231 cells has been shown to down-regulate vascular endothelial growth factor expression, which would be expected to attenuate angiogenesis (38). Direct inhibitors of osteoclast function have also been shown to inhibit the formation of bone metastasis (39, 40). Consistent with the lack of promiscuous binding described above, a significant amount of ATN-161 (~40%), which was not distributed to the tissue, remains free in plasma even 2 hours after i.v. injection and is presumably available for binding to its target in a tumor.[4] A recently completed phase I study of ATN-161 showed that at doses >0.5 mg/kg in man, a $C_{max}$ of ~10 μmol/L or greater can be achieved, which exceeds the *in vitro* $IC_{50}$ for integrin binding, indicating that it is possible to reach a sufficiently high enough concentration of the peptide in plasma to nearly saturate its targets (41). Furthermore, ATN-161 antitumor activity has been described in several *in vivo* studies, confirming that sufficient peptide is able to remain free to elicit an antitumor effect (12, 13). Thus, we evaluated whether ATN-161 could inhibit MDA-MB-231 growth and metastasis in nude mice. ATN-161 significantly inhibited the growth of primary MDA-MB-231 tumors. Immunohistochemical analysis of sections obtained from these tumors indicated that MAPK activation was inhibited, whereas FAK was not, consistent with the *in vitro* results. In addition, there was a significant decrease in the proliferative index measured by Ki-67 immunostaining in the tumors from ATN-161–treated animals. Because the inhibition of MAPK activation *in vitro* was insufficient to directly inhibit the proliferation of these cells, it is likely that the inhibition of angiogenesis observed using CD31 immunostaining contributed to the inhibition of proliferation observed *in vivo*, and that a combined inhibition of angiogenesis/tumor cell MAPK activation resulted in the observed antitumor effects. Despite the inhibition of proliferation observed *in vivo*, there did not seem to be any effect on cell survival as no difference in terminal nucleotidyl transferase (TdT)–mediated nick end labeling staining was observed between the treated and untreated groups (data not shown).

The observation of antitumor activity in s.c. MDA-MB-231 tumors was extended in a model of MDA-MB-231 experimental metastasis. Inoculation of tumor cells via the intracardiac route results in metastasis to the bone, as well as to soft tissue, and ATN-161 significantly inhibited the outgrowth of metastases at all metastatic sites. In some animals, ATN-161 completely inhibited the formation of bone metastases in a model which is historically refractory to systemic antitumor treatments. This observation was extremely encouraging in that very few agents, especially noncytotoxic agents, have any effect on the formation of metastatic lesions in the bone. The results presented herein, combined with previously published results of the synergistic activity of ATN-161 with chemotherapy (12), provide a basis for future studies of ATN-161 in breast cancer models in combination with chemotherapeutic agents such as docetaxel. The demonstration of enhanced antitumor activity against bone metastasis with a combination treatment of ATN-161 and chemotherapy would provide the rationale for developing ATN-161 combinations for the treatment of patients with advanced breast cancer.

**Acknowledgments**

The authors thank Dr. Ida Khalili, Department of Radiology, McGill University Health Centre, for carefully reviewing all X-rays.

**References**

1. Schwartz MA, Schaller MD, Ginsberg MH. Integrins: emerging paradigms of signal transduction. Annu Rev Cell Dev Biol 1995;11:549–99.

2. Brakebusch C, Bouvard D, Stanchi F, Sakai T, Fassler R. Integrins in invasive growth. J Clin Invest 2002;109:999–1006.

3. Abdel-Ghany M, Cheng HC, Elble RC, Pauli BU. The breast cancer β4 integrin and endothelial human CLCA2 mediate lung metastasis. J Biol Chem 2001;276:25438–46.

4. Matsuura N, Puzon-McLaughlin W, Irie A, Morikawa Y, Kakudo K, Takada Y. Induction of experimental bone metastasis in mice by transfection of integrin α4β1 into tumor cells. Am J Pathol 1996;148:55–61.

5. Koukoulis GK, Virtanen I, Korhonen M, Laitinen L, Quaranta V, Gould VE. Immunohistochemical localization of integrins in the normal, hyperplastic, and neoplastic breast. Correlations with their functions as receptors and cell adhesion molecules. Am J Pathol 1991;139:787–99.

6. Liapis H, Flath A, Kitazawa S. Integrin αVβ3 expression by bone-residing breast cancer metastases. Diagn Mol Pathol 1996;5:127–35.

7. Plow EF, Haas TA, Zhang L, Loftus J, Smith JW. Ligand binding to integrins. J Biol Chem 2000;275:21785–8.

8. Pecheur I, Peyruchaud O, Serre CM, et al. Integrin α(v)β3 expression confers on tumor cells a greater propensity to metastasize to bone. FASEB J 2002;16:1266–8.

9. Carron CP, Meyer DM, Engleman VW, et al. Peptidomimetic antagonists of αvβ3 inhibit bone resorption by inhibiting osteoclast bone resorptive activity, not osteoclast adhesion to bone. J Endocrinol 2000;165:587–98.

10. Hwang R, Varner J. The role of integrins in tumor angiogenesis. Hematol Oncol Clin North Am 2004;8:991–1006, vii.

11. Bernstein L. Epidemiology of endocrine-related risk factors for breast cancer. J Mammary Gland Biol Neoplasia 2002;7:3–15.

12. Stoeltzing O, Liu W, Reinmuth N, et al. Inhibition of integrin α5β1 function with a small peptide (ATN-161) plus continuous 5-FU infusion

reduces colorectal liver metastases and improves survival in mice. Int J Cancer 2003;104:496 – 530.

13. Livant DL, Brabec RK, Pienta KJ, et al. Anti-invasive, antitumorigenic, and antimetastatic activities of the PHSCN sequence in prostate carcinoma. Cancer Res 2000;60:309 – 20.

14. Guo Y-J, Higazi AA-R, Arakelian A, et al. A peptide derived from the non-receptor binding region of urokinase plasminogen activator (uPA) inhibits tumor progression and angiogenesis and induces tumor cell death *in vivo*. FASEB J 2000;14:1400 – 10.

15. Pakneshan P, Szyf M, Farias-Eisner R, Rabbani SA. Reversal of the hypomethylation status of urokinase (uPA) promoter blocks breast cancer growth and metastasis. J Biol Chem 2004;279:31735 – 44.

16. Doñate F, Guan X, Callahan JA, Mazar AP, Parry GC. ATN-161 (Ac-PHSCN-NH2) has potent anti-angiogenic activity through multiple mechanisms of action and localizes to newly formed blood vessels *in vivo*. Proc Am Assoc Cancer Res 2005;44:63.

17. Khalili P, Arakelian A, Chen G, Singh G, Rabbani SA. Role of Herceptin in abrogating the progression of skeletal metastases in a xenograft model of human breast cancer. Oncogene 2005;24:6657 – 66.

18. Gurber AD, Pauli BU. Tumorigenicity of human breast cancer is associated with loss of the $Ca^{+}$-activated chloride channel CLCA2. Cancer Res 1999;59:5488 – 91.

19. Rabbani SA, Khalili P, Arakelian A, Pizzi H, Chen G, Goltzman D. Regulation of parathyroid hormone related peptide by estradiol (E2): effect of tumor growth and metastasis *in vitro* and *in vivo*. Endocrinology 2005;146:2885 – 94.

20. El Abdaimi K, Dion N, Papavasiliou V, et al. The vitamin D analogue EB 1089 prevents skeletal metastasis and prolongs survival time in nude mice transplanted with human breast cancer cells. Cancer Res 2000;60:4412 – 8.

21. Yin JJ, Selander K, Chirgwin JM, et al. TGF-β signaling blockade inhibits PTHrP secretion by breast cancer cells and bone metastases development. J Clin Invest 1999;103:197 – 206.

22. Chen G, Shukeir N, Potti A, Sircar K, Aprikian A, Goltzman D, Rabbani SA. Upregulation of Wnt-1 and β-catenin production in advanced metastatic human prostate cancer: potential pathogenetic and prognostic implications. Cancer 2004;101:1345 – 56.

23. Wilson JW, Potten CS. The effect of exogenous prostaglandin administration on tumor size and yield in Min/+ mice. Cancer Res 2000; 60:4645 – 53.

24. Byzova TV, Kim W, Midura RJ, Plow EF. Activation of integrin α(V)β(3) regulates cell adhesion and migration to bone sialoprotein. Exp Cell Res 2000;254:299 – 308.

25. Stupack DG, Cheresh DA. Integrins and angiogenesis. Curr Top Dev Biol 2004;64:207 – 38.

26. Danese S, Sans M, Spencer D, et al. Starving the inflamed gut: angiogenesis blockade as a novel therapeutic approach to experimental colitis. Gastroenterology 2005;128:A40.

27. Winding B, Misander H, Sveigaard C, et al. Human breast cancer cells induced angiogenesis, recruitment, and activation of osteoclasts in osteolytic metastasis. J Cancer Res Clin Oncol 2000;126:631 – 40.

28. Kim S, Bell K, Mousa SA, Varner JA. Regulation of angiogenesis *in vivo* by ligation of integrin α5β1 with the central cell-binding domain of fibronectin. Am J Pathol 2000;156:1345 – 6.

29. Tani N, Higashiyama S, Kawaguchi N, et al. Expression level of integrin α5 on tumour cells affects the rate of metastasis to the kidney. Br J Cancer 2003;88:327 – 33.

30. Mould AP, Askari JA, Aota S, et al. Defining the topology of integrin α5β1-fibronectin interactions using inhibitory anti-α5 and anti-β1 monoclonal antibodies. Evidence that the synergy sequence of fibronectin is recognized by the amino-terminal repeats of the α5 subunit. J Biol Chem 1997;272:17283 – 92.

31. Adderley SR, Fitzgerald DJ. Glycoprotein IIb/IIIa antagonists induce apoptosis in rat cardiomyocytes by caspase-3 activation. J Biol Chem 2000;275:5760 – 6.

32. Krueger JS, Keshamouni VG, Antanaskova N, Reddy KB. Temporal and quantitative regulation of mitogen-activated protein kinase (MAPK) modulates cell motility and invasion. Oncogene 2001;20:4209 – 18.

33. Vellon L, Menendez JA, Lupu R. αVβ3 integrin regulates heregulin (HRG)-induced cell proliferation and survival in breast cancer. Oncogene 2005;24:3759 – 73.

34. Wong NC, Mueller BM, Barbas CF, et al. α-v integrins mediate adhesion and migration of breast carcinoma cell lines. Clin Exp Metastasis 1998;16:50 – 61.

35. Lev DC, Kim LS, Melnikova V, Ruiz M, Ananthaswamy HN, Price JE. Dual blockade of EGFR and ERK1/2 phosphorylation potentiates growth inhibition of breast cancer cells. Br J Cancer 2004;91:795 – 802.

36. Campbell S, Otis M, Cote M, Gallo-Payet N, Payet MD. Connection between integrins and cell activation in rat adrenal glomerulosa cells: a role for Arg-Gly-Asp peptide in the activation of the p42/p44(mapk) pathway and intracellular calcium. Endocrinology 2003;144:1486 – 95.

37. Panka DJ, Atkins MB, Mier JW. Targeting the mitogen-activated protein kinase pathway in the treatment of malignant melanoma. Clin Cancer Res 2006;12:2371s – 5s.

38. Chelouche-Lev D, Miller CP, Tellez C, Ruiz M, Bar-Eli M, Price JE. Different signalling pathways regulate VEGF and IL-8 expression in breast cancer: implications for therapy. Eur J Cancer 2004;40:2509 – 18.

39. Peyruchaud O, Serre CM, NicAmhlaoibh R, Fournier P, Clezardin P. Angiostatin inhibits bone metastasis formation in nude mice through a direct anti-osteoclastic activity. J Biol Chem 2003;278:45826 – 32.

40. Keller ET. The role of osteoclastic activity in prostate cancer skeletal metastases. Drugs Today (Barc) 2002;38:91 – 102.

41. Cianfrocca ME, Kimmel KA, Gallo J, et al. Phase I trial of the antiangiogenic peptide ATN-161 (Ac-PHSCN-NH2), a β integrin antagonist, in patients with solid tumors. Br J Cancer 2006;94:1621 – 6.

# SPECTROPHOTOMETRIC STUDIES

## II. PREPARATIONS FROM WASHED BLOOD CELLS; NITRIC OXIDE HEMOGLOBIN AND SULFHEMOGLOBIN

By DAVID L. DRABKIN and J. HAROLD AUSTIN

*(From the Department of Physiological Chemistry and the John Herr Musser Department of Research Medicine, School of Medicine, University of Pennsylvania, Philadelphia)*

(Received for publication, June 10, 1935)

In this paper evidence will be presented which indicates that spectrophotometric constants are more precisely reproducible with solutions prepared from washed erythrocytes than from hemolyzed whole blood, used in our earlier analyses (1). The data, obtained under standard conditions which will be defined, include the absorption curves of $HbO_2$, Hb, HbCO, MHbCN, HbNO (nitric oxide hemoglobin), and SHb (sulfhemoglobin). The two latter pigments were the main subjects of the investigation.

HbNO was prepared under conditions which excluded the presence of higher oxides of nitrogen and the possible formation of MHb. These precautions were not taken in previous studies of HbNO (2) and rendered doubtful the older spectroscopic data.

SHb probably has not been prepared in a pure state, as claimed (3). We have derived the spectrum of this pigment by extrapolation from absorption data upon mixtures of Hb and SHb. We were thus able to establish the identity of the abnormal pigment present in the blood of a patient with clinical sulfhemoglobinemia (4).

### *Methods*

The spectrophotometer and technique employed were those described in our previous publication (1), except for the following modifications.

*Preparation of Hemoglobin Solutions*—Dog blood was obtained

by cardiac puncture from normal, unfed animals. It was defibrinated. The serum was separated by centrifuging and the cells were washed three times with about 4 volumes of 0.9 per cent saline. The washed erythrocytes were hemolyzed by the addition of enough distilled water to make 10 times the original volume of blood employed. This solution was filtered to remove cell debris. It was kept on ice and was not used longer than for a period of 4 days. From the 1:10 stock solution the more dilute solutions (1:50 or 1:100) were prepared.

*Notation*—In our absorption curves $\epsilon$ values are plotted both against wave-length, $\lambda$, in $m\mu$, and wave number, $\nu$, which may be defined as the *frequency per cm.* (5) and which is the reciprocal of $\lambda$ expressed in centimeters ($\nu = 1/(\lambda \text{ in } m\mu \times 10^{-7})$). Although most spectrometers are calibrated in terms of $\lambda$, $\nu$ is more useful in the interpretation of spectroscopic data (6).

Our extinction coefficients, $\epsilon$, are qualified by the concentration of pigment, $c$, expressed in mM per liter where 1 M indicates 1 mole of porphyrin, which for hemoglobin is equivalent to 1 gm. atomic weight of Fe or 1 mole of $O_2$ capacity. Standard values are given as $\epsilon(c = 1 \text{ mM per liter})$, obtained from the equation

$$\epsilon(c = 1 \text{ mM per liter}) = \frac{\epsilon_{\text{observed}}}{d(\text{depth})_{\text{cm.}} \times c(\text{actual concentration in mM per liter})}$$

$\epsilon$ values at standard concentrations are far more useful than the archaic absorption constant $A = \check{c}/\epsilon$. The use of molar units for $c$ permits ready comparison of the absorption spectra of all derivatives and relatives of hemoglobin.

For comparison with Table III of our earlier paper (1) $\epsilon(c = 1$ mM per liter$) = 1/60A = 167/(A \times 10^4)$. In Fig. 1 of that paper the ordinates designated as $1/A$ are actually $1/(A \times 10^4)$. For convenience we have introduced at the right of our graphs a scale of $\epsilon(c = 1$ gm. Hb per 100 cc.$) = \frac{1}{1.67}\epsilon(c = 1$ mM per liter$)$.

*Quantitative Estimation of Pigment Concentration*—Total pigment was determined by measuring the absorption of cyanmethemoglobin (cyanhemoglobin), MHbCN, prepared from suitable aliquots by the addition of $K_3Fe(CN)_6$ to a final concentration of 0.6 mM per liter and KCN to a concentration of 0.8 mM per liter, the pigment concentration being of the order of 0.1 to 0.2 mM per

liter. The constants for MHbCN which were utilized in this determination are: $\epsilon(c = 1$ mM per liter$) = 11.1$ at $\lambda$ 551, 11.5 at $\lambda$ 545, and 11.5 at $\lambda$ 540 $m\mu$ (1). At these wave-lengths the molar extinction coefficient of $K_4Fe(CN)_6$ has an average value of only 0.28 ($\epsilon(c = 1$ mM per liter$) = 0.00028$); the absorption of $K_4Fe(CN)_6$ in this spectral region is even less. Hence no correction was made for the absorption of ferri- or ferrocyanide. The use of the absorption of MHbCN as a standard of reference has the following advantages. We have attained a higher precision of measurement of hemoglobin spectrophotometrically (1) than by gasometric technique. It is the most direct procedure, and avoids such highly questionable practices as the estimation of total pigment colorimetrically as a basis for absorption constants (7). MHbCN is an ideal pigment for the determination of total concentration. Hb, $HbO_2$, HbCO, HbNO (Fig. 2), and MHb are all readily convertible into MHbCN. Within fairly wide limits (Fig. 1) pH does not influence the conversion or the spectrum, and the characteristic absorption of MHbCN is maximal in the region of greatest visual sensitivity.

Very recently Brooks (8) published her conclusion "that the absorption curve for cyanhemoglobin was identical with that for oxyhemoglobin." She apparently studied mixtures rather than single pigment derivatives and drew her conclusion from a consideration of measurements at only two wave-lengths, calculating the ratio of extinction coefficients at $\lambda$ 560 and $\lambda$ 540 $m\mu$. The use of extinction ratios at two points in the spectrum has been advocated as a guide to the detection of impurities in $HbO_2$ and not for the identification of pigments. Consideration of the shape of the entire spectrophotometric curves of $HbO_2$ and MHbCN (Fig. 1), in fact so different in their character, would, we believe, have led her to a different conclusion.

*Preparation of HbNO and SHb*—In the preparation of HbNO the absence of oxygen (to avoid the formation of higher oxides of $N_2$) was insured by the use of reduced hemoglobin solutions and exposure to NO in an atmosphere of nitrogen. Washed defibrinated dog erythrocytes were hemolyzed in water to 10 times the volume of the initial blood and filtered. 20 cc. of this solution + 20 cc. of 133 mM per liter of phosphate buffer (pH 7.0) were diluted to 100 cc. The diluted solution was repeatedly evacuated in a

tonometer (capacity of 400 cc.) and equilibrated with $CO_2 + N_2$, then with $N_2$. The solution was filtered and again repeatedly evacuated and equilibrated. A sample was converted to MHbCN for determination of concentration; another sample was run into the spectroscopic cell with minimal exposure to air and read to establish completeness of reduction. Reduction having been demonstrated, successive additions of NO were run into the tonometer, the diluting gas being $N_2$. As equilibrations with successive increases in NO tension were completed, samples were quickly sealed in the spectroscopic cell for reading. The NO was generated by delivering 33 per cent $HNO_3$ upon thin strips of pure Cu suspended in an air-tight cylinder over water. The cylinder and connection were previously evacuated and flushed with $N_2$. Details of special experiments appear in the legends accompanying the figures.

SHb was prepared with $H_2S$ generated in a Kipp apparatus with HCl and washed in water. The gas was delivered at a rate of approximately 150 bubbles per minute from an outlet tube of 3 mm. bore. The foaming of the dilute solutions of hemolyzed washed blood cells receiving the gas was minimized with minute amounts of caprylic alcohol. The duration of exposure to $H_2S$ was variable and is indicated in the legends accompanying the figures. Alternate exposure to $H_2S$ and air or oxygen (3) was found unnecessary, sufficient oxygen being furnished by carrying out the reaction in open flasks.

The pH of solutions was determined by means of the glass electrode.

### *Results*

Fig. 1 shows the absorption curves of solutions of $HbO_2$, HbCO, Hb, and MHbCN, prepared from hemolyzed, washed erythrocytes. It is evident that with these pigments fairly wide variations in pH did not affect the absorption curve. Table I indicates that greater precision of measurement was attained upon solutions prepared from hemolyzed, washed blood cells than from hemolyzed whole blood. The ratios of absorption of the peaks of the curve to the trough were somewhat higher for $HbO_2$ and HbCO prepared by the present technique than for the corresponding pigments prepared from whole blood (Table I, last two columns).

The differences in the two sets of preparations are most probably related to physical factors such as very slight turbidity, unavoid-

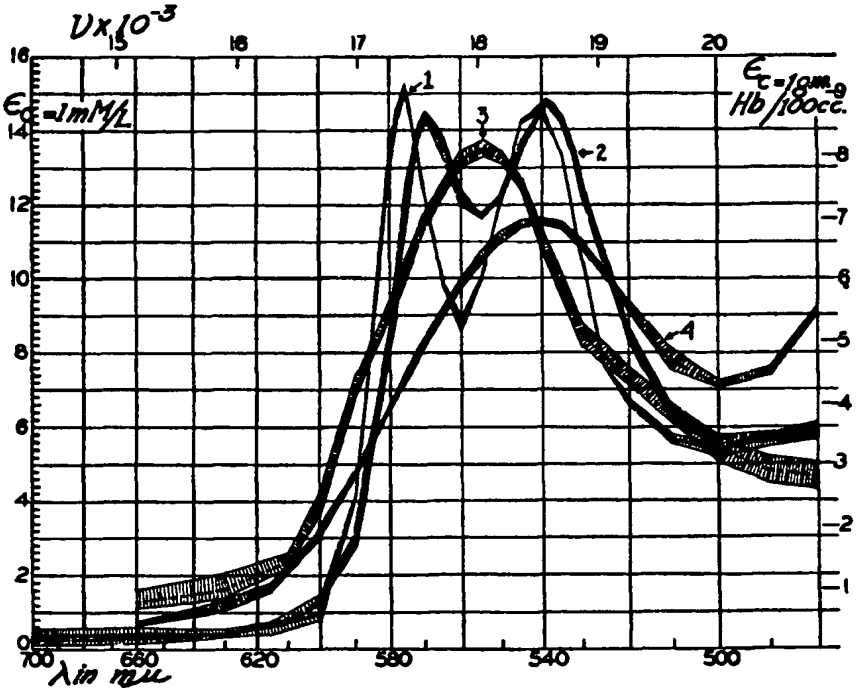


FIG. 1. Absorption curves of $HbO_2$, HbCO, Hb, and MHbCN, cross-hatched to show the spread of the determinations. Curve 1 represents $HbO_2$ (eight solutions) 0.070 to 0.205 mM per liter, buffers 33 mM per liter of phosphate, 25 mM per liter of borate (two unbuffered solutions), pH 5.9 to 9.2; Curve 2, HbCO (six solutions) 0.0942 to 0.205 mM per liter, buffers 33 mM per liter of phosphate, 10 to 27 mM per liter of borate (one unbuffered solution and one with 100 mM per liter of $NH_4OH$), pH 5.9 to 11.0; Curve 3, Hb (seven solutions) 0.107 to 0.205 mM per liter, buffers 13 to 27 mM per liter of phosphate, 24 mM per liter of borate (two unbuffered solutions), pH 4.5 to 9.2. Reduction was by evacuation in one solution, in the others with $Na_2S_2O_4$, 4 mM per liter; Curve 4, MHbCN (seven solutions) 0.113 to 0.205 mM per liter, buffers 15 to 33 mM per liter of phosphate, 11 to 25 mM per liter of borate (one unbuffered solution), pH 5.9 to 9.2. $K_3Fe(CN)_6$ 0.8 to 0.9 mM per liter and KCN 0.7 to 0.8 mM per liter.

able when whole blood is used. It is well recognized that lower ratios for $HbO_2$ will be obtained when MHb is present, but it is

TABLE I

*Precision of Measurement of Absorption Constants*

| Pigment | Source* | No. of specimens | λ | ε(c = 1 mM per liter) | | | | $\sqrt{\frac{\Sigma\delta^2}{n-1}}$ † | Ratio, ε/ε‡ | |
|---|---|---|---|---|---|---|---|---|---|---|
| | | | | Average | High | Low | Δ, high to low | | $\frac{\lambda\ 575\ m\mu}{\lambda\ 560\ m\mu}$ | $\frac{\lambda\ 540\ m\mu}{\lambda\ 560\ m\mu}$ |
| | | | mμ | | | | | | | |
| $HbO_2$ | A | 17 | 575 | 15.79 | 16.7 | 15.3 | 1.4 | 0.31 ± 0.05 | 1.67 | 1.62 |
| | | | 560 | 9.43 | 10.2 | 9.0 | 1.2 | 0.26 ± 0.04 | | |
| | | | 540 | 15.29 | 16.5 | 14.8 | 1.7 | 0.38 ± 0.07 | | |
| " | B | 8 | 575 | 15.13 | 15.26 | 15.06 | 0.20 | 0.07 ± 0.02 | 1.73 | 1.68 |
| | | | 560 | 8.73 | 8.95 | 8.56 | 0.39 | 0.13 ± 0.03 | | |
| | | | 540 | 14.62 | 14.70 | 14.52 | 0.18 | 0.06 ± 0.01 | | |
| HbCO | A | 16 | 569 | 14.71 | 15.48 | 13.22 | 2.26 | 0.48 ± 0.08 | 1.22 | 1.23 |
| | | | 558 | 12.09 | 12.50 | 11.80 | 0.70 | 0.29 ± 0.05 | | |
| | | | 539 | 14.83 | 15.64 | 13.31 | 2.33 | 0.49 ± 0.09 | | |
| " | B | 6 | 569 | 14.39 | 14.54 | 14.08 | 0.46 | 0.16 ± 0.05 | 1.23 | 1.26 |
| | | | 558 | 11.81 | 11.92 | 11.70 | 0.22 | 0.08 ± 0.02 | | |
| | | | 555§ | 11.70 | 11.74 | 11.65 | 0.09 | 0.05 ± 0.02 | | |
| | | | 539 | 14.77 | 14.82 | 14.69 | 0.13 | 0.05 ± 0.01 | | |
| Hb | " | 7 | 560 | 13.24 | 13.51 | 13.00 | 0.51 | 0.21 ± 0.06 | | |
| | | | 555 | 13.50 | 13.66 | 13.28 | 0.38 | 0.14 ± 0.04 | | |
| | | | 550 | 13.28 | 13.45 | 13.12 | 0.33 | 0.12 ± 0.03 | | |
| MHbCN | " | 7 | 551 | 11.10‖ | 11.28 | 10.97 | 0.31 | 0.10 ± 0.03 | | |
| | | | 545 | 11.52‖ | 11.60 | 11.40 | 0.20 | 0.08 ± 0.02 | | |
| | | | 540 | 11.53‖ | 11.63 | 11.47 | 0.16 | 0.05 ± 0.01 | | |

* Solutions prepared from hemolyzed, whole dog blood are listed as Source A, those prepared from hemolyzed, washed dog erythrocytes, as Source B.

† The figures after the ± represent the standard error of the standard deviation.

‡ Ratios of extinction coefficients at the maxima of absorption to the minimum between the two bands.

§ Only three determinations at this wave-length were made.

‖ The average constants have been assumed on the basis of our earlier work (1) so that only the spread of determinations is of significance in the case of this pigment.

not justifiable to conclude (9) that admixture with the oxidized form of hemoglobin is the sole cause of this phenomenon. The reasons for this will be made more apparent in two of the following papers.

Fig. 2 is typical of the data obtained in experiments with HbNO. The absorption curve of HbNO is evidently that of an analogue of $HbO_2$. The spectrum is distinguishable from that of $HbO_2$ by the shallowness of the trough between the two max-

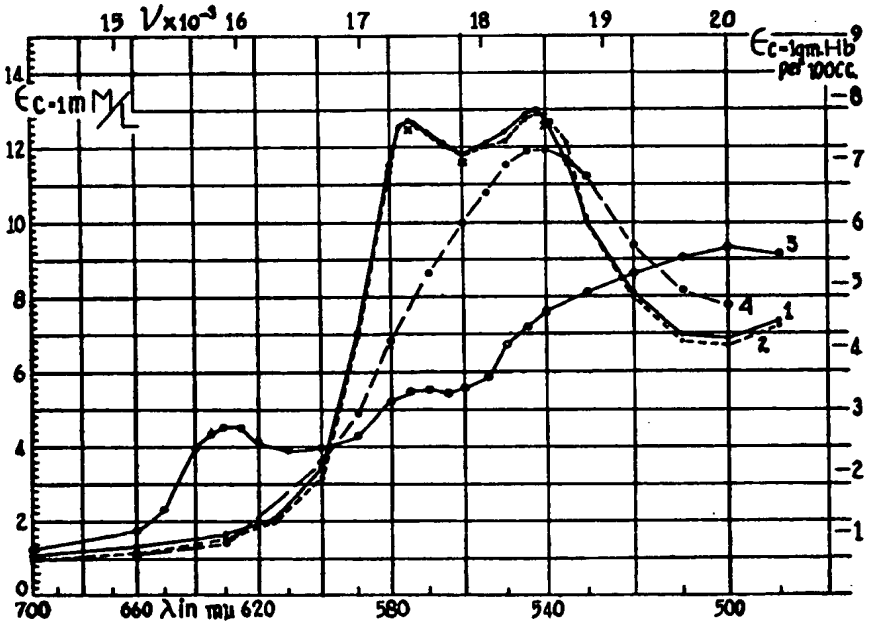


FIG. 2. HbNO and its conversion to MHb and MHbCN. Curve 1 represents HbNO, 0.204 mM per liter, $PO_4$ buffer (pH 7.0) 25 mM per liter, pH 7.1, tension of NO 87 mm. of Hg; Curve 2, HbNO, 0.204 mM per liter, $PO_4$ buffer (pH 7.0) 25 mM per liter, pH 7.0, tension of NO 244 mm. of Hg; Curve 3, MHb, 0.186 mM per liter, prepared from HbNO solution with $K_3Fe(CN)_6$, 3.6 mM per liter; Curve 4, MHbCN, 0.168 mM per liter, prepared from the above MHb solution with KCN, 1.4 mM per liter. The cross marks are for HbNO, the solution of Curve 2 after evacuation and equilibration with $CO_2 + N_2$.

ima of absorption. This results in unusually low ratios of extinction coefficients of peaks to trough.

$$\frac{\epsilon_{\lambda\ 575\ m\mu}}{\epsilon_{\lambda\ 560\ m\mu}} = 1.08 \qquad \frac{\epsilon_{\lambda\ 543\ m\mu}}{\epsilon_{\lambda\ 560\ m\mu}} = 1.10$$

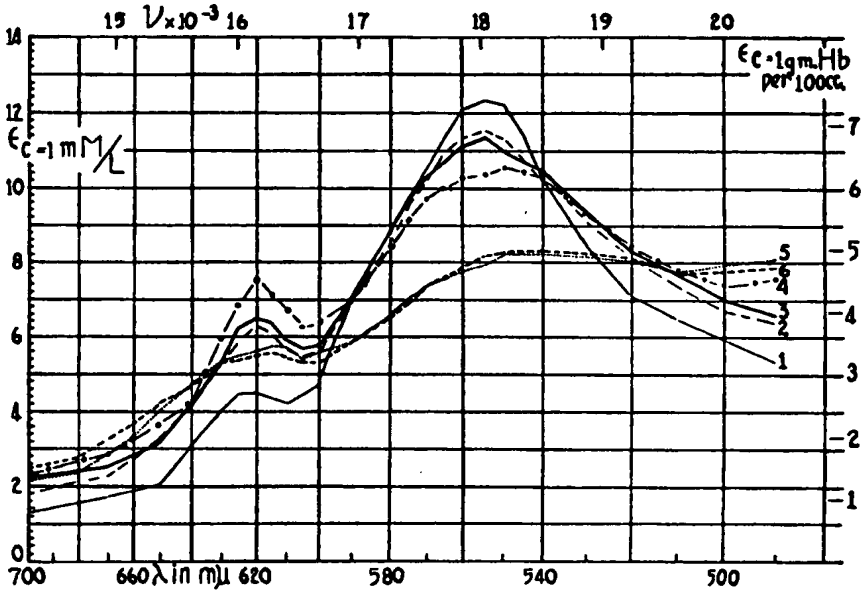


FIG. 3. Effect of duration of treatment with $H_2S$ upon absorption curve of hemoglobin solutions. Curve 1 represents 4 minutes exposure to $H_2S$, interpreted as 69 to 74 per cent Hb and 31 to 26 per cent SHb. Total pigment 0.201 mM per liter, borate buffer (pH 9.2) 10 mM per liter; Curve 2, 8 minutes exposure to $H_2S$, interpreted as 47 to 55 per cent Hb and 53 to 45 per cent SHb; Curve 3, 8 minutes exposure to $H_2S$ followed by evacuation, interpreted as 44 to 52 per cent Hb and 56 to 48 per cent SHb. No change on adding $Na_2S_2O_4$ or KCN; Curve 4, 50 minutes exposure to $H_2S$, interpreted as 28 to 37 per cent Hb and 72 to 63 per cent SHb. Total pigment 0.158 mM per liter, borate buffer (pH 9.2) 10 mM per liter; Curve 5, 90 hours exposure to $H_2S$. Total pigment at start 0.171 mM per liter, phosphate buffer (pH 7.0) 13.3 mM per liter, final pH 6.91. Centrifuged and filtered to remove copious precipitate, mainly S; Curve 6, 4 hours exposure to mixed $H_2S$ and air and 86 hours exposure to $H_2S$. Total pigment at start 0.171 mM per liter, phosphate buffer (pH 7.0) 13.3 mM per liter, final pH 6.83. Centrifuged and filtered to remove precipitate. $\epsilon$ values raised by 13.8 per cent to bring level of curve to that of preceding solution, assuming greater loss of pigment.

The locations of the absorption maxima are not materially different than for $HbO_2$. The apparent slight shift of the $\beta$ band towards the red may be significant, but our data are insufficient to establish this point.

HbNO was quantitatively converted by the addition of $K_3Fe(CN)_6$ into MHb. In the experiment reported in Fig. 2 the conversion was at pH 7.0 and the spectrum obtained is very similar to that yielded by MHb prepared from $HbO_2$ at the same H ion concentration (10). The quantitative conversion of the MHb formed from HbNO into MHbCN was also demonstrated. This would appear definitely to establish HbNO as a true analogue of $HbO_2$.

HbNO, buffered at pH 7.0, was not converted to Hb (Fig. 2) by repeated evacuation and equilibration with $CO_2 + N_2$, then with $N_2$— conditions under which $HbO_2$ would have been completely reduced. The union of Hb with NO is apparently more firm than with $O_2$. HbNO appeared also to be more stable to alteration in H ion concentration than $HbO_2$. We observed no changes in spectrum in the wide pH range of 3.4 to 11.2.

Fig. 3 presents the data obtained in a group of experiments in which $HbO_2$ was exposed to $H_2S$ for varying periods of time. In Curves 1 to 4 it is obvious that there is a progressive change in spectrum involving simultaneously an increase of absorption in the red at $\lambda$ 620 $m\mu$ and a decrease in the green at $\lambda$ 555 $m\mu$. A consideration of the absorption curve of Hb (Fig. 1) led to the assumption that at least Curves 1 to 3 of Fig. 3 were due to mixtures of Hb and SHb. It was assumed at first that Curve 4 (50 minutes exposure to $H_2S$) represented complete conversion to SHb.

Curves 5 and 6 (Fig. 3) were obtained after long exposure of hemoglobin to $H_2S$, followed by centrifuging and filtration to remove copious precipitates mainly of colloidal S. Precipitation with the possible loss of pigment invariably occurred when solutions of $HbO_2$ were exposed to $H_2S$ for 1 hour or longer. The precipitate from the solution represented by Curve 5 had no appreciable color. There was a greater loss of pigment from the solution represented by Curve 6 (exposed actively to $H_2S$ and air), and the level of this curve has been adjusted to the concentration of the pigment in the solution represented by Curve 5. Both solutions gave optical evidence (Tyndall effect) of slight turbidity. The shape of these absorption curves sets them apart from the others reported in Fig. 3.[1] The proportional decrease

[1] The exact level of the curves is uncertain, since the concentration of pigment in these experiments could not be determined by conversion to

in the two maxima of absorption in comparison with Curve 4 and a relative increase in absorption at the red and blue ends of the spectrum could be due to a combination of the factors of loss of pigment and presence of turbidity. This explanation, however, demands a greater loss of pigment than appears to have actually taken place and does not account for the shift of the absorption maxima towards the blue. It is, therefore, also probable that, after long exposure to $H_2S$, secondary pigment changes may have occurred. We believe that Haurowitz's SHb studies (3) may be interpreted in a similar manner. Our curves are not inconsistent with the changes in spectrum which would occur were appreciable amounts of a hemin-like derivative (11) produced.

Examples of the absorption spectra yielded by the hemolyzed blood of a patient with clinical sulfhemoglobinemia[2] as well as of specially prepared control mixtures of normal $HbO_2$ treated with a solution of $H_2S$ are presented in Fig. 4 (Curves 1 and 2). It is evident that these curves are similar. However, when we constructed theoretical curves of mixtures of $HbO_2$ and SHb, assuming that Curve 4 of Fig. 3 (repeated in Fig. 4 for convenience) was pure SHb, we failed to get any curve the shape of which resembled the curves yielded by the pathological blood and the control blood treated with $H_2S$ water. This led us to the conclusion that Curve 4, like Curves 1 to 3 in Fig. 3, was that of a mixture of Hb and SHb. This curve represented the maximum conversion to SHb attained in our experiments before precipitation and perhaps other changes occurred.

The absorption spectrum of SHb (Curve 4, Fig. 4) has been deduced mathematically from the data at four wave-lengths, $\lambda$ 620, $\lambda$ 575, $\lambda$ 560, and $\lambda$ 540 $m\mu$, for Curves 1 to 4 in Fig. 3. The underlying assumption was that these curves represented a

MHbCN. The addition of KCN alone produced no change in spectrum, while the addition of $K_3Fe(CN)_6$ resulted in the precipitation of highly pigmented material.

[2] The patient had chronic acetanilide poisoning, in this respect resembling one of the patients described by Harrop (4). Solutions prepared from the blood showed spectroscopically the usual bands of $HbO_2$ and besides a band at $\lambda$ 620 $m\mu$. Most of the pigment in the blood was convertible into Hb by means of $Na_2S_2O_4$ and into MHbCN by the addition of $K_3Fe(CN)_6$ and KCN, but the band in the red persisted unaltered in strength in each case.

progressive change from Hb to SHb. We determined by successive approximations the values for the concentration of Hb ($c_{Hb}$) and SHb ($1-c_{Hb}$) for each of the four solutions and the

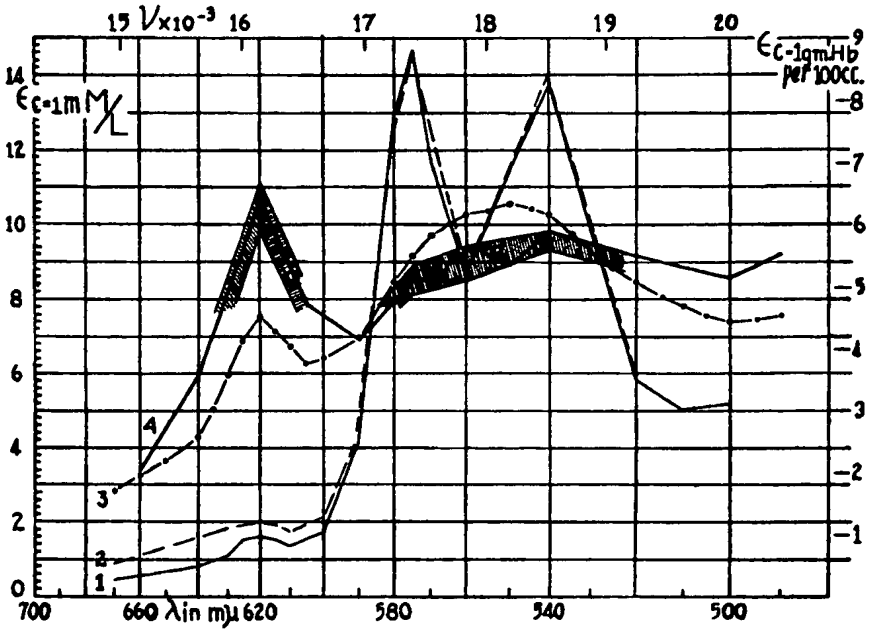


FIG. 4. Absorption spectrum of blood of a patient with clinical sulfhemoglobinemia and our extrapolated spectrum of pure SHb. Curve 1 represents pathological blood. Total pigment 0.141 mM per liter, $HbO_2$ 0.124 to 0.126 mM per liter, SHb 0.015 to 0.017 mM per liter; Curve 2, control from normal human blood treated with $H_2S$. Total pigment 0.226 mM per liter, as determined both upon original $HbO_2$ and after conversion, $HbO_2$ 0.192 to 0.196 mM per liter, SHb 0.030 to 0.035 mM per liter. Prepared by adding 0.1 cc. of a saturated aqueous solution of $H_2S$ to 5 cc. of dilute solution of hemolyzed washed erythrocytes; Curve 3, Hb + SHb, same as Curve 4, Fig. 3; Curve 4, extrapolated spectrum of SHb (see text). Cross-hatched areas indicate zone of uncertainty.

absorption constants of SHb ($\epsilon_{SHb}$) at the four chosen wavelengths which satisfied best sixteen equations which can be set up under these circumstances. The equations were of the form

$$c_{Hb} \times \epsilon_{Hb} + (1 - c_{Hb}) \times \epsilon_{SHb} - \epsilon_{observed} = 0$$

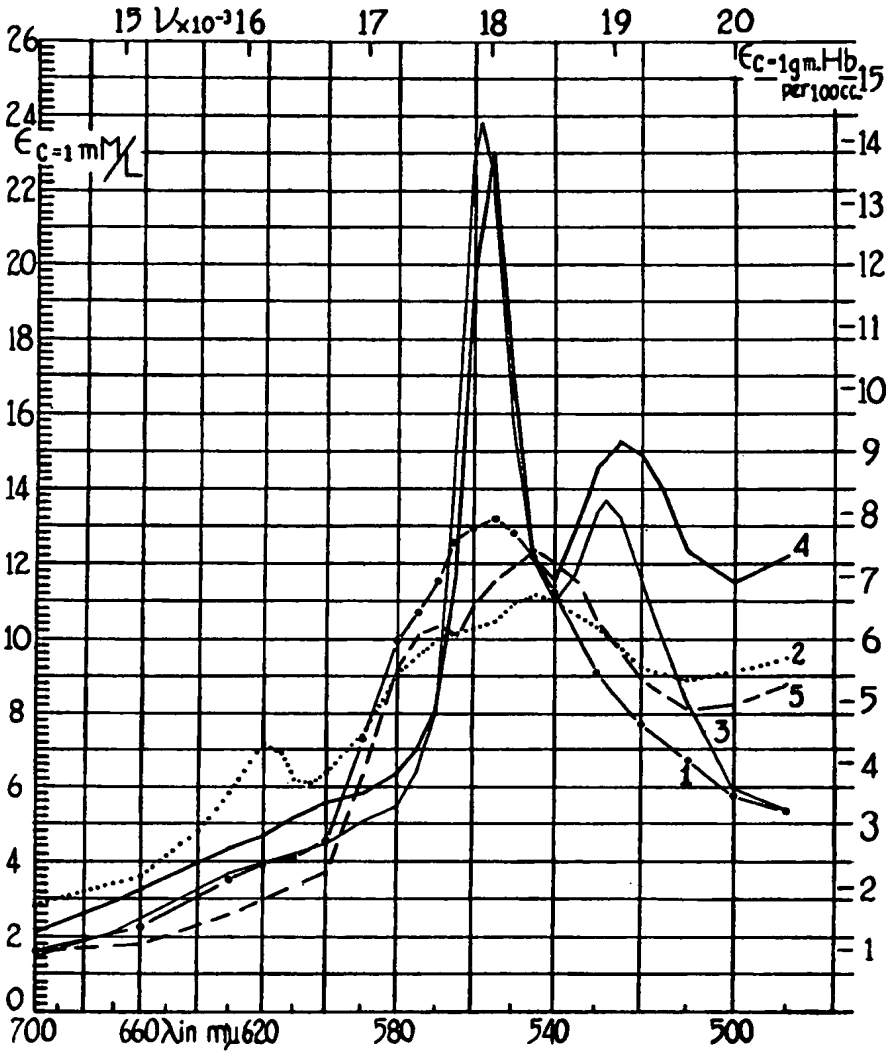


FIG. 5. Curves for reduced hemochromogens, prepared from mixtures of Hb and SHb, and for sulfmethemoglobin, SMHb. Curve 1 represents Hb exposed to $H_2S$. Total pigment 0.151 mM per liter, phosphate buffer (pH 7.0) 13.3 mM per liter, reduced in tonometer by evacuation and equilibration

The sixteen equations contained eight unknowns. The data permitted each of the unknowns to be evaluated within certain limits. The $\epsilon_{SHb}$ values so obtained were used to plot our deduced spectrum of pure SHb, the cross-hatched areas indicating the limits of the approximation. Proof of the validity of our assumptions was furnished by the ability to construct theoretical curves of mixtures of $HbO_2$ and SHb or of Hb and SHb which agreed excellently with the observed spectra from the patient's blood, both before and after the addition of $Na_2S_2O_4$, and with normal hemolyzed blood treated with a solution of $H_2S$. The percentage composition of the mixtures of pigments which appear in the legends of Fig. 3 and 4 and the total pigment concentration of the clinical case were calculated from the absorption data of $HbO_2$ and Hb (Fig. 1) and of SHb (Fig. 4). This is, we believe, the first time that quantitative estimation of sulfhemoglobin concentration in a clinical case has been accomplished.

No consistent changes in the absorption spectra of mixtures of Hb and SHb took place with variations in pH from 6.2 to 10.4. It is of interest, however, that solutions of hemoglobin through which $H_2S$ was bubbled became somewhat more acid. The acidity of $H_2S$ ($K_1 = 9.0 \times 10^{-10}$) may partly account for a marked drop in pH, 9.2 to 6.7, observed in solutions buffered with $Na_2B_4O_7$. This explanation, however, cannot be applied to a slight though consistent lowering of pH, 7.0 to 6.83 and 7.0 to 6.23, of solutions buffered with phosphate. The possibility that acid was produced by the oxidation of $H_2S$ must be considered.

---

with $CO_2 + N_2$, then with $N_2$, equilibrated with pure $H_2S$ in tonometer, transferred to cell with minimal exposure to air, and read; Curve 2, Hb + SHb, preceding solution after exposure to air; Curve 3, reduced hemochromogen. Total pigment 0.087 mM per liter, borate buffer (pH 9.2) 5 mM per liter, exposed to $H_2S$ for 4 minutes, NaOH then added to 87 mM per liter, no change on adding $Na_2S_2O_4$; Curve 4, reduced hemochromogen. Total pigment 0.101 mM per liter, borate buffer (pH 9.2) 5 mM per liter, exposed to $H_2S$ for 4 minutes, pyridine added to 50 per cent, no change on adding $Na_2S_2O_4$; Curve 5, SMHb. Total pigment 0.151 mM per liter, transformed to MHb by addition of $K_3Fe(CN)_6$, 0.158 mM per liter, phosphate buffer (pH 5.9) 7 mM per liter. The acid MHb was exposed to $H_2S$ for 5 seconds. An identical spectrum was obtained from MHbCN by treatment with $H_2S$.

Reduced hemoglobin was not converted to SHb upon exposure to $H_2S$, unless $O_2$ was available (Fig. 5, Curves 1 and 2). Mixtures of Hb + SHb were converted to typical reduced hemochromogens (11) by the addition of pyridine or alkali in excess (Fig. 5, Curves 3 and 4). Conversion to reduced hemochromogen suggests that our preparations of SHb are in a reduced condition.

In confirmation of Keilin's experiments (12) we have found that a characteristic pigment, which may be designated as sulfmethemoglobin (SMHb), was produced when MHb was exposed to $H_2S$ (Fig. 5, Curve 5). In these experiments it was important to avoid any excess of $K_3Fe(CN)_6$ to insure against the precipitation of pigmented material which otherwise occurred. SMHb, in contrast to SHb (see Curve 3, Fig. 3), could be converted to its parent pigment. Upon exposure to air, reconversion of SMHb to MHb took place; the MHb so formed was convertible to typical MHbCN upon the addition of KCN and to typical Hb upon the addition of $Na_2S_2O_4$.

We have not found a suitable explanation for the need of $O_2$ in the production of SHb from Hb. The formation of SHb did not occur in solutions of $HbO_2$ exposed to $SO_2$.

## SUMMARY

The absorption spectra of $HbO_2$, Hb, HbCO, and MHbCN yielded by solutions prepared from hemolyzed washed erythrocytes have been presented. Such solutions have been found preferable for precise spectrophotometric analysis rather than corresponding preparations from hemolyzed whole blood.

The absorption spectrum of HbNO was obtained under conditions which excluded the presence of $O_2$. The conversion of this pigment to MHb has been demonstrated. HbNO is probably a relatively stable analogue of $HbO_2$.

Data have been presented which indicate that the absorption spectrum of pure SHb probably has not been described heretofore. The absorption curve of this pigment has been extrapolated from our data upon mixtures of Hb + SHb. For the first time the quantitative estimation of SHb in the blood of a patient with clinical sulfhemoglobinemia has been accomplished. SHb was formed from Hb only in the presence of oxygen. The pigment was not convertible to Hb or MHbCN, but was readily changed

into typical hemochromogens. Solutions of Hb increase in acidity upon exposure to $H_2S$.

SMHb, a characteristic pigment described by Keilin (12), was obtained from MHb by treatment with $H_2S$. A pigment yielding the spectrum of SMHb was obtained also by the exposure of MHbCN to $H_2S$.

BIBLIOGRAPHY

1. Drabkin, D. L., and Austin, J. H., *J. Biol. Chem.*, **98**, 719 (1932).
2. Haurowitz, F., *Z. physiol. Chem.*, **138**, 68 (1924). Haldane, J., Makgill, R. H., and Mavrogordato, A. E., *J. Physiol.*, **21**, 160 (1897).
3. Haurowitz, F., *Z. physiol. Chem.*, **151**, 130 (1926).
4. Clarke, T. W., and Hartley, W. H., *J. Physiol.*, **36**, 62 (1907–08). Van Lier, H. W., Over de Parhaemoglobinaemieen, Utrecht, 61 (1933). Harrop, G. A., Jr., *Internat. Clin.*, **3**, 86 (1931).
5. Birge, R. T., in Washburn, E. W., International critical tables of numerical data, physics, chemistry and technology, New York, **5**, 409 (1929).
6. Walsh, J. W. T., Photometry, New York, 18, 460 (1926). Zeeman, P., in Washburn, E. W., International critical tables of numerical data, physics, chemistry and technology, New York, **5**, 418 (1929).
7. Ray, G. B., and Isaac, L. A., *J. Biol. Chem.*, **85**, 549 (1929–30).
8. Brooks, M. M., *Proc. Soc. Exp. Biol. and Med.*, **32**, 1113 (1935).
9. Winegarden, H. M., and Borsook, H., *J. Cell. and Comp. Physiol.*, **3**, 437 (1933).
10. Austin, J. H., and Drabkin, D. L., *J. Biol. Chem.*, **112**, 67 (1935–36).
11. Drabkin, D. L., and Austin, J. H., *J. Biol. Chem.*, **112**, 89 (1935–36).
12. Keilin, D., *Proc. Roy. Soc. London, Series B*, **113**, 393 (1933).

Exhibit 5

Figure 1

The effect of ATN-161 and ATN-220 on growth factor induced angiogenesis was tested in the matrigel plug assay in the presence or absence of the PKA inhibitor HA1004. As shown in the upper panel ATN-161 significantly inhibited growth factor induced angiogenesis and this inhibition was in large part attenuated by the presence of HA1004. In contrast, although ATN-220 significantly inhibited angiogenesis (lower panel) this inhibition was not affected by the presence of HA1004.